STUDY OF INTERNAL OVERVOLTAGES AND DESIGN OF DAMPING CIRCUIT FOR HVDC THYRISTOR VALVES

By

ADAPA RAMBABU

DEPARTMENT OF ELECTRICAL ENGINEERING
INDIAN INSTITUTE OF TECHNOLOGY, KANPUR

AUGUST, 1981

STUDY OF INTERNAL OVERVOLTAGES AND DESIGN OF DAMPING CIRCUIT FOR HVDC THYRISTOR VALVES

A Thesis Submitted
in Partial Fulfilment of the Requirements
for the Degree of
MASTER OF TECHNOLOGY

By

ADAPA RAMBABU

to the
DEPARTMENT OF ELECTRICAL ENGINEERING
INDIAN INSTITUTE OF TECHNOLOGY, KANPUR
AUGUST, 1981

EE-1981-M-RAM-STU

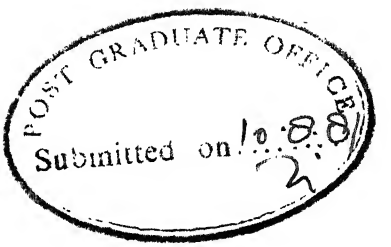

CERTIFICATE

Certified that the work entitled , "Study of Internal Overvoltages and Design of Damping Circuit for HVDC Thyristor Valves" by Mr. Adapa Rambabu has been carried out under my supervision and has not been submitted elsewhere for the award of a degree.

(Dr. K.R. Padiyar)
Professor
Department of Electrical Engineering
Indian Institute of Technology
KANPUR

ACKNOWLEDGEMENT

I express my deep sense of gratitude to Dr. K.R. Padiyar who initiated the problem and provided excellent guidance throughout the course of this work.

I am thankful to all my friends especially Mr. Sachchidanand for the constant help rendered to me at all stages of this thesis.

I thank Mr. K.N. Tewari for his patient and skilful typing.

Adapa Rambabu

TABLE OF CONTENTS

LIST OF TABLES

LIST OF FIGURES

LIST OF PRINCIPAL SYMBOLS

v_a, v_b, and v_c	:	a, b, and c phase voltages respectively
E_L	:	line-to-line r.m.s. voltage
L_t	:	transformer leakage inductance/phase
C_t	:	lumped transformer capacitance/phase
C_y	:	lumped switchyard capacitance/phase
R_a	:	anode damper resistance
L_a	:	anode damper inductance
R_g	:	grading circuit resistance/thyristor
C_g	:	grading circuit capacitance/thyristor
R_d	:	damping circuit resistance
C_d	:	damping circuit capacitance
I_d	:	direct current
t_d	:	delay time of a thyristor
t_r	:	rise time of a thyristor
t_{on}	:	turn-on time of a thyristor
N	:	total number of thyristors in a valve
n	:	number of thyristor groups in a valve
F(t)	:	overvoltage factor
I_o	:	peak reverse current through a valve
Q_{rr}	:	storage charge of a thyristor
ΔQ	:	incremental storage charge

Q_{min}	:	minimum value of Q_{rr}
$\delta(t)$	:	unit impulse function
i_{R_d}	:	current flowing through the damping resistance R_d
α	:	delay (or firing) angle
μ	:	commutation (or overlap) angle
δ	:	extinction angle
C_s	:	stray capacitance across the valve
f(or f_1)	:	fundamental frequency (power frequency)
T	:	power frequency period
ζ	:	damping factor
ω_n	:	undamped angular frequency, rad./sec.
η	:	performance index
Q	:	weighting matrix
P	:	symmetric positive semidefinite matrix
K	:	weightage given to the power loss component
F, G	:	system matrices
x, u	:	state variable and control vectors respectively

Subscript zero with variable denote initial condition of variables.

ABSTRACT

A thyristor valve for HVDC systems must contain a large number of devices connected in series and in parallel to accommodate large voltage and current requirements. As the turn on and turn-off characteristics of the individual thyristors vary, the thyristors are subjected to overvoltages and overcurrents during the turn-on and commutation of a valve. The overvoltages are controlled by the grading and damping circuits. Computer programs are developed to calculate turn-on and turn-off overvoltages in a HVDC valve having thyristors connected in series.

Power loss in the damping circuit is a significant component of the overall convertor losses and hence has a bearing on its design. A method is developed for the exact calculation of losses in the damping circuit. The effect of bridge operation and damping circuit parameters on losses is analysed.

A computer program is developed to calculate the sensitivities of the valve voltage with respect to damping circuit resistance and capacitance in Time Domain using Adjoint network approach. A method of parameter optimization is used to select the values of damping circuit parameters which reduce the recovery voltage without undue increase in losses.

CHAPTER 1

INTRODUCTION

1.1 Status of HVDC Transmission

Despite the general acceptance of A.C. transmission, D.C. Transmission is preferred for certain applications because of its advantages. In particular it can be considered for the following applications.

(1) Submarine cables of length more than 20 miles,

(2) Interconnecting A.C. systems of different frequencies,

(3) For transmitting large amounts of power over long distance by overhead lines,

(4) For transmission by cables in congested urban areas.

Ratings of HVDC link have grown continuously and at present a power rating of more than 2000 MW with transmission voltage upto $\pm$ 600 KV are feasible. The use of better converter transformers, harmonic filters, sophisticated methods of converter control and protection, 12 pulse converters has improved the performance of HVDC to a great extent. The modern trends towards the use of multiterminal systems and the developments in the design of HVDC circuit breakers will certainly increase the application of HVDC in future.

1.2 HVDC Thyristor Valve [7, 13-16]

The major component of the converter station is the valve which allows current flow only in one direction and the instant of starting the conduction through a valve can be controlled with the help of grid (firing angle) control.

The very high current density of the cathode spot in mercury arc valves, together with high breakdown level of mercury vapour, established the superiority of mercury arc valves during early thirties of this century. Mercury arc valves are now displaced by thyristor valves which have proved to be more reliable. In particular, with thyristor valves

1) there is no problem of arc backs (reverse conduction)
2) the converter is of modular construction and the design and maintenance are easy
3) the operation is more reliable and capable of fast control.

A thyristor valve consists of a number of individual thyristors connected in series and parallel to accommodate the large voltage and current requirements because of the limited voltage and current carrying capability of individual thyristors. The thyristor is a three terminal, semiconductor device made of alternate layers of p and n type silicon. The diagram of the device and electric

symbol is shown in Fig.1.1. The device can carry current only in one direction from anode to cathode and the instant of initiation of conduction can be controlled by gate.

The characteristic of the device is shown in Fig.1.2 with the three states of the device (1) Reverse bias and blocking (2) forward bias and blocking and (3) forward bias and conducting.

A thyristor is turned on by applying an electrical signal to gate when the device is forward biased. Voltage and current waveforms during S.C.R. turn-on time are shown in Fig.1.3. When firing current is delivered to the gate of the device, it does not switch immediately from the blocking to the full conduction state. Indeed for a short period of time, the device continues to block the anode voltage applied to it in almost the same way as it would had the firing pulse not yet been delivered. Thereafter, the forward impedance starts to decrease, but not until a further time period has elapsed does the device become fully turned on. The total turn-on time of the device is subdivided into two distinct periods, called the delay time and the rise time. Both the delay time and the rise time are related to the rise time and amplitude of the gate firing current. The total turn-on time is of the order of 2-4 microseconds.

Turn-off of a device implies that the forward conduction has stopped and the application of a positive voltage to the anode

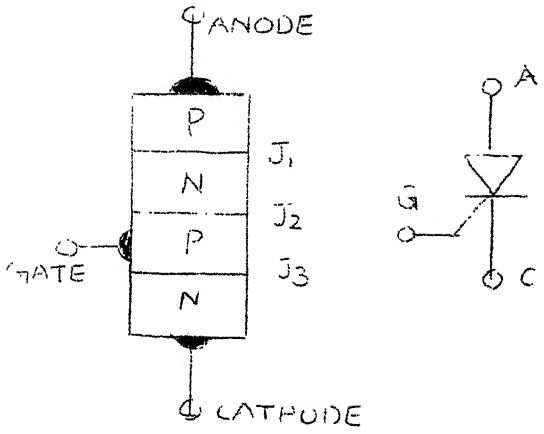

IG 1.1 THE DIAGRAM AND LECTRICAL SYMBOL OF THYRISTOR

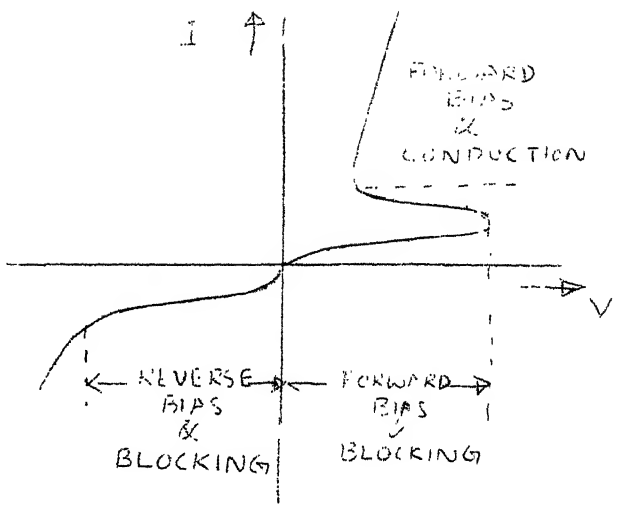

FIG 1.2 V-I Characteristic of THYRISTOR

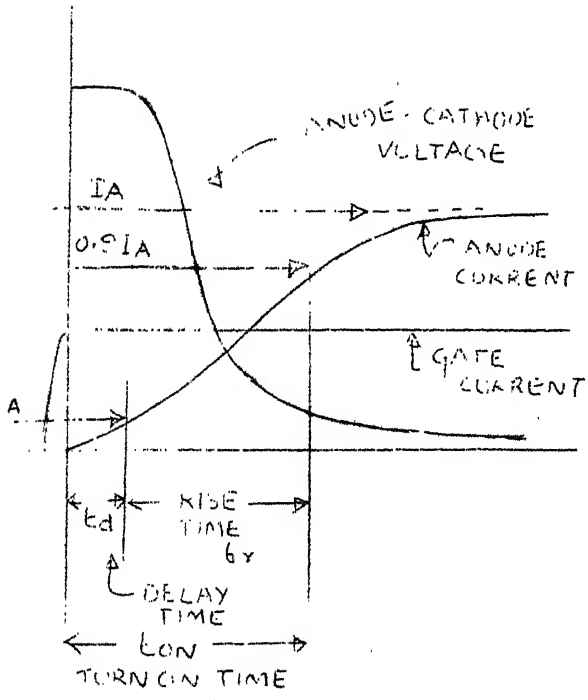

1.3 Voltage and current eforms during thyristor n on time

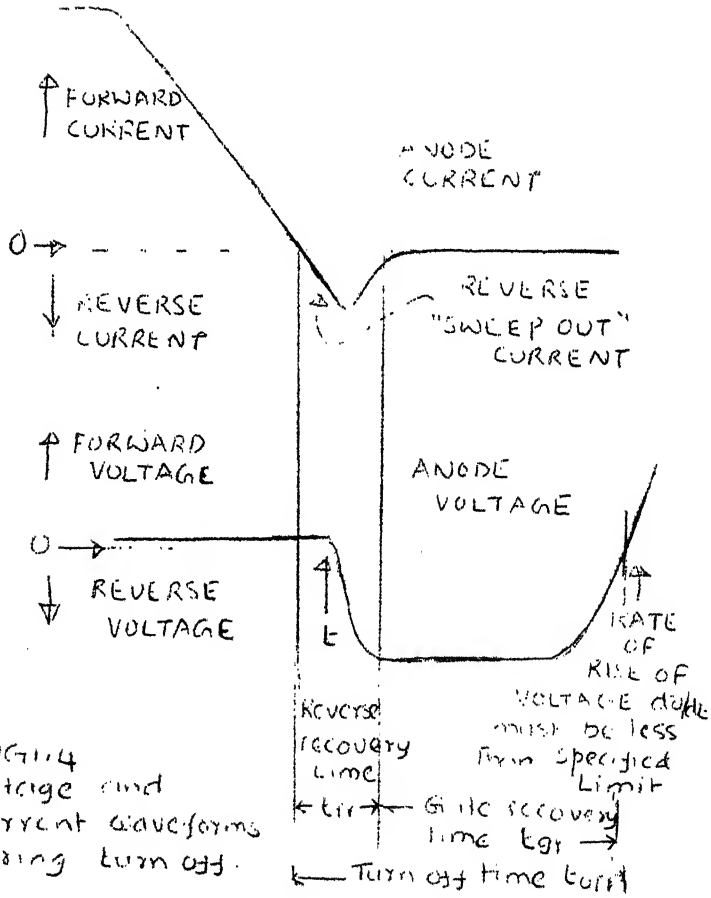

FIG 1.4 Voltage and current waveforms during turn off.

will not cause any current to flow if there is no gate signal. Voltage and current waveforms during SCR turn-off time are shown in Fig. 1.4. The total turn-off time is subdivided into two regions, called the reverse recovery time, and the gate recovery time. When a reverse voltage is applied across the thyristor its current reduces to zero value. Because of the storage charge present in the device, it continues to conduct in the reverse direction until its storage charge is neutralised. The reverse recovery time is a function of forward current and the rate of decay of forward current.

During the gate recovery time, reverse voltage must be maintained across the device. Not until the end of the gate recovery time is the device capable of blocking reapplied forward anode voltage. This time is dependent upon junction temperature of the device and the rate of reapplication of forward voltage.

The current rating of a thyristor depends upon the dimensions of the device as well as cooling arrangements. The voltage rating of a thyristor indicates the maximum reverse voltage it can block without excessive reverse current. At present, the thyristors used in HVDC valves have a maximum voltage rating of 3.5 KV and a current rating of 1800 Amps.

The proper sharing of voltage by the individual devices in the series connected thyristors in steady state is achieved by connecting a resistance or a zener diode across each device. Transient voltage sharing is ensured by a grading circuit which consists of series connected resistance and capacitance connecting across each device.

Cooling of a HVDC valve is required because the thyristors are thermally limited devices. A variety of fluids such as air, oil, water and SF_6 can be used for this purpose. Air cooling is simpler and more reliable. The insulation of the valve can also be through air, oil or SF_6 gas.

Overvoltages in a HVDC Valve

The electrical design of HVDC valves depends upon the overvoltages generated in the system and those generated within the valve. The valve is subjected to internal overvoltages and voltage stresses caused by the external system conditions. Switching surges from the A.C. side and voltage surges from D.C. side may cause overvoltages across a valve. The overvoltages can also occur during abnormal conditions (maloperation of the valve) such as arc back, arc through, quenching and misfire.

The turn-on and turn-off overvoltages constitute internal overvoltages in a valve. As the characteristics of thyristors vary due to manufacturing tolerances, the

individual thyristors turn-on and turn-off at different times because of which the thyristors and the valve are subjected to overvoltages. And also, a recovery overvoltage is developed across the valve after commutation. Grading and damping circuits are used to limit these overvoltages.

1.3 Objective of the Thesis

The objective of this thesis is to study in detail the turn-on and turn-off overvoltages in a HVDC Thyristor Valve and design of damping circuit. The turn-on and turn-off processes in a valve have to be simulated accurately to know the overvoltages developed across it. Digital simulation, based on network equations derived from topological considerations, is used to calculate these overvoltages. Effect of the valve and the system parameters is also investigated.

The considerations in the damping circuit design are overvoltage and power loss. An accurate evaluation of the overvoltage and power loss and the variation with damping circuit parameters is essential in the optimal design of the damping circuit. A mathematical technique to optimize the parameters is also investigated.

1.4 Review of the Literature

A detailed method of calculating turn-on overvoltages in a HVDC valve having thyristors in series is presented in

ref.[1] by G. Karady and T. Gilsig, in which a cumulative delay time distribution curve is used to select the number of thyristors that are turned on at any instant. The thyristor is modelled by a voltage source in series with a switch which closes at the instant of delay time of the thyristor. During the rise time the voltage across a thyristor will decrease exponentially. The effect of various system and valve parameters on turn-on overvoltages is analysed taking a representative thyristor valve. An IBM supplied ECAP program is used for circuit analysis. An extension of this work is carried out in ref.[2], in which parallel thyristor strings are also considered, which are necessary to meet the current requirements. Effects on overvoltages, of parallel strings of various turn-on delay time distributions and the effect of series string inductances on current sharing and overvoltages are considered. The system is described by a set of state equations and solved numerically.

Ref.[3] gives an exact method of calculating turn-off overvoltages which consist of both the overvoltages caused due to non-simultaneous turn-off of individual thyristors and the recovery overvoltages occurring during and after the turn-off process. A statistical distribution of storage charge is assumed for the thyristors. The thyristors are divided into a number of groups and each group of thyristors is represented by a step change in impedance from a small value to a very high value. The results are evaluated using ECAP program.

In ref.[7], a simplified analysis is carried out to calculate the valve voltage waveform. In ref.[4], a detailed equivalent circuit is presented to calculate the recovery voltage, neglecting the turn-off process.

Turn-on and turn-off overvoltages can be controlled by providing proper grading and damping circuits. Because of the presence of voltage across a valve during its non-conducting state the losses take place in the damping circuit. An approximate formulae are suggested by Ainsworth [17] to calculate the valve damping loss. An improvement to this method is made in ref.[4], by taking a second order model for generating voltage oscillations, which are superimposed on the ideal valve voltage. A hybrid computer is used to evaluate the power loss.

The design of the damping circuit requires the determination of the capacitance and resistance which limit the recovery voltage to a predetermined level without undue increase in losses. The various considerations to be taken in designing a damping circuit are given in ref.[4].

1.5 Summary of the Thesis

A chapterwise summary of the thesis is given below.

Chapter 2 deals with the calculation of turn-on overvoltages and the effect of system and valve parameters on it. A general computer program has been developed to

simulate the turn-on process of thyristors in a valve. The approach adopted for simulation of a valve during turn-on period is along the lines given in refs. [1,2]. The equivalent circuit is simulated by developing the state equations on the basis of topological considerations.

A method of calculation of turn-off overvoltages using a digital simulation is presented in Chapter 3. During the turn-off period the valve is represented by a time varying resistance in series with a time varying capacitance based on the approach given in ref. [3]. The effect of system and valve parameters on turn-off overvoltages is studied. The recovery voltage neglecting turn-off process is also calculated.

Chapter 4 deals with the calculation of sensitivities of the valve voltage with respect to damping circuit resistance and capacitance using adjoint network approach. The effect of damping circuit parameters on the sensitivities has also been studied.

An exact method of calculating the damping circuit loss is presented in Chapter 5, using the equivalent circuit representation of the converter system during different intervals of conduction. The results are compared with the results obtained using an approximate second order system model for valve voltage oscillations and with the results obtained by the approximate formulas given by Ainsworth.

A method of evaluation of optimal damping circuit parameters is presented in Chapter 6, by minimizing an objective function which takes into account both recovery voltage transient and damping circuit loss.

Conclusions of this thesis are given in Chapter 7.

CHAPTER 2

CALCULATION OF TURN-ON OVERVOLTAGES

2.1 Introduction

A thyristor valve used for HVDC transmission systems must contain a large number of thyristors connected in series, because of the limited voltage capabilities of a single thyristor. Because of the unequal turn-on characteristics of the individual thyristors, the thyristors turn-on non-simultaneously due to which the thyristors are subjected to overvoltages during this transitional period. A computer program is developed to calculate the turn-on overvoltages in a HVDC valve having number of thyristors in series. The effect of critical system and valve parameters on turn-on over-voltages is studied by considering a numerical example. This study is useful for valve design and for optimization of system and valve parameters.

2.2 Equivalent Circuit for the Turn-On Process of a Thyristor Valve.

2.2.1 Equivalent Circuit of the Supply Network:

The thyristor valve converter system [1], is shown in Fig. 2.1. Each thyristor valve will operate as one leg of the three phase bridge circuit. Each valve is shunted by the damping circuit, which consists of a resistance (R_d) and a capacitance (C_d), and has in series a parallel combination

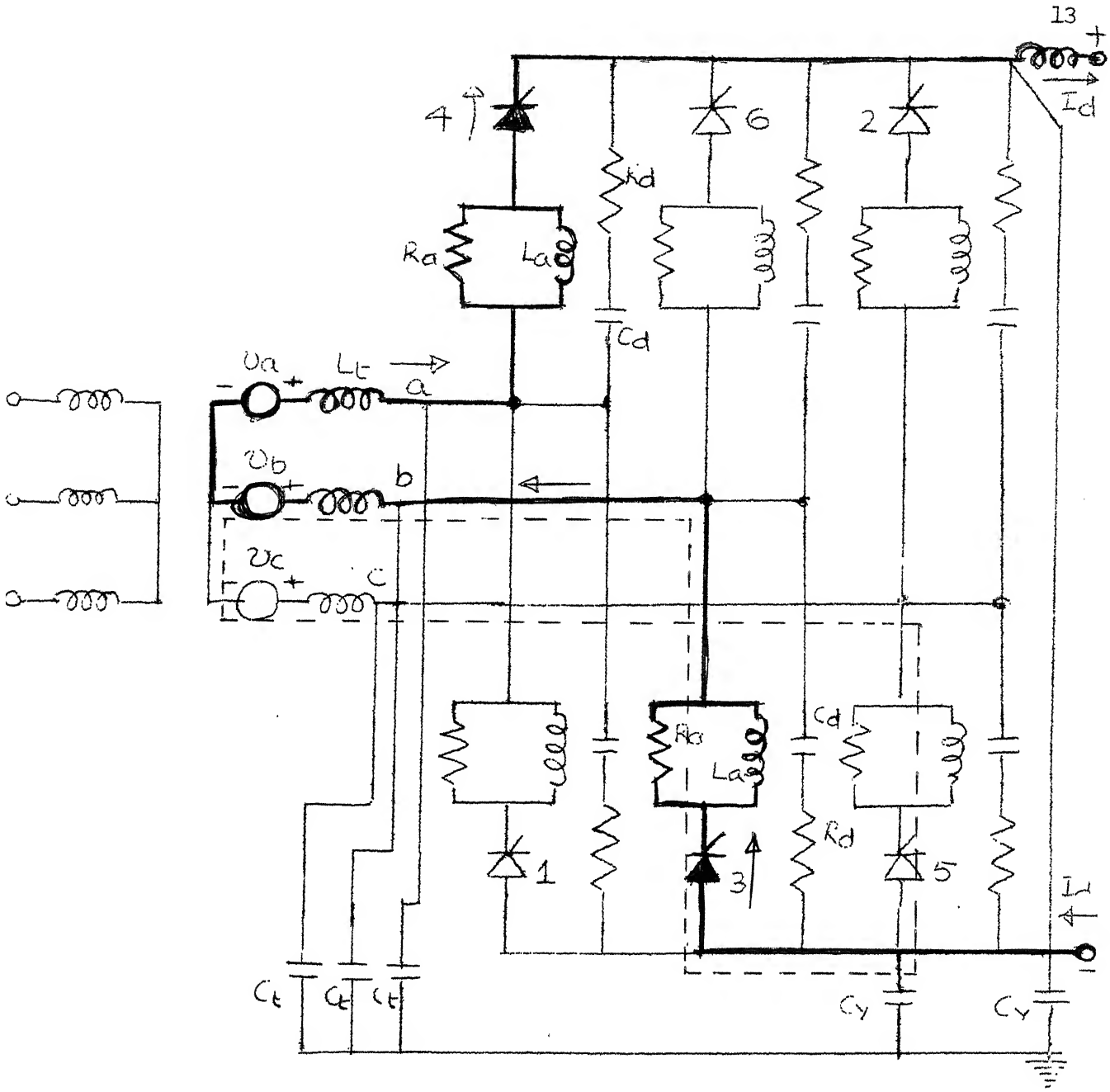

FIG 2.1 THREE PHASE BRIDGE CIRCUIT

of R_a-L_a, which is known as anode damper. The distributed transformer and switchyard capacitances are treated as lumped elements C_t and C_y, respectively.

During the normal operation of the three phase bridge, two and three valves conduct alternately. The current conduction through valves 3 and 4, is shown by the solid line in Fig.2.1. At the end of the conduction period of valves 3 and 4, valve 5 starts to conduct resulting in three valves (3, 4 and 5) conduction during the commutation period. The current transfer from valve 3 to valve 5 during commutation is shown by the dotted line in Fig. 2.1. During this commutation period, the voltage across valve 5 reduces to zero, and the current through valve 5 increases to I_d. The transient distribution of the collapsing forward voltage across the individual thyristors of valve 5 is studied in this chapter.

In practice, the turn-on period is a few microseconds which is small compared to the time constant of damping circuit. So there is no effective connection between phase a and phases b and c. Accordingly, valve 5 turn-on process is represented by the dotted path of Fig.2.1 with the associated stray capacitances. A further simplification is done, through a star-delta transformation of capacitances, and neglecting R_d-C_d circuits across valves 3 and 5 as their effect can be neglected compared to R_a-L_a circuits and valve stray capacitance (C_y). The stray capacitance across

the valve 5 is neglected. The simplified equivalent circuit of the supply network is shown in Fig.2.2. The two voltage sources v_b and v_c are combined to an equivalent voltage source V_o, which is expressed as $V_o = v_b - v_c$ where v_b and v_c are b and c phase voltages, using Thevenin's theorem. Since the peak voltage across the valve is of interest in calculating turn-on overvoltages, V_o is assumed to be at the maximum value corresponding to $\alpha = 90^o$, in this analysis. The delta equivalent capacitances C_{bc}, C_{yc} and C_{by} in terms of the star connected capacitances C_t and C_y are given as

$$C_{bc} = C_t^2/(2C_t + C_y)$$

$$C_{by} = C_{yc} = C_t C_y/(2C_t + C_y) \qquad (2.1)$$

The capacitance C_{by} which comes across valve 3 is neglected.

2.2.2 Equivalent Circuit of a Thyristor Valve:

A thyristor valve having N number of series connected thyristors, with a voltage grading circuit consisting of R_g and C_g across each thyristor is shown in Fig.2.3. Prior to the turn-on of each thyristor, a positive voltage is developed across each thyristor. Accordingly, during turn-on process, each thyristor can be represented as a voltage source, which starts decreasing as the gate signal is applied. The voltage across a thyristor does not start to collapse until a finite time after the gate pulse is applied, because of the finite speed of charge carriers, and takes some further finite time

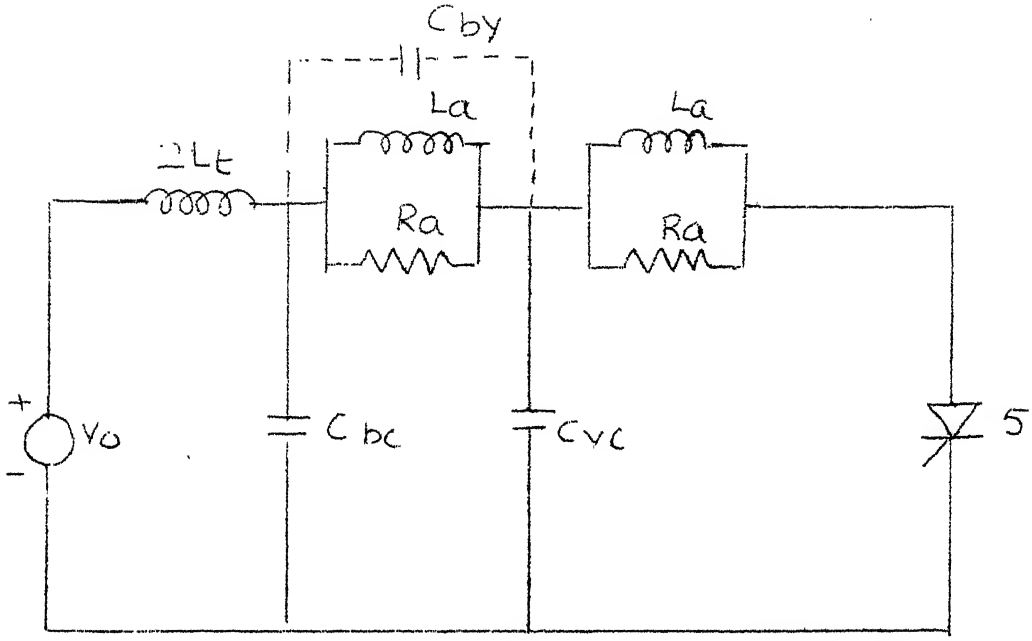

FIG 2.2 SIMPLIFIED EQUIVALENT CIRCUIT OF THE SUPPLY NETWORK

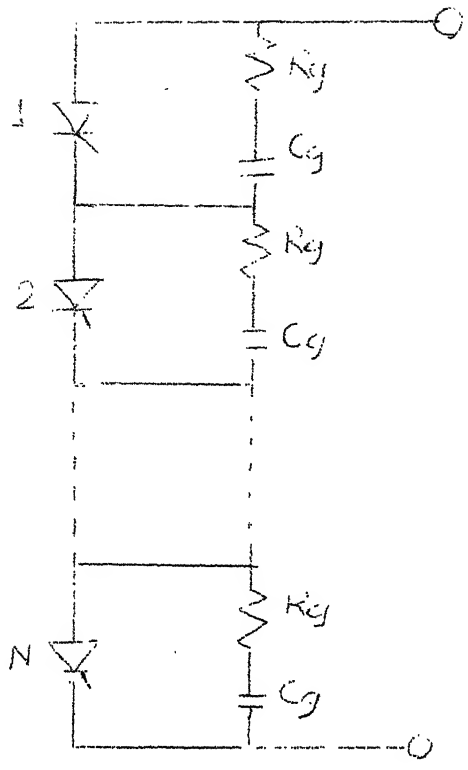

FIG 2.3 THYRISTOR VALVE WITH N NUMBER OF THYRISTORS CONNECTED IN SERIES

to collapse to the conduction value. Accordingly, turn-on time (t_{on}) is the sum of delay time (t_d) and rise time (t_r) which is shown in Fig.2.4.

The parameters t_d and t_r for a given type of thyristor, under specific test conditions and for a given gate current waveform can be obtained from the specifications given by the thyristor manufacturers. In this analysis, the thyristor is represented by a switch closing at the instant t_d, in series with a voltage source given by

$$v(t) = v_o \, e^{-\delta(t-t_d)} \qquad (2.2)$$

where

$$\delta = \left| \frac{\ln 9}{t_r} \right| \qquad (2.3)$$

For a given type of thyristor, there will be a range of values of delay time because of manufacturing tolerances. Therefore, a statistical distribution is considered for the delay times. A cumulative delay time distribution curve, based on the measurements of a sample taken from a particular thyristor type, is shown in Fig. 2.5 [1].

Using the curve shown in Fig.2.5, we can obtain the number of thyristors in the on condition as a function of time after the gate pulse is applied. The curve is approximated as a finite number of steps, where each step represents a group of thyristors and the time at which that group turns-on.

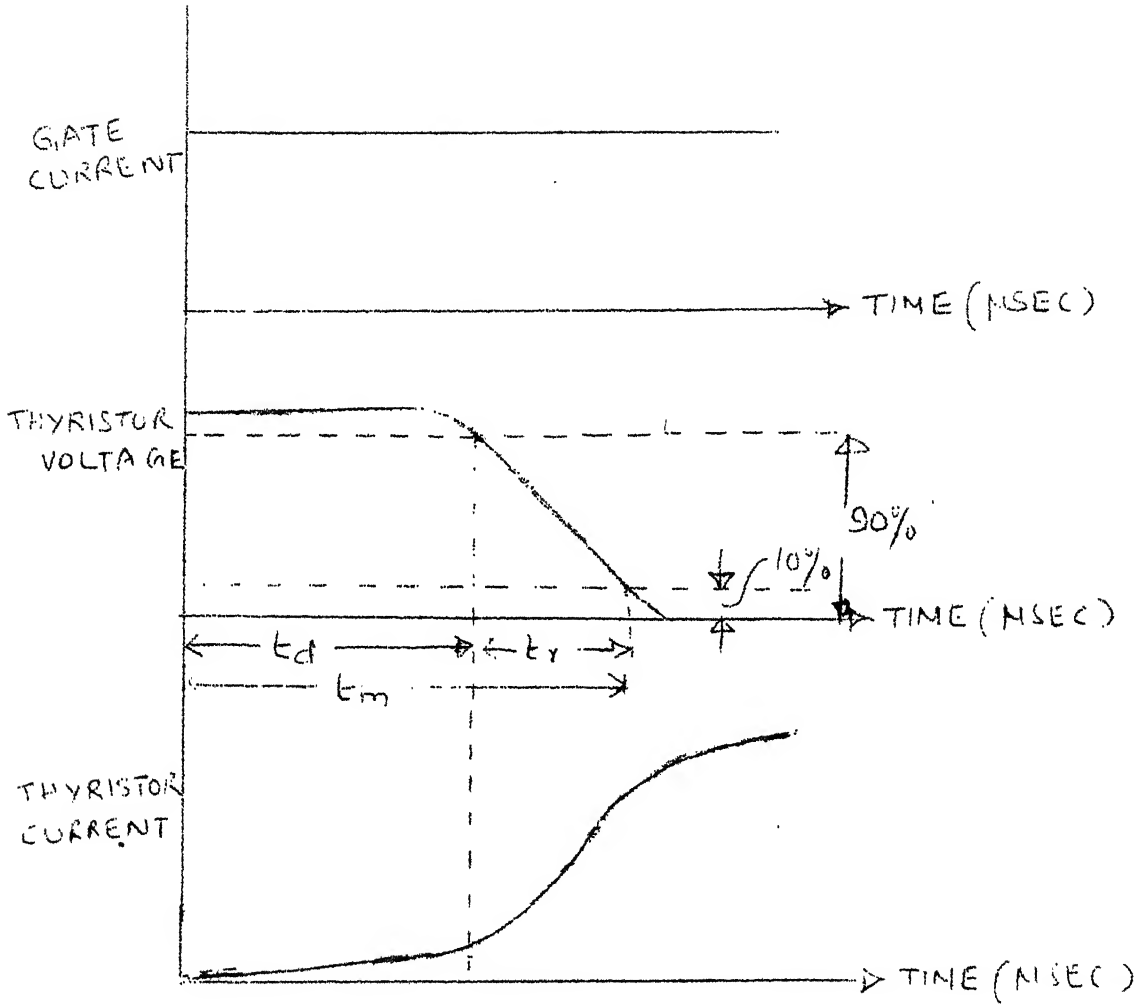

FIG 2.4 THYRISTOR TURN ON VOLTAGE AND CURRENT

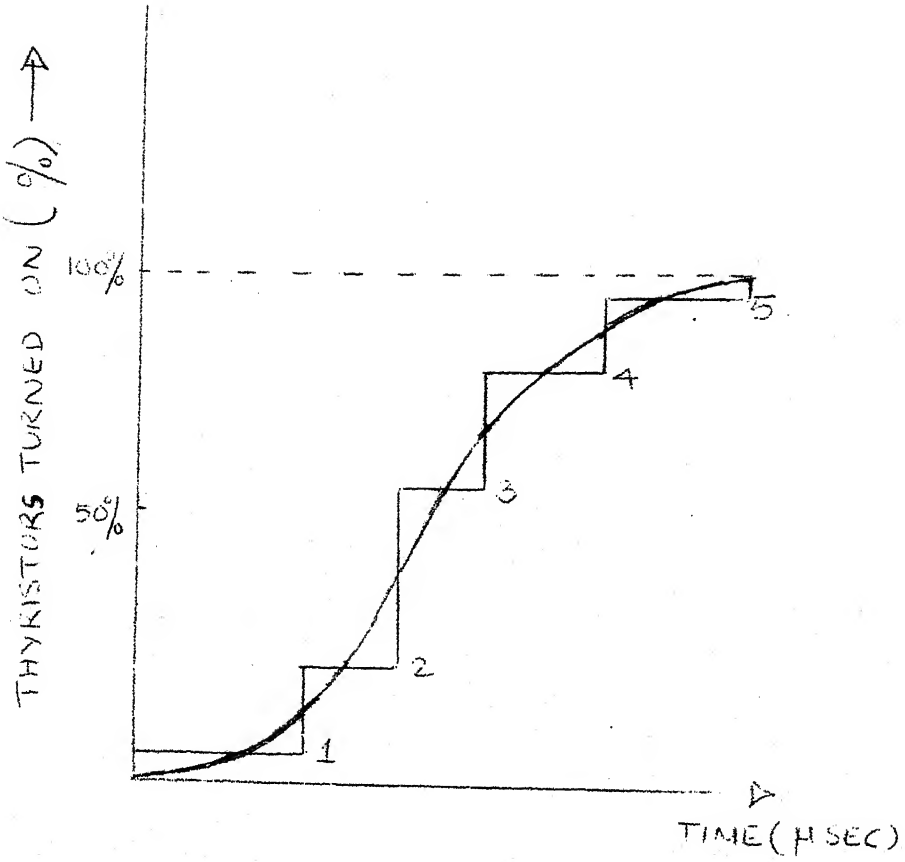

FIG 2·5 THYRISTOR DELAY TIME DISTRIBUTION

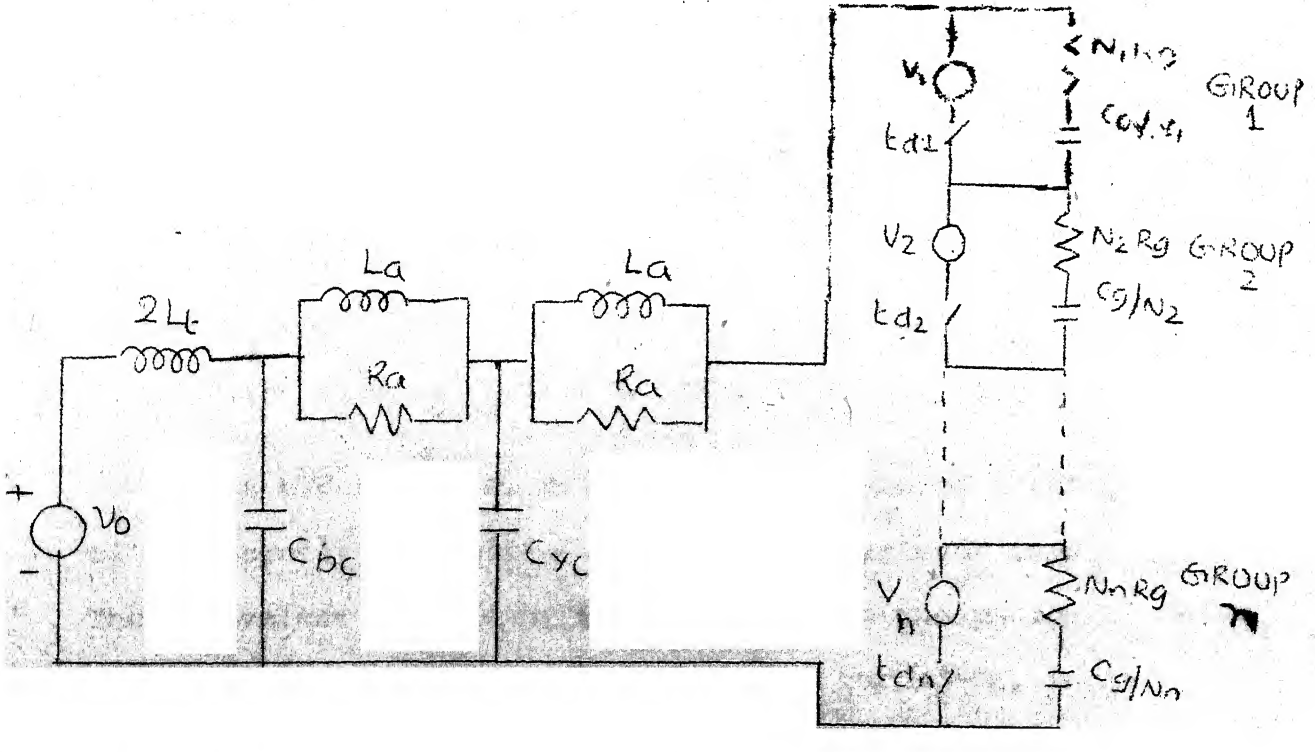

FIG 2·6 EQUIVALENT CIRCUIT FOR CALCULATION OF TURN-ON OVERVOLTAGES

For a given thyristor type, the rise times between individual thyristors also vary, which cause second order effect on turn-on overvoltages. A representative value of t_r can be chosen to calculate the value of δ which is used in Eq. (2.3). For a number of high power thyristors, δ ranges from $2.0 - 3.5 \times 10^6$ sec^{-1} [1].

2.2.3 Combined Equivalent Circuit:

The complete equivalent circuit for the supply system and thyristor valve is shown in Fig. 2.6.

2.2.4 Simplification of the Equivalent Circuit:

The equivalent circuit shown in Fig.2.6 is simplified for computer calculation and is shown in Fig.2.7. During the turn-on process the valve is represented by a time varying voltage source in series with a time varying R_g and C_g.

The total number of thyristors (N) are divided into n groups. The ith group with N_i thyristors is represented by a switch which closes at t_{di}, in series with a voltage source $V_i(t) = N_i . v_i(t)$. Using the switching function of Fig.2.5, the time t_{di} for each group of thyristors is obtained.

At $t < t_{d1}$, i.e. prior to the turn-on of first group of thyristors, the voltage across each thyristor is $v_o = V_o/N$. The equivalent circuit of the valve during the period $t_{d1} < t < t_{d2}$ is shown in Fig.2.8(a). Group 1 having turned-on, it is represented by a voltage source

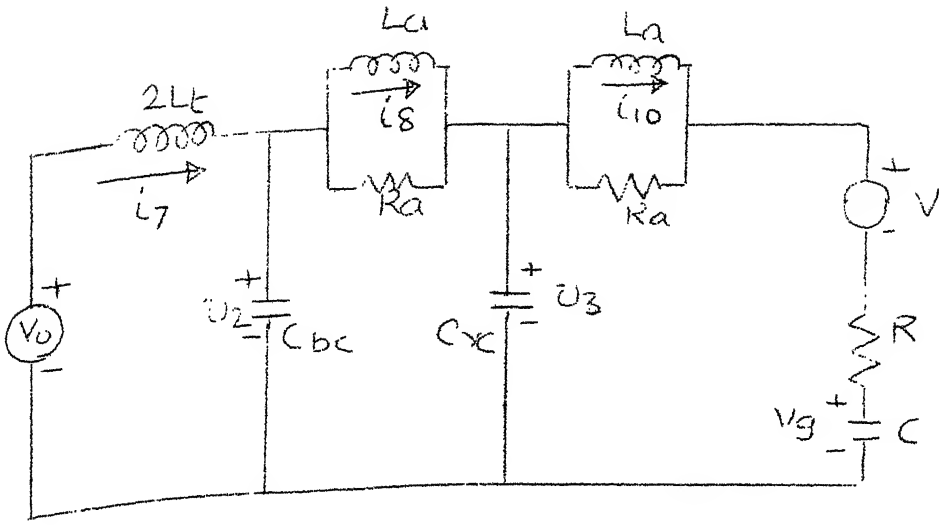

FIG 2.7 SIMPLIFIED EQUIVALENT CIRCUIT FOR COMPUTER CALCULATION

$$V_1(t - t_{d1}) = N_1 v_{o1} e^{-\delta(t-t_{d1})} \qquad (2.4)$$

where $v_{o1} = v_o$. The remainder of the valve is represented by $(N-N_1)R_g$ in series with $C_g/(N-N_1)$ with an initial voltage of $V_{g1}(t_{d1})$ where

$$V_{g1}(t_{d1}) = (N - N_1) v_o \qquad (2.5)$$

At $t = t_{d2}$, group 2 turns-on and the equivalent circuit of the valve is shown in Fig. 2.8(b). Group 2 is represented by the voltage source

$$V_2(t-t_{d2}) = N_2 v_{o2} e^{-\delta(t-t_{d2})} \qquad (2.6)$$

where v_{o2} is the voltage across a non-conducting thyristor which is given by

$$v_{o2} = [I_1(t_{d2}) R_g (N-N_1) + V_{g1}(t_{d2})]/(N-N_1) \qquad (2.7)$$

The remainder of the valve is represented by $(N-\overline{N_1+N_2})R_g$ in series with a capacitor $C_g/(N-\overline{N_1+N_2})$ with an initial voltage of $V_{g2}(t_{d2})$ where

$$V_{g2}(t_{d2}) = v_{o2} (N - \overline{N_1+N_2}) \qquad (2.8)$$

The above process continues through the switching of successive groups at t_{d3}, t_{d4}, ..., $t_{d(n-1)}$. During the period $t_{d(n-1)} < t < t_{dn}$ the equivalent circuit of the valve is shown in Fig. 2.8(c). The voltage applied across last group of thyristors at $t = t_{dn}$ is obtained from this circuit. As a measure to the overvoltage across each thyristor an

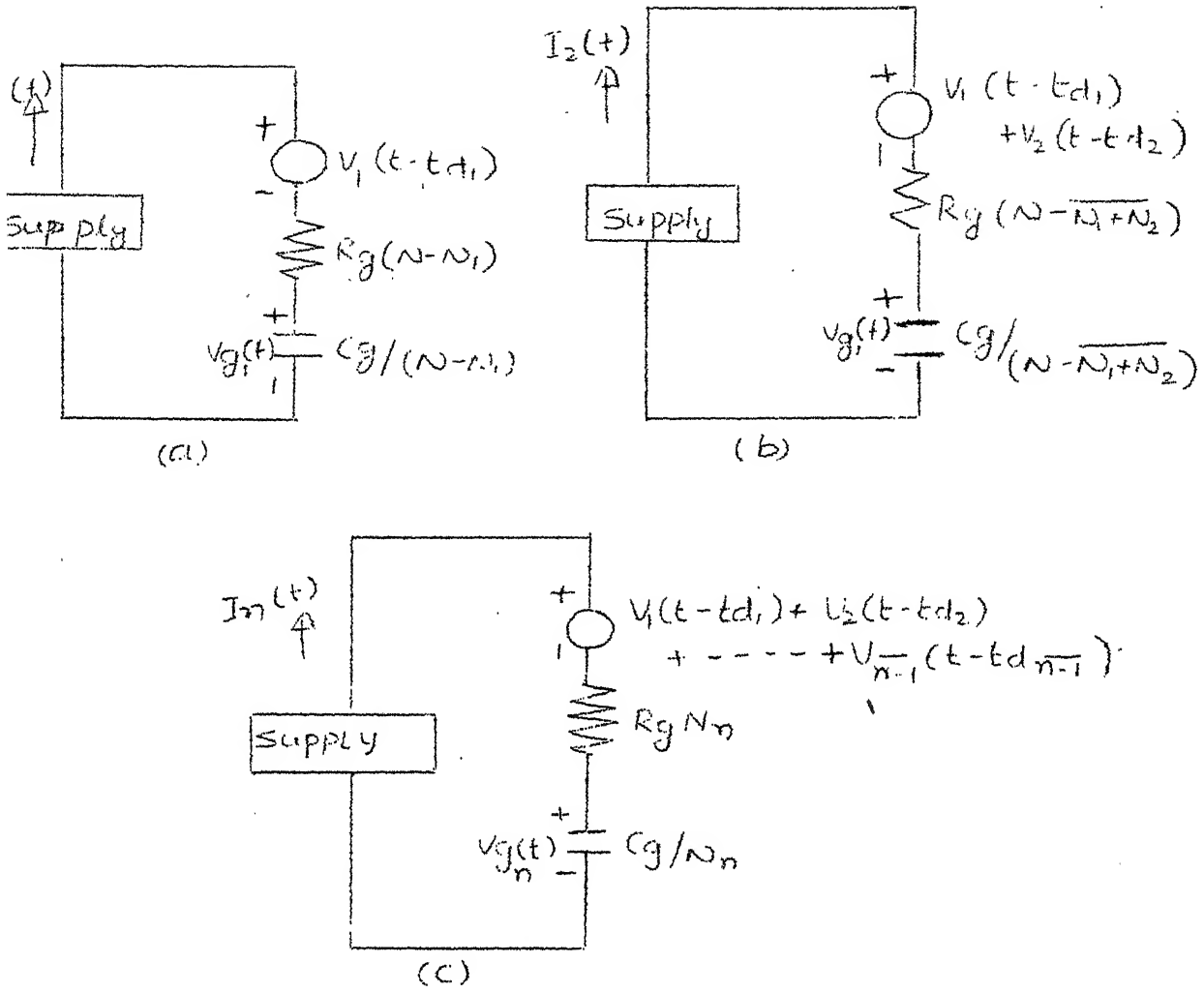

fig 2.8 VARIATION OF THE VALVE EQUIVALENT CIRCUIT DURING TURN ON

(a) AFTER TURN ON OF GROUP 1

(b) AFTER TURN ON OF GROUP 2

(c) AFTER TURN ON OF GROUP (n-1)

overvoltage factor F(t) is defined as

$$F(t) = v_i/v_o \qquad (2.9)$$

where v_i is the voltage across each thyristor in ith group given as

$$v_i = [I_i(t)\, R_g(N - \overline{N_1+\ldots+N_{i-1}}) + V_{gi}(t)]/(N - \overline{N_1+N_2+\ldots+N_{i-1}}) \qquad (2.10)$$

v_o is the initial voltage across each thyristor prior to the turn-on of first group and the time t is in the period $t_{\overline{di-1}} < t < t_{di}$.

2.3 Calculation of Turn-On Overvoltages

2.3.1 System State Equations:

The state equations are derived for Fig.2.7 using the algorithm given in Appendix A. The final state variable equations are given by Eq. (A.13) of Appendix A.

2.3.2 Computer Program:

The state equations are solved numerically by using Runge-Kutta fourth order method. The flow chart of the computer program is shown in Fig. 2.9.

2.4 An Example

2.4.1 Description of the Problem:

A valve which contains 200 thyristors and which operates at a peak repetitive voltage of 200 KV is considered

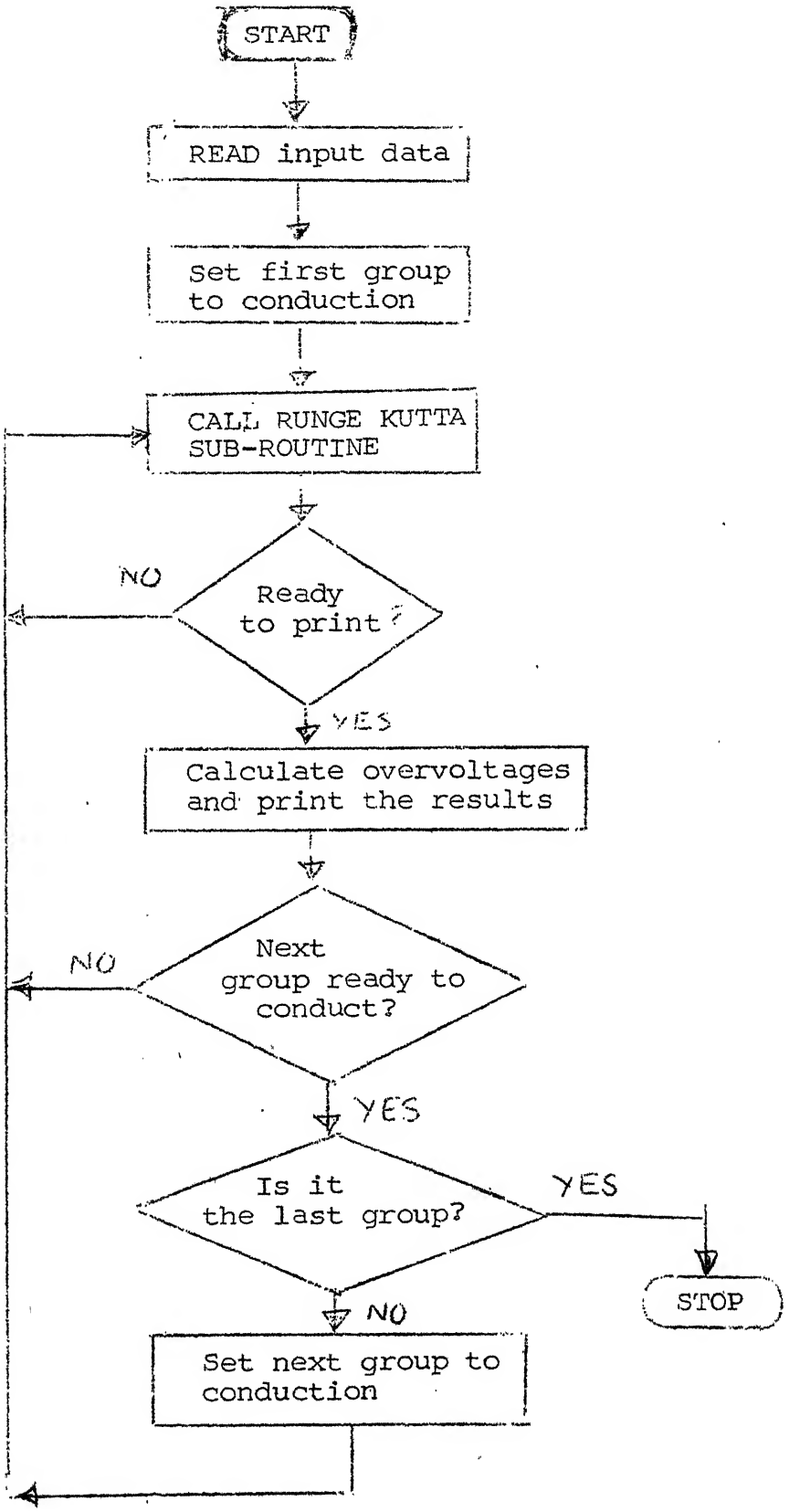

Fig. 2.9: Flow chart of the computer program.

to show the effect of certain critical parameters on turn-on overvoltages with the following supply system and valve parameters. This example is taken from ref.[1].

Supply system:

V_o = 200 KV

$2L_t$ = 0.15 H

C_{bc} = 2.0 nF ; C_{yc} = 2.0 to 20.0 nF

L_a = 1 mH

R_a = 4 M-ohm.

Valve: R_g = 1 to 100 ohms

C_g = 0.1 to 10 micro F.

δ = 2.0×10^6 sec^{-1}

Number of thyristor groups considered in a valve = 14.

The number of thyristors in each group and their switching times are shown in Table 2.1.

The step length used in Runge-Kutta subroutine is 0.01 microseconds, and the initial state variable vector is as follows.

$v_2(o)$ = 200,000 volts

$v_3(o)$ = 200,000 volts

$V_g(o)$ = 200,000 volts

$i_7(o)$ = 0

$i_8(o)$ = 0

$i_{10}(o)$ = 0

TABLE 2.1: Number of Thyristors in each Group and Their Switching Times.

Group	Number of thyristors in each group	Switching time for each group (microseconds)
1	3	0.2
2	4	0.4
3	7	0.6
4	16	0.8
5	30	1.0
6	32	1.2
7	31	1.4
8	27	1.6
9	16	1.8
10	14	2.0
11	7	2.2
12	6	2.4
13	4	2.6
14	3	2.75

2.4.2 Results:

The computed valve voltage and valve current waveforms during turn-on process are shown in Fig. 2.10. The valve voltage is reduced from 200 KV to zero, and the valve current has increased from zero to 291 Amps. during the turn-on process of the valve.

The effect of valve parameters R_g and C_g on turn-on overvoltages:

The variation of overvoltage factor with time for different R_g is shown in Fig. 2.11. For a particular R_g and C_g the overvoltage factor increases with time, as the voltage across a late firing thyristor is the sum of the resistive and capacitive components. Fig. 2.11 shows that reducing the value of R_g can reduce the overvoltage factor significantly. For a value of R_g = 1 ohm, the overvoltage factor is much less compared to the higher values of R_g. But the value of R_g as low as 1 ohm is impractical, as this would result in excessive values of di/dt during turn-on, and insufficient damping during transients [1]. Hence a practical minimum value is taken as of the order of 5 - 10 ohms.

The variation of overvoltage factor with time for different C_g is shown in Fig. 2.12. The effect of increasing the value of C_g is not significant at lower times, since the capacitance voltage is proportional to the time integral of

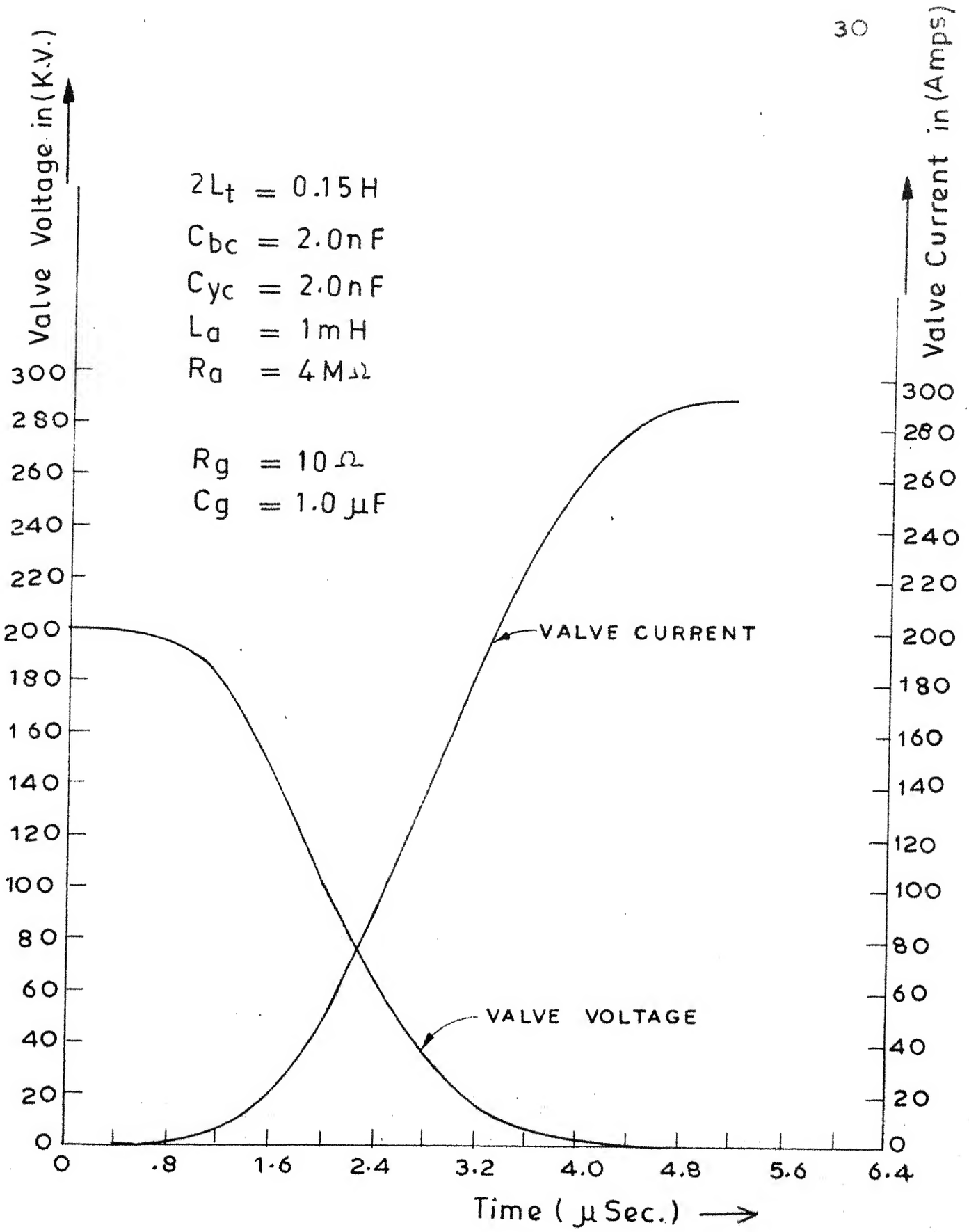

FIG.2.10 Computed valve voltage and Current waveforms during turn-on process.

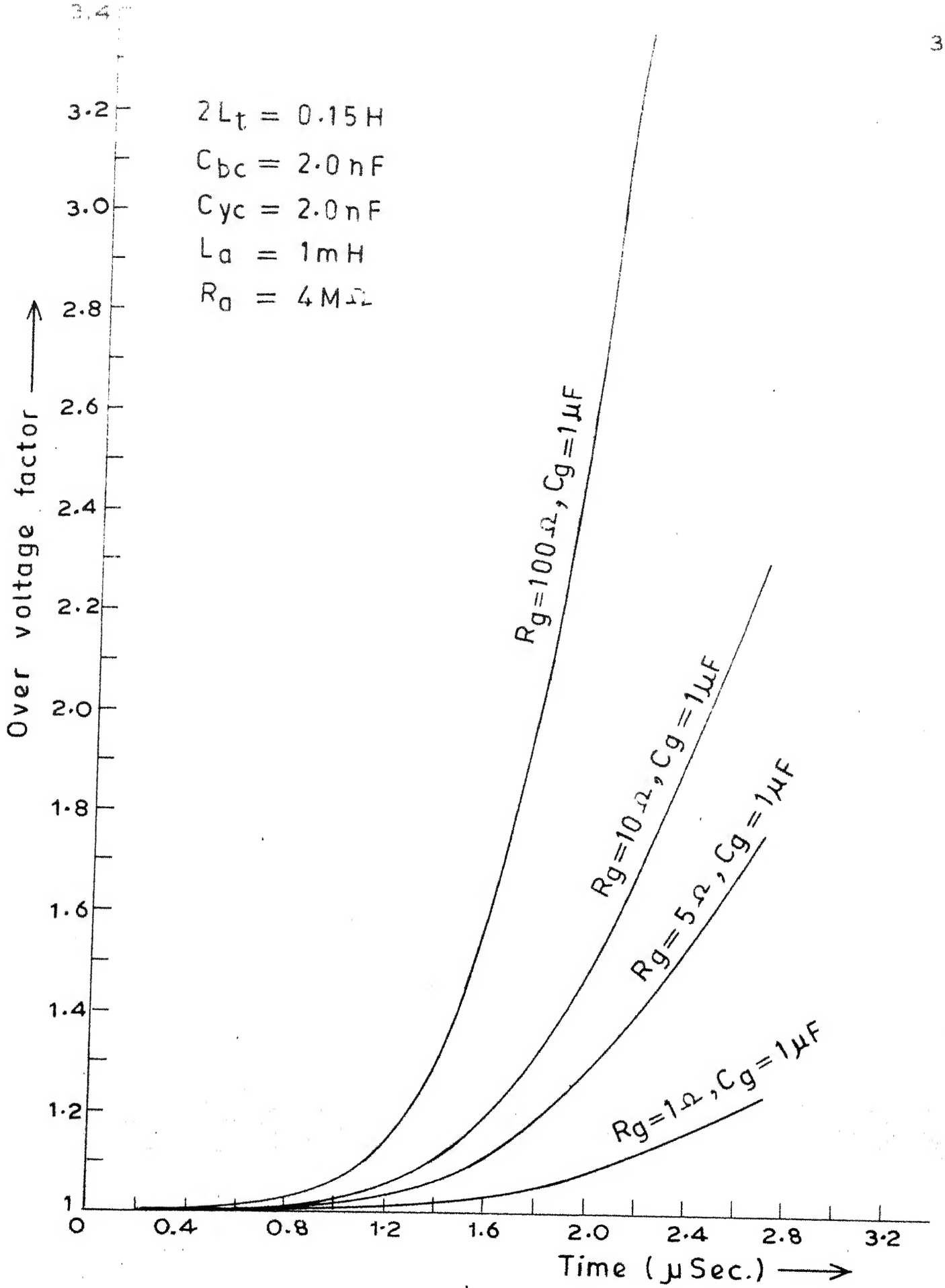

FIG.2.11 The effect of the Resistance of the Voltage grading circuit (Rg)

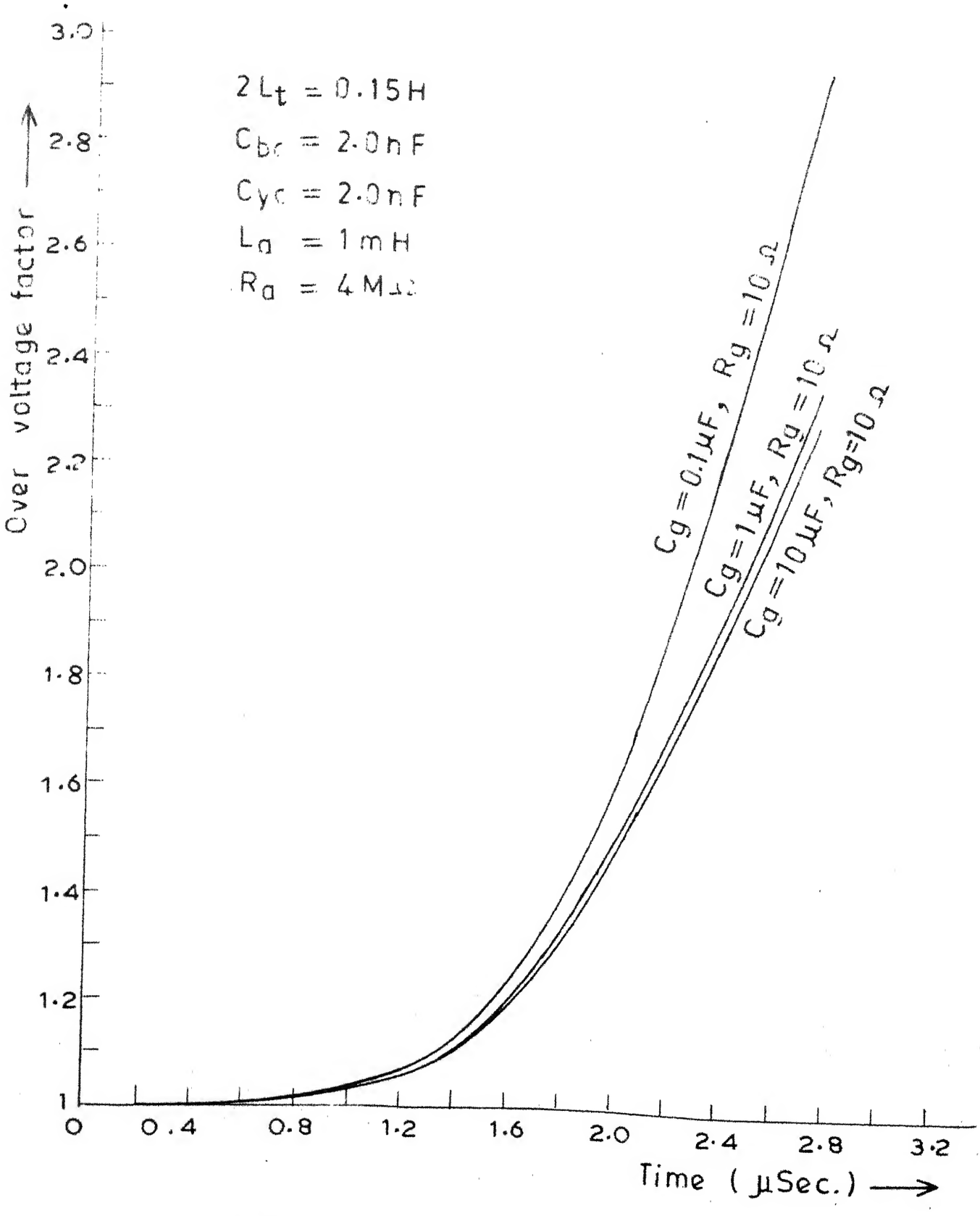

FIG. 2.12 The effect of grading circuit Capacitance (Cg)

the current. For a value of R_g = 10 ohms, increasing C_g beyond about 1.0 micro farad is not useful, since the dominant component of voltage is due to resistance. Increase in C_g beyond a certain value is not advisable, since the grading circuit losses increase with increase in C_g [1].

The effect of switchyard capacitance:

The variation of overvoltage factor with time for two different values of C_{yc} is shown in Fig. 2.13. Decreasing C_{yc} from 20 nF to 2 nF reduces overvoltage factor and also the reduction in overvoltage factor increases with time.

The effect of number of thyristors (N):

The variation of overvoltage for different N is shown in Fig. 2.14. The overvoltage factor is reducing with decreasing N. This is an important observation which can be followed in building a valve with the highest voltage thyristors available.

2.4.3 Discussion:

In ref. [1], for the transient solution, an IBM-modified ECAP (Electronic Circuit Analysis Program) program is used as a subroutine. A data preparation program written in FORTRAN and a monitor program to link this with ECAP program are also used. A complete solution for a valve containing 200 thyristors divided into 16 groups took 276 seconds c.p.u. time on an IBM 360-50 computer [1].

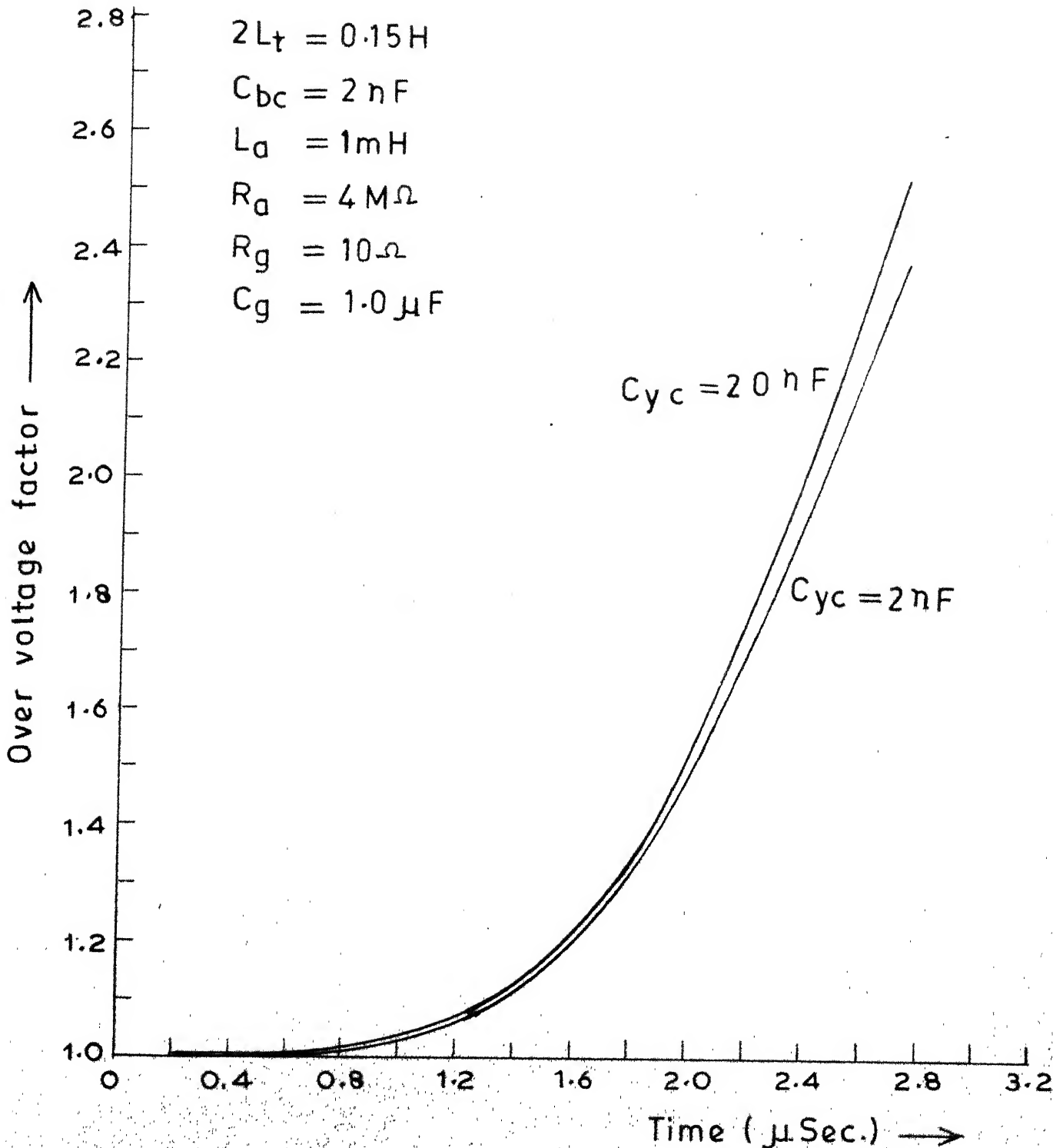

FIG.2.13 The effect of switch yard Capacitance (C_{yc})

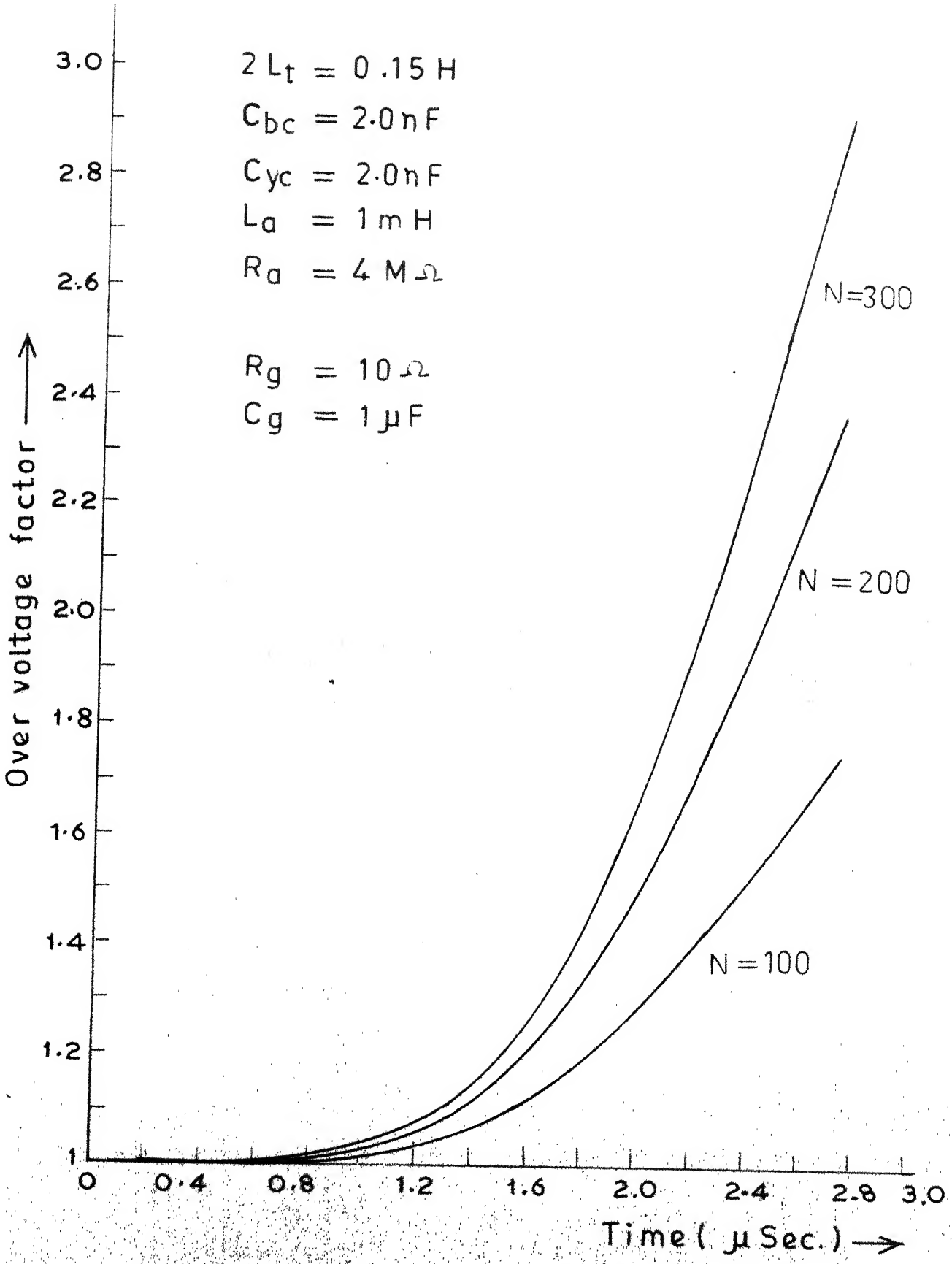

FIG. 2.14 The effect of number of thyristors (N)

In this analysis, the system is represented by a set of state variable equations and are solved numerically. A complete solution for a valve containing 200 thyristors divided into 14 groups took 0.66 seconds c.p.u. time on DEC-1090 computer.

The results obtained in this analysis agree with the results of ref.[1] qualitatively, but slightly differ quantitatively. This difference is expected to be due to difference in the value of δ and number of groups considered in the two analyses.

2.5 Conclusions

A general computer program to calculate the turn-on overvoltages in a HVDC thyristor valve has been developed, which simulates the turn-on process with the scatter in delay times of the series connected thyristors of the valve. The effect of varying the valve parameters R_g and C_g for a representative valve has been demonstrated. Minimizing the resistance of the voltage grading circuit decreases thyristor overvoltages. Increasing the value of capacitance has the same effect, but the incremental improvement is small for practical values of resistance.

The valve current during turn-on period is supplied mostly from stray capacitances, the transformer current being small. For the times of the order of 1-3 microseconds, the switchyard capacitance will act as a principal current

source. The current supplied by the switchyard and transformer capacitances is limited by the parallel connected anode resistance and inductance, the latter being more effective.

Thyristors of the highest available voltage rating should be used, to reduce turn-on overvoltages.

CHAPTER 3

CALCULATION OF TURN-OFF OVERVOLTAGES

3.1 Introduction

A thyristor valve used for HVDC systems must contain a large number of thyristors connected in series, because of the limited voltage capability of a single thyristor. Because of the difference in turn-off characteristics of the individual thyristors, the thyristors turn-off non-simultaneously, because of which they are subjected to overvoltages during this transitional period. Also, the valve is subjected to recovery overvoltages, which occur during and after the turn-off period. A computer program is developed to calculate the turn-off overvoltages which consist of both recovery overvoltages and overvoltages caused due to non-simultaneous turn-off of thyristors in a HVDC valve. The effects of critical system and valve parameters on turn-off overvoltages are studied by taking a representative thyristor valve. This study is useful for valve design and for optimization of system and valve parameters. A method of calculating the recovery overvoltage neglecting turn-off process has also been presented.

3.2 Equivalent Circuit for the Turn-Off Process of a Valve:

3.2.1 Equivalent Circuit of the Supply System:

The thyristor valve convertor system is shown in Fig.3.1 [3]. Each valve is shunted by the damping circuit R_d-C_d, and

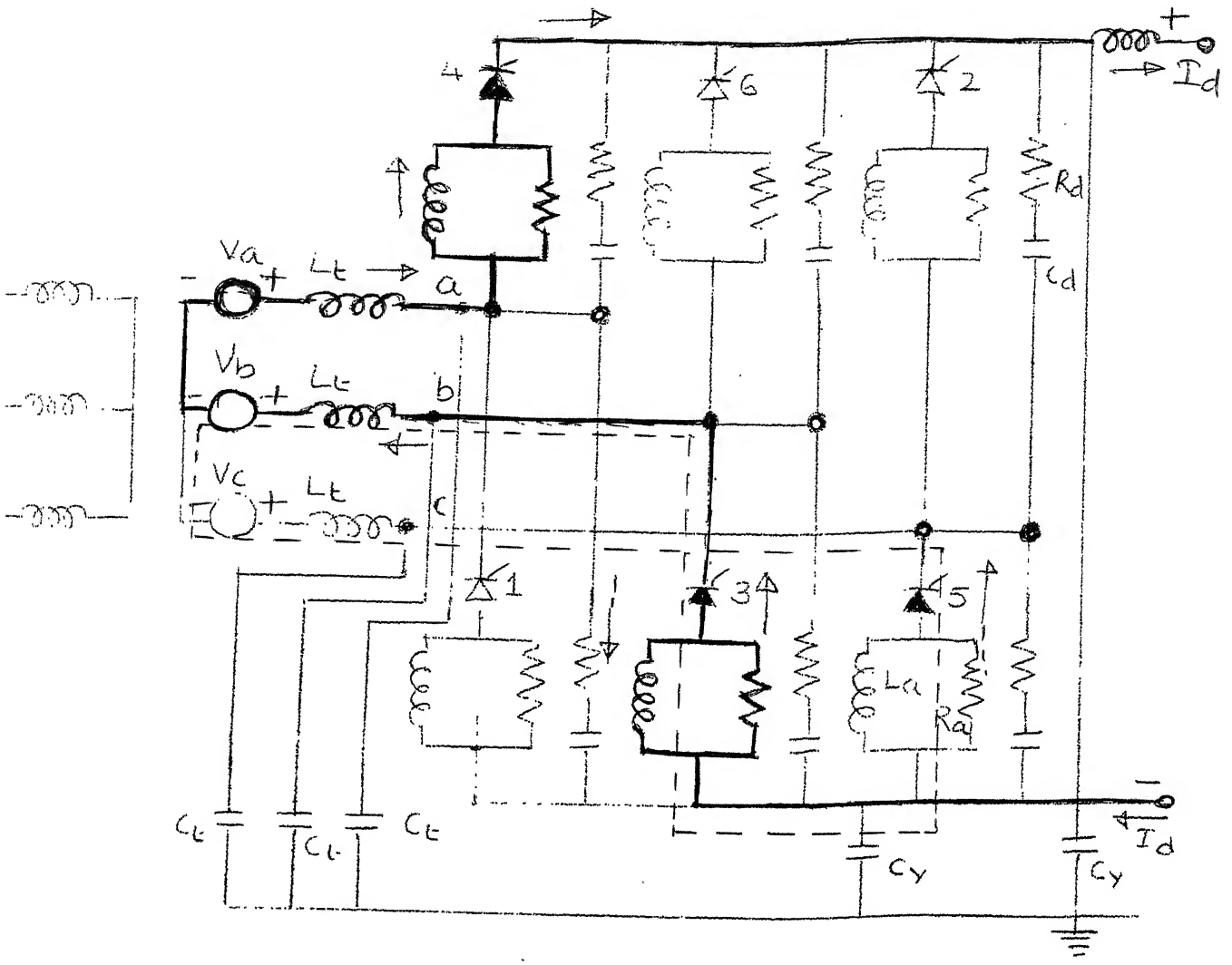

FIG 3.1 THREE PHASE BRIDGE CIRCUIT

has in series a parallel combination of R_a-L_a, which is known as anode damper. The distributed transformer and switchyard capacitances are represented by the lumped parameters C_t and C_y, respectively.

During the normal operation of the three phase bridge circuit, two and three valves conduct alternately. The current conduction through valves 3 and 4 is shown by the solid line in Fig.3.1. As the valve 5 turns on, the current through valve 3 decreases to zero, while the current through valve 5 increases to I_d as shown in Fig.3.2(a). During this commutation period, the voltage across valve 5 decreases to zero in a few microseconds, while a reverse voltage is developed across the valve 3 as shown in Fig.3.2(b). The turn-off of valve 3 is considered as a representative case to calculate the turn-off overvoltages.

Even after the current through valve 3 goes to zero, valve 3 continues to conduct in the reverse direction, because of the presence of storage charge represented by unneutralised carriers in the thyristors of valve 3. The reverse current of peak value I_o, which also flows as a forward current through valve 5 superimposed on I_d is shown by the dotted line in Fig.3.1. The time during which reverse current flows is some tens of microseconds and is enlarged for clarity in Fig.3.2.

As the values of storage charge for individual thyristors differ, the thyristors of valve 3 turn-off sequentially, thus

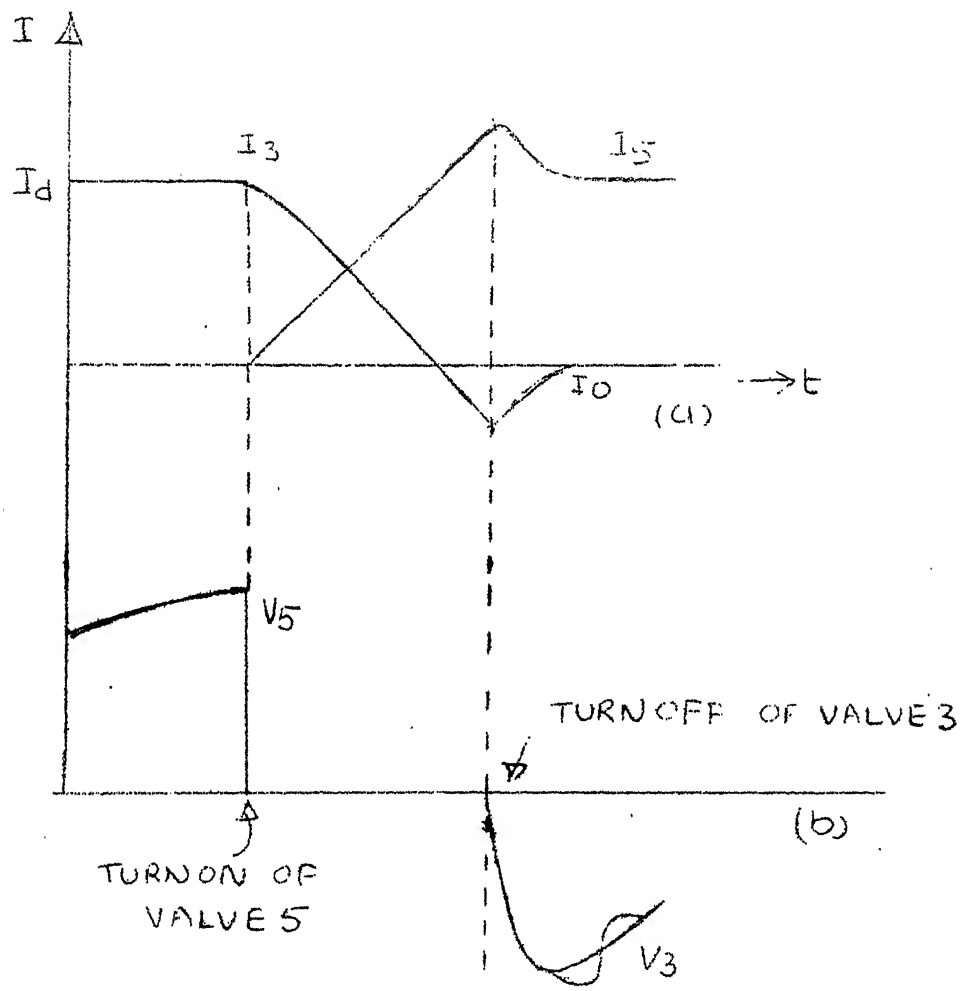

FIG 3.2 VALVE TURN OFF WAVEFORMS

a) CURRENT

b) VOLTAGE

increasing the impedance of the outgoing valve at a finite rate. The voltage across valve 3 continues to increase till all thyristors are turned-off. The transient voltage across valve 3 will oscillate initially as shown in Fig.3.2(b), and will finally approach the steady state line voltage V_{cb}.

A valve consists of a number of series connected thyristors with a voltage grading network R_g-C_g across each thyristor. The equivalent circuit of valve 3 turning-off is shown in Fig.3.3. It is developed from Fig.3.1, by representing each of the non-conducting valves (6, 2, and 1) by its damping circuit R_d-C_d in parallel with its grading network R_g-C_g, and the conducting valves, 5 and 4, by short circuits. The anode damper R_a-L_a is neglected for all the valves, except for valve 3. The capacitances C_{ab}, C_{bc}, and C_{ac} of Fig.3.3 are given by the following expressions obtained from star-delta capacitance transformations.

$$C_{ab} = C_{bc} = \frac{C_t(C_t + C_y)}{3C_t + 2C_y} \qquad (3.1)$$

$$C_{ac} = \frac{(C_t + C_y)^2}{3C_t + 2C_y} \qquad (3.2)$$

The maximum turn-off overvoltages occur when the voltage across the valve is maximum. This corresponds to the instant $\alpha + \mu = 90^\circ$, and when $v_a = 0$, $v_b = -E_L/\sqrt{2}$, and $v_c = +E_L/\sqrt{2}$. In Fig.3.3, the voltage V_o is assumed to be constant equal to

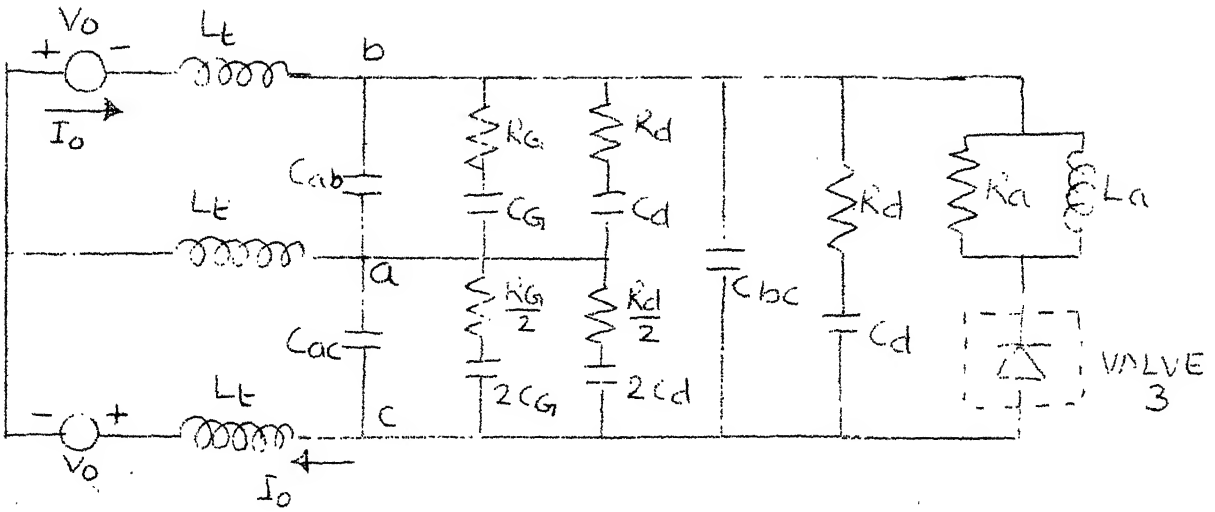

FIG 3.3 EQUIVALENT SUPPLY CIRCUIT FOR CALCULATION OF TURN OFF OVER VOLTAGE

$E_L/\sqrt{2}$, as the variation in phase voltages is small during the turn-off process. The initial rate of change of current is given by

$$\frac{di}{dt} = \frac{V_o}{L_t} \qquad (3.3)$$

3.2.2 Equivalent Circuit of a Thyristor Valve

Even after the current through a thyristor falls to zero, it will continue to conduct, because of unneutralised carriers present in it. The negative current-time integral of Fig.3.2(a) is shown in detail in Fig.3.4. It is assumed that the thyristor turns-off at the instant when the reverse current reaches its peak, and a reverse voltage is suddenly applied across it. Accordingly, the storage charge is taken as the shaded area of Fig.3.4; and each thyristor is represented as an ideal switch which is opened at the instant when the reverse current reaches its maximum value. It is important to note that the turn-off process considered in this analysis does not imply ability of the thyristor to support forward voltage.

Storage charge will depend upon forward current, rate of change of current through zero, and junction temperature[3]. For a given thyristor type, a range of values of storage charge will exist because of manufacturing tolerances. A cumulative charge distribution curve based on measurements on a sample quantity of a particular type of high power thyristor is shown in Fig.3.5 [3].

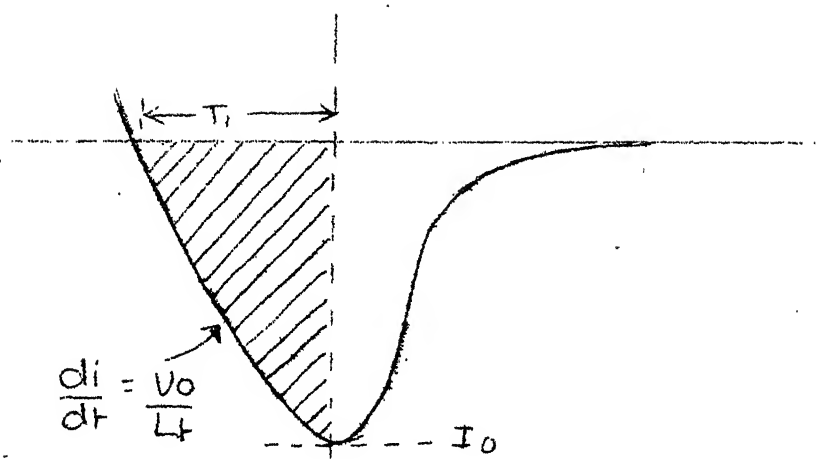

FIG 3.4 .

THYRISTOR REVERSE CURRENT SHOWING STORAGE CHARGE

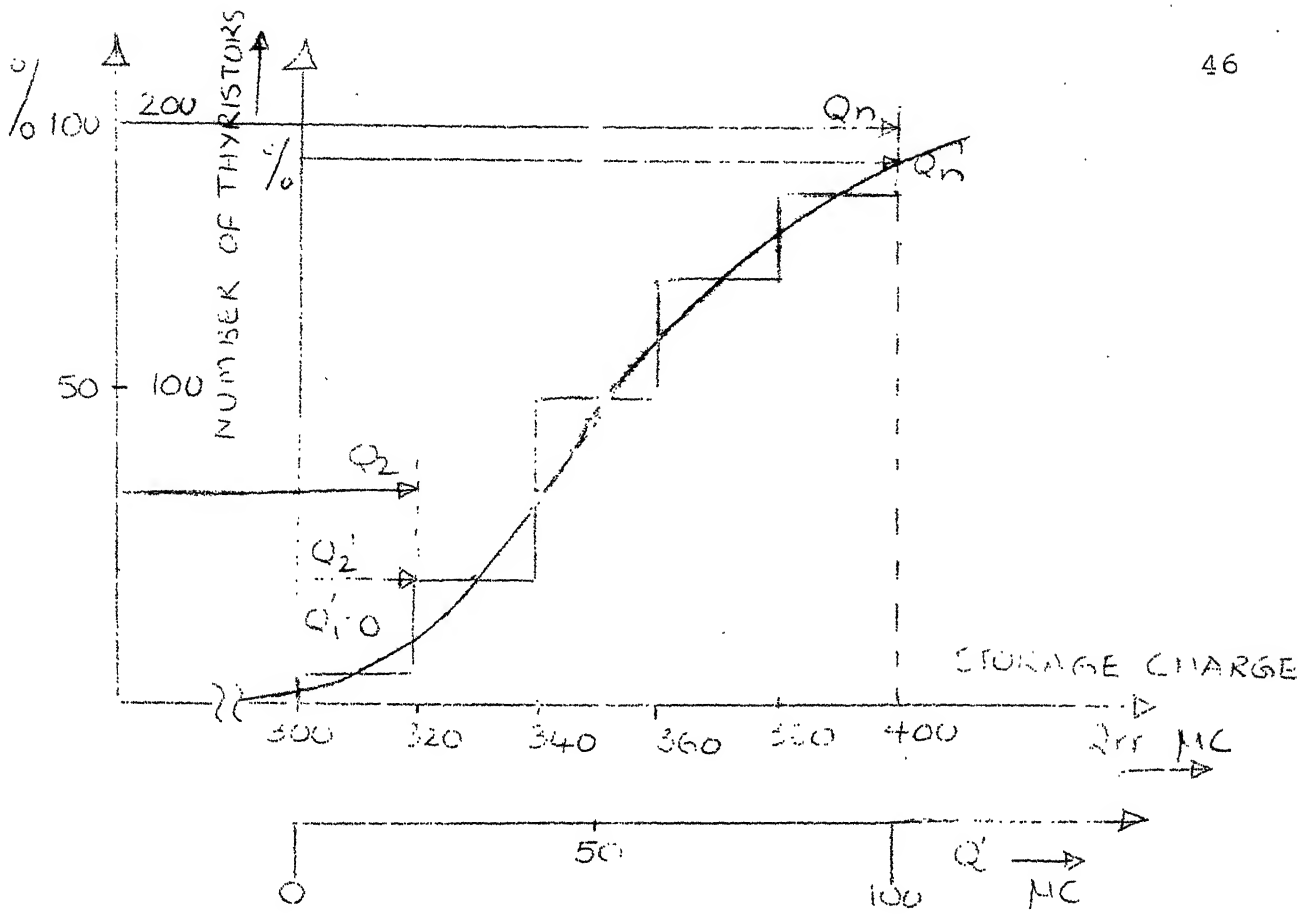

FIG 3·5 STORAGE CHARGE DISTRIBUTION CURVE

The cumulative charge distribution curve can be approximated by dividing the thyristors into a number of groups, with all the thyristors in a group having equal storage charge. In Fig.3.5, group 1 consists of 10 thyristors (5 percent of the total) with Q_{rr} = 300 micro C, while group 2 consists of 40 thyristors (20 percent of the total) with Q_{rr} = 320 micro C, etc.

For convenience, a second scale is introduced with origin as minimum value of Q_{rr}, Q_{min}. The increment in Q_{rr} with respect to group 1 is designated as Q', the values corresponding to the groups of thyristors are $Q'_1 = 0$, $Q'_2 = 20$ micro C, etc.

3.2.3 Combined Equivalent Circuit:

The combined equivalent circuit for the supply system and thyristor valve is shown in Fig.3.6. The valve is considered to be having N number of thyristors divided into n groups, each thyristor having in parallel a grading network R_g-C_g. In general, the ith group of N_i thyristors is represented by a switch S_i, having in parallel a resistance $N_i R_g$ in series with a capacitance C_g/N_i.

3.2.4 Simplification of the Equivalent Circuit:

The equivalent circuit shown in Fig.3.6 is simplified for computer calculation and is shown in Fig.3.7. During the turn-off process the valve is represented by a time varying resistance (R) and capacitance (C).

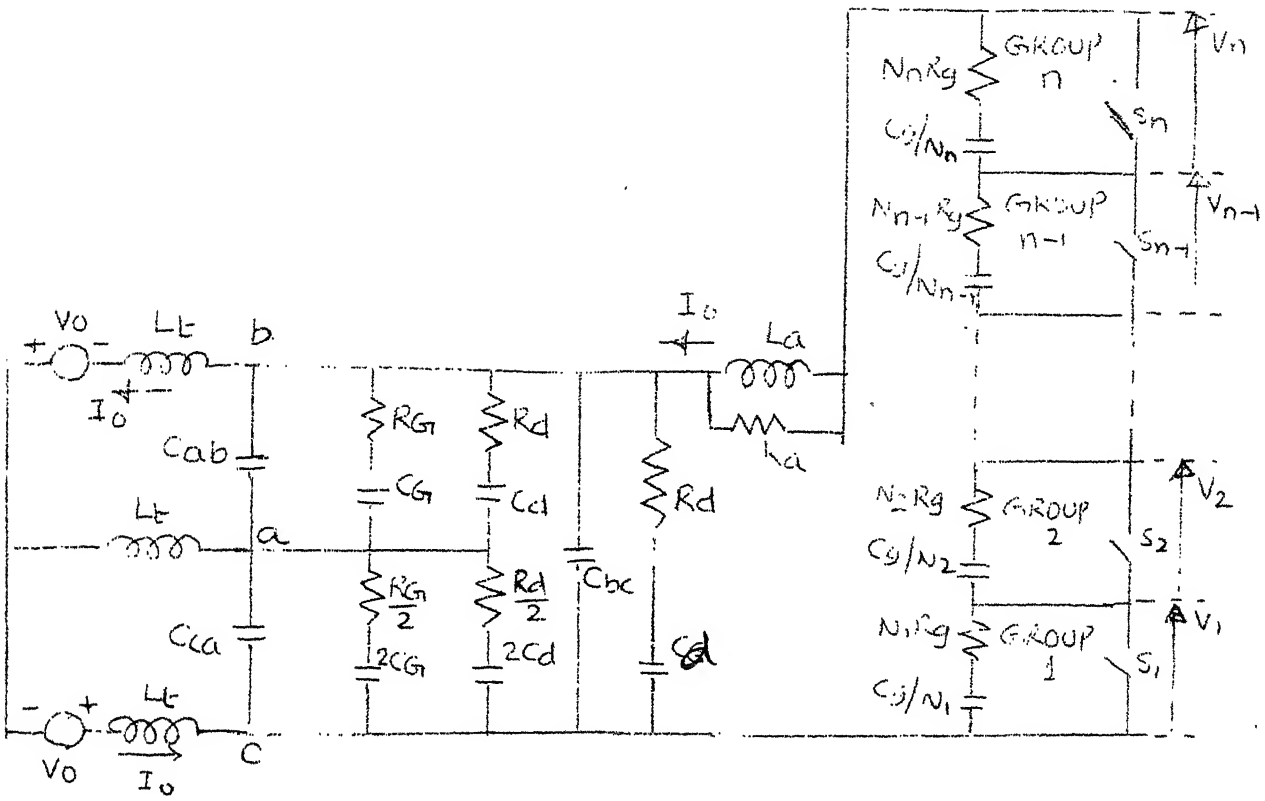

FIG 3.6 COMPLETE EQUIVALENT CIRCUIT FOR CALCULATION OF TURN OFF OVERVOLTAGES

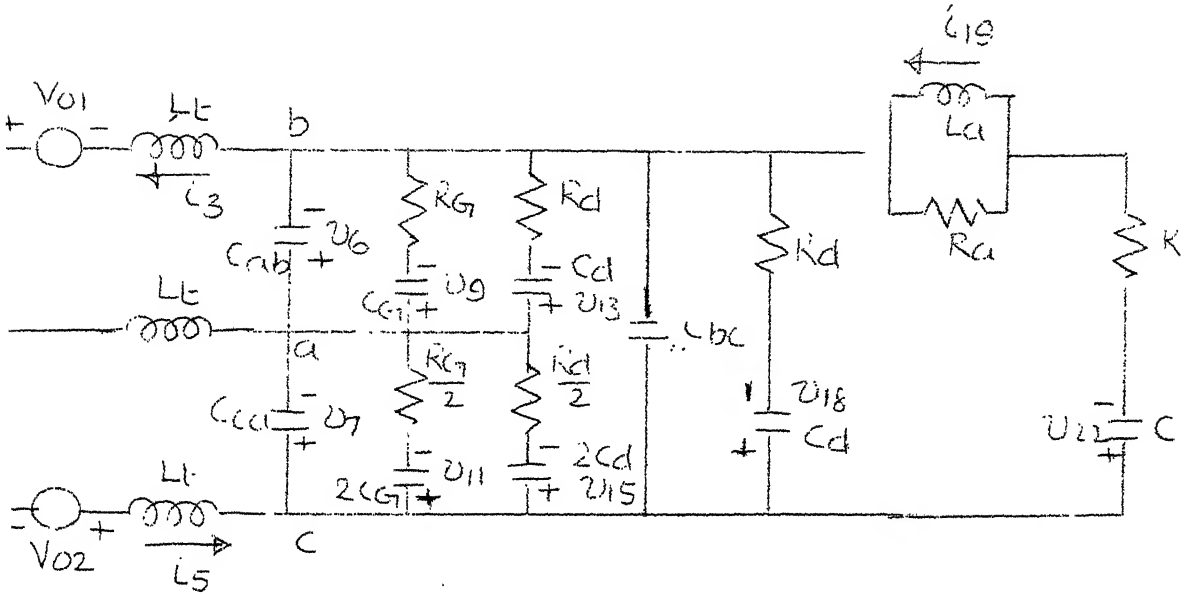

FIG 3.7 SIMPLIFIED EQUIVALENT CIRCUIT FOR COMPUTER CALCULATION

3.3 Calculation of Turn-Off Overvoltages

Fig.3.4 is considered as the reverse current characteristic of the thyristors of group 1. The storage charge of thyristors of group 1 is neutralised at time $t = T_1$, and the thyristors of this group turn-off which is simulated by opening the switch S_1 of Fig.3.6. At this instant the current I_o flows through the voltage grading network of group 1.

The initial conditions for turning-off of group 1 are calculated, using the rate of change of current of Eq.(3.3), as follows,

$$I_o = \frac{V_o}{L_t} T_1 \tag{3.4}$$

$$Q_1 = \int_o^{T_1} I \, dt = \frac{V_o}{2L_t} T_1^2 \tag{3.5}$$

From (3.4) and (3.5),

$$I_o = \sqrt{(2V_o Q_1 / L_t)} \tag{3.6}$$

and

$$T_1 = \sqrt{(2Q_1 / (V_o / L_t))} \tag{3.7}$$

After the switch S_1 is opened, the voltage V_1 across group 1 increases from zero as the current is diverted into its voltage grading network, while it continues to flow through the remaining switches $S_2 - S_n$. After some time T_2, the total current time integral will neutralise the storage charge of group 2, and S_2 is opened. Voltage will now start to build up

on the thyristors of group 2, as the current is diverted into its grading circuit.

This process of opening of switches continues until all the thyristors are turned-off. As the group 1 turns-off first, it experiences the highest voltage, while the group n experiences the lowest voltage. Starting with the turn-off of group 1, a fast rising recovery voltage is generated, and is superimposed on the overvoltages caused due to non-simultaneous turn-off of thyristors.

3.3.1 System State Equations:

The state equations are derived for Fig.3.7 using the algorithm given in Appendix A. These equations arewritten in the form

$$p\,x = F\,x + G\,u \tag{3.8}$$

where x is the state variable vector with 11 state variables given by

$$[x] = [v_6,\ v_7,\ v_9,\ v_{11},\ v_{13},\ v_{15},\ v_{18},\ v_{22},\ i_3,\ i_5,\ i_{19}]^T \tag{3.9}$$

F is a 11x11 matrix and G is a 11x2 matrix which are given in Appendix E. u is a vector given by

$$u = [v_{o1}\quad v_{o2}]^T \tag{3.10}$$

3.3.2 Computer Program:

The state equations are solved numerically using Runge-Kutta fourth order method. Trapezoidal rule [10] is used to

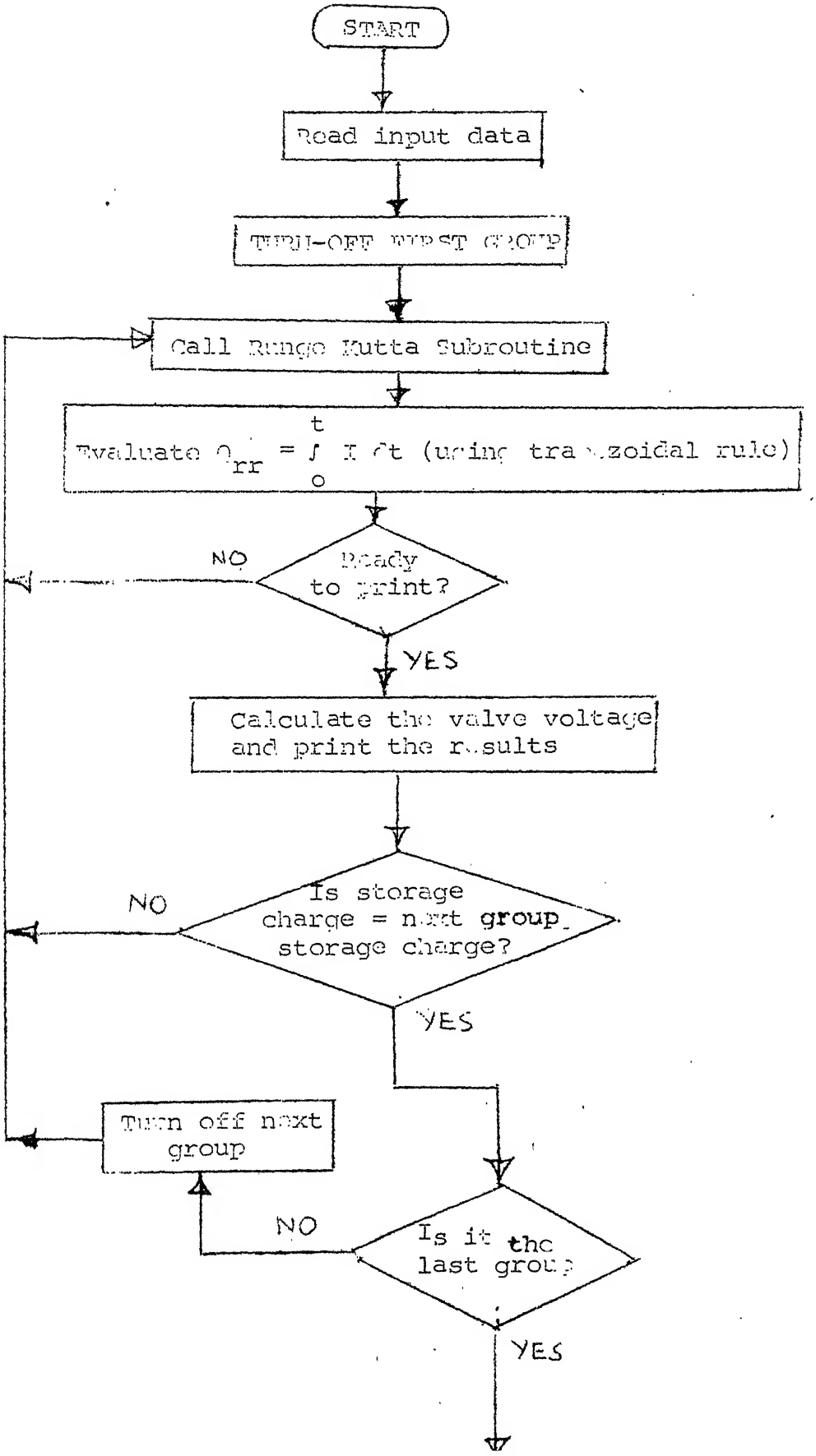
START
Read input data
TURN-OFF FIRST GROUP
Call Runge Kutta Subroutine
Evaluate $Q_{rr} = \int_0^t I\,dt$ (using trapezoidal rule)
Ready to print?
NO
YES
Calculate the valve voltage and print the results
Is storage charge = next group storage charge?
NO
YES
Turn off next group
Is it the last group?
NO
YES

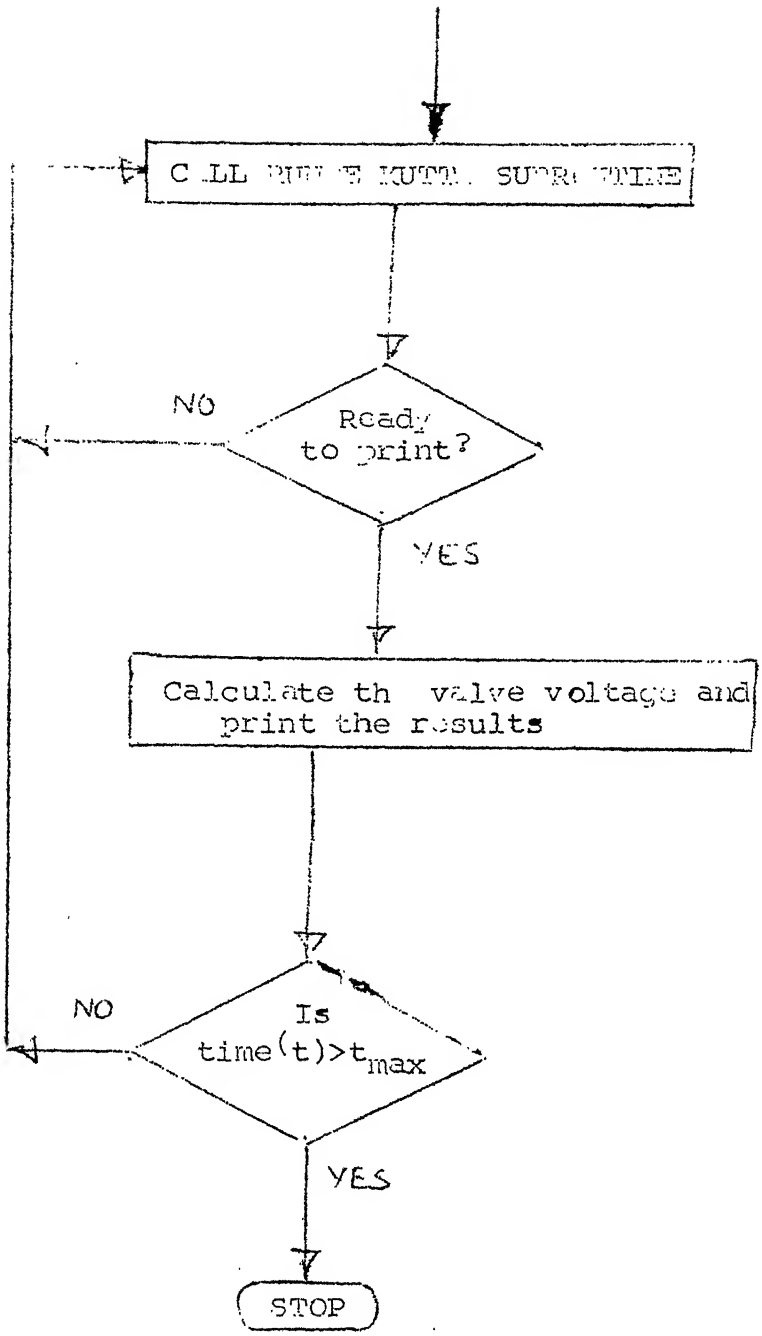

Fig.3.8 Flow chart of the computer program.

integrate the current numerically for obtaining storage charge. The flow chart of the computer program is shown in Fig. 3.8.

3.4 An Example

3.4.1 Description of the Problem:

A valve which contains 200 thyristors and operates at a peak repetitive voltage of 200 kV [3], is considered to show the effect of certain critical parameters on turn-off overvoltages with the following supply system and valve parameters.

Supply system:

L_t = 0.05 to 0.3 H

C_t = 2 nF

C_y = 2 nF

L_a = 1 mH

V_o = 100 KV

Valve:

R_d = 1 to 10 K-ohm

C_d = 10 to 500 nF

R_g = 5 to 30 ohms

C_g = 1 to 20 micro-F

Q_{min} = 300 micro-C.

ΔQ = 100 micro-C.

A valve consisting of 6 groups of thyristors is considered in this analysis. Table 3.1 shows the number of thyristors in each group and their corresponding storage charges.

Table 3.1

Group	No. of thyristors in each group	Storage charge (Q_{rr} in micro C) for each group
1	10	190
2	30	210
3	70	230
4	60	255
5	20	275
6	10	290

The initial capacitor voltages are assumed to be zero. The initial conditions for the inductor currents are

$$i_3(T_1) = -20 \text{ Amps}$$

$$i_5(T_1) = -20 \text{ Amps}$$

$$i_{19}(T_1) = -20 \text{ Amps}$$

where $T_1 = 30$ microseconds.

The integration step size used in Runge-Kutta subroutine is 0.1 microsecond.

3.4.2 Results:

Fig. 3.9 shows the current and voltage waveforms during turn-off. Equations(3.6)and(3.7) are used to calculate the

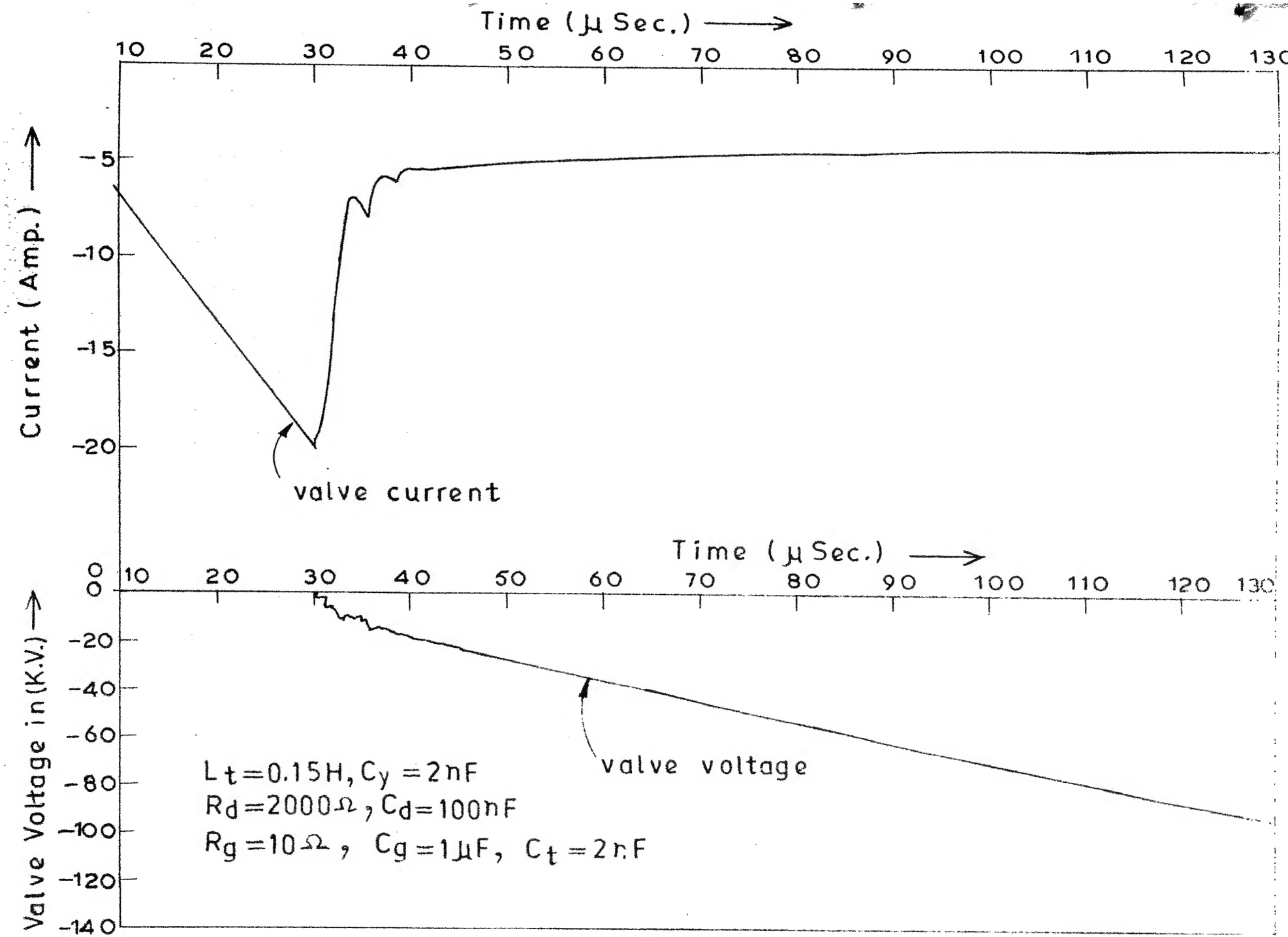

FIG.3.9 Computed Current and Voltage waveforms.

current, I_o, and the time at which group 1 turns-off, T_1. At the time T_1, the impedance of the valve increases as the switch S_1 opens, and the current is diverted into the parallel grading circuit. The initial voltage at time T_1 across the grading circuit of group 1 thyristors, is $N_1 R_g I_o$, which is same as the voltage across the entire valve as the other groups are still conducting. The voltage across the first group of thyristors increases after time T_1 as the capacitors of the grading circuit become charged, although the magnitude of the valve current decreases.

As the groups are turned-off successively, the magnitude of the current decreases, but the voltage across each group of thyristors which has already turned off, increases. At time T_n, the last group of thyristors will be turned off, and the recovery voltage builds up across the valve.

Effect of network parameters:

The voltage developed across the first group of thyristors to turn-off, is a function of the current furnished by the supply network. Investigation of the current distribution in a representative supply network during turn-off period leads to the following conclusions.

The di/dt during turn-off is relatively low, and current flows through the parallel anode inductance L_a. As the current flowing through anode resistance is negligible,

R_a can be neglected from the equivalent circuit [3]. Accordingly, Eq.(3.8) is modified and used in the analysis.

Although the valve capacitance affects the turn-on overvoltages [1], its effect is negligible here as the overvoltages during turn-off are controlled by the low impedance damping and grading circuits.

The effect of varying transformer inductance, L_t, on turn-off overvoltages is shown in Fig.3.10. For a particular set of the values of the parameters of the network and valve, increasing in L_t increases the peak valve voltage, while reducing the value of dV/dt.

Fig.3.11 shows the effect of damping circuit capacitance, C_d, on turn-off overvoltages. Both the valve voltage and dV/dt are reduced with the increase of damping circuit capacitance. But the very high values of C_d are not preferable, as the losses in this circuit are proportional to the value of capacitance.

The effect of damping circuit resistance, R_d, on turn-off overvoltages is shown in Fig.3.12. The value of dV/dt increases with the increase in R_d. By observing the voltage waveforms for R_d = 1000 ohms, 5000 ohms and 10,000 ohms, it can be seen that there exists an optimum R_d for a particular value of C_d, at which the valve voltage is minimum.

3.4.3 Discussion:

The various results obtained are compared with that of ref.[3], and it is found that there is no significant difference which validates the program developed. In ref.[3], an IBM supplied ECAP program is used for network analysis. Also the switching of individual thyristor group is represented by a step change in the impedance from a very small value to a large value. However, in this program, ideal switch is used and the entire valve is represented by a variable impedance of R and C in series. This simplifies the equivalent circuit. The valve voltage calculation for a particular set of parameters is taken 19 seconds C.P.U. time on DEC-1090 computer.

3.5 Calculation of Recovery Overvoltage Neglecting Turn-off Process

In the case of thyristor valves, because of the un-neutralized carriers (i.e. storage charge) present, a negative current flows through the valve during turn-off process, which delays the rise of reverse voltage across each valve. As it has been observed in the previous sections of this chapter, the recovery voltage across the valve is less dependent on storage charge distribution. Accordingly, the calculations in this section are carried out neglecting the turn-off process, i.e., all the thyristors of the valve are considered to be turned-off at the same instant [4].

Equation (3.8) is used for valve voltage calculations. The valve voltage variations with time for different damping circuit resistances and capacitances are shown in Fig. 3.15. The results are similar to those obtained in the previous section considering the turn-off process. The frequency of oscillation and overshoot for particular values of R_d and C_d, are calculated which are useful for calculating the damping circuit losses considering an approximate second order system model used in the next chapter. With R_d= 8K-ohm, C_d= 50 nF, the overshoot(from Fig.3.15) is approx.25.9 percent.

The expressions given by equations (3.14) and (3.15) [6] are used to calculate the damping factor of the oscillation and the frequency of oscillation respectively.

$$M_p = 100 \exp(-\pi\zeta/\sqrt{(1-\zeta^2)}) \qquad (3.14)$$

$$t_p = \pi/[\omega_n \sqrt{(1-\zeta^2)}] \qquad (3.15)$$

where M_p and t_p are peak percentage overshoot and time to peak, respectively.

For 25.9 percent overshoot, the calculated values of damping factor and frequency of oscillation are 0.40 and 4.5 KHz, respectively.

The results obtained in this section tally with the results given in ref.[4] without any significant difference.

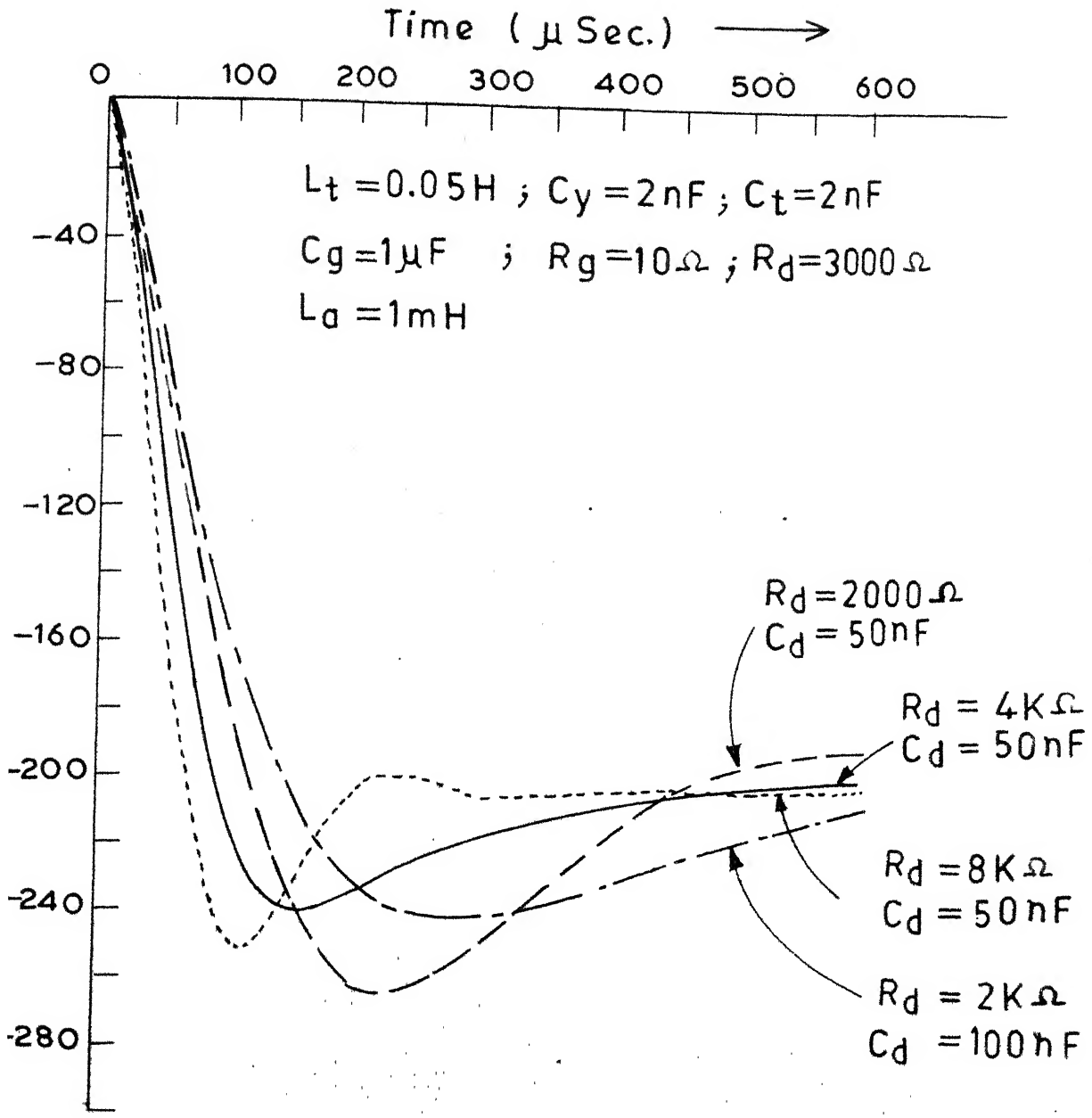

FIG. 3.15 Effect of damping resistance R_d on recovery over voltage.

3.6 Conclusions

A general computer program to calculate both recovery overvoltages and overvoltages due to non-simultaneous turn-off of thyristors in a HVDC valve has been developed. The effect of varying the system and valve parameters on turn-off overvoltages has been demonstrated by considering a representative thyristor valve.

Although the effect of switchyard capacitance, transformer capacitance, on turn-on overvoltages is significant, their effect on turn-off overvoltages is negligible. There is a significant increase in recovery overvoltage with the increase in transformer leakage inductance.

Both the thyristor and valve voltages are limited by choosing proper damping and grading circuits. The overvoltages can be limited only by a grading circuit without any external damping circuit, but the values chosen for grading circuit resistance and capacitance are not feasible if we consider both turn-on overvoltages and losses into account.

Consideration of turn-off process in detail has no significant effect on recovery overvoltages across the valve, though its effect is considerable if we consider the voltage across each thyristor of a valve. A computer program has been developed for calculation of recovery overvoltages neglecting the turn-off process.

CHAPTER 4

TIME DOMAIN SENSITIVITY CALCULATIONS USING ADJOINT NETWORK APPROACH

4.1 Introduction

In the design of any system, it is important to know the effect on the system performance due to variations of some system parameters. A method of calculating the sensitivities of the valve voltage with respect to damping circuit resistance and capacitance in time domain using adjoint network approach is presented. The results for a representative valve are presented. This sensitivity information is useful in the design of valve damping circuit.

4.2 Network considered and its Adjoint

The equivalent circuit considered is the same as that presented in Chapter 3 neglecting turn-off process. This network (N) is shown in Fig.4.1 [4]. The adjoint network $\hat{N}$ corresponding to the given network N is shown in Fig.4.2, which is constructed using the algorithm given in ref.[5,11]. The details of the algorithm are given in Appendix B.

4.3 Sensitivity Calculations

4.3.1 System Equations:

The state equations for the original network shown in Fig.4.1 are given by Eq.(E.1) (Appendix E). The state

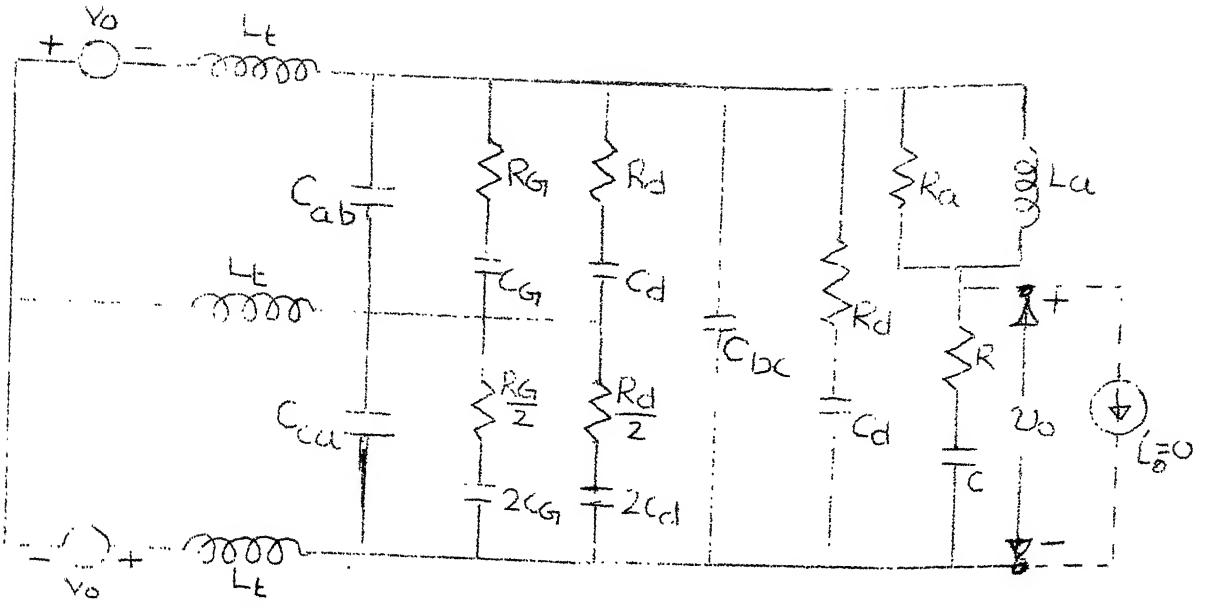

FIG 4.1 ORIGINAL NET WORK (N)

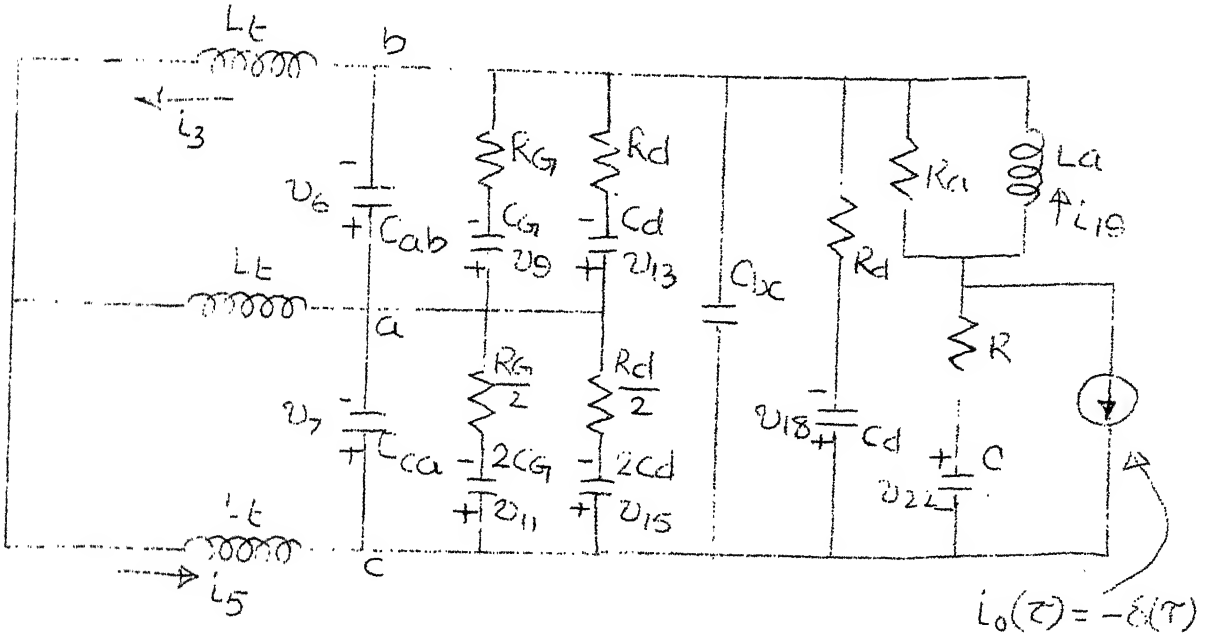

FIG 4.2 ADJOINT NETWORK ($\hat{N}$)

equations for the adjoint network are derived similarly and can be expressed as

$$p\,x = F\,x + G'u' \tag{4.1}$$

where x is the state vector given as

$$x = [v_6, v_7, v_9, v_{11}, v_{13}, v_{15}, v_{18}, v_{22}, i_3, i_5, i_{19}]^T \tag{4.2}$$

F is a 11 x 11 matrix given by Eq.(E.3) of Appendix E. G' is a 11 x 1 matrix. The non-zero elements of G' are as follows:

$$G'(1,1) = 1 - [R_a/(R+R_a)]$$

$$G'(2,1) = -1 - [R_a/(R+R_a)] \tag{4.3}$$

$$G'(11,1) = -RR_a/L_t(R+R_a)$$

For studying the sensitivity of the valve voltage with respect to damping circuit parameters a current source (impulse function) is connected across R-C circuit of Fig.4.2.

Therefore u' is a vector given by

$$u' = [i_c(t)] = [-\delta(t)] \tag{4.4}$$

The initial state vectors for both original and adjoint network are zero valued.

Substituting the above expression for the u' in Eq.(4.1), and integrating it between 0^- and 0^+ gives

$$x(0^+) = G' \tag{4.5}$$

Therefore, solving the forced system Eq.(4.1) is equivalent to solving an unforced system

$$\dot{x} = F\,x \tag{4.6}$$

with the initial state vector as G'.

4.3.2 Calculation of Sensitivities of the Valve Voltage with respect to Damping Circuit Resistance and Capacitance:

The perturbation observed in the valve voltage due to perturbations in the damping circuit parameters is given by the following equation (see Appendix B).

$$\Delta V_o(t_f) = \sum_{\text{all } R_d} \int_o^{t_f} \left[\hat{i}_{R_d}(\tau)\, i_{R_d}(t)dt\right]_{\tau = t_f - t} \Delta R_d$$

$$- \sum_{\text{all } C_d} \int_o^{t_f} \left(\hat{v}_{C_d}(\tau)\, \dot{v}_{C_d}(t)dt\right]_{\tau = t_f - t} \Delta C_d \tag{4.7}$$

The expressions for sensitivities are obtained from Eq.(4.7), which are given by

$$\partial V_o(t_f)/\partial R_d = \sum_{\text{all } R_d} \int_o^{t_f} \left[\hat{i}_{R_d}(\tau)\, i_{R_d}(t)dt\right]_{\tau = t_f - t} \tag{4.8}$$

$$\partial V_o(t_f)/\partial C_d = -\sum_{\text{all } C_d} \int_o^{t_f} \left[\hat{v}_{C_d}(\tau)\, \dot{v}_{C_d}(t)dt\right]_{\tau = t_f - t} \tag{4.9}$$

Using Eqs.(4.8) and (4.9), the expressions that are used for calculating the sensitivities in this analysis are developed which are given by

$$\frac{\partial V_o(t_f)}{\partial R_d} = \Big[\int_o^{t_f} \hat{i}_{12}(\tau)\, i_{12}(t)\, dt + \frac{1}{2} \int_o^{t_f} \hat{i}_{14}(\tau)\, i_{14}(t)\, dt + \int_o^{t_f} \hat{i}_{17}(\tau)\, i_{17}(t)\, dt \Big]_{\tau = t_f - t} \qquad (4.10)$$

$$\frac{\partial V_o(t_f)}{\partial C_d} = -\Big[\int_o^{t_f} \hat{v}_{13}(\tau)\, \dot{v}_{13}(t)dt + 2 \int_o^{t_f} \hat{v}_{15}(\tau)\, \dot{v}_{15}(t)dt + \int_o^{t_f} \hat{v}_{18}(\tau)\, \dot{v}_{18}(t)dt \Big]_{\tau = t_f - t} \qquad (4.11)$$

The currents, voltages and the derivatives of the capacitor voltages, used in Eqs.(4.10) and (4.11) are obtained from the transient analyses of both original and adjoint networks which are carried out numerically using Runge-Kutta fourth order method. The integrals in Eqs.(4.10) and (4.11) are evaluated numerically using Trapezoidal rule [10]. For example, the integral is approximated by the following summation (with $t_f = 5h$) given by

$$I = \int_o^{t_f} \big[\hat{i}(\tau)\, i(t) \big] dt \Big|_{\tau = t_f - t}$$

$$\simeq \frac{h}{2} \big[\hat{i}(5h) i(o) + 2 \big[\hat{i}(4h)\, i(h) + \hat{i}(3h)\, i(2h) + \hat{i}(2h)\, i(3h) + \hat{i}(h)\, i(4h) \big] + \hat{i}(o)\, i(5h) \big] \qquad (4.12)$$

4.4 An example

4.4.1 Description of the Problem:

A valve which contains 200 thyristors and which operates at a peak repetitive voltage of 200 kV, is considered to show the effect of damping circuit parameters on sensitivities with the following supply system and valve parameters.

Supply system:

L_t = 0.05 H

C_t = 2 nF

C_y = 2 nF

L_a = 1 mH

R_a = 3 K-ohm

V_o = 100 KV

Valve:

R_d = 2 to 4 K-ohm

C_d = 50 to 100 nF

R_g = 10 ohm

C_g = 1 microfarad

The step length used in Runge-Kutta subroutine is 0.5 micro-seconds. A C.P.U. time of 42 seconds is taken on DEC-1090 computer for the evaluation of the sensitivities.

4.4.2 Results:

The transient analysis of the original network (N) is carried out and the effect of damping circuit resistance (R_d)

on valve voltage has been shown in Chapter 3 which is reproduced here in Fig. 4.3. The variation of the sensitivity of the valve voltage with respect to damping circuit resistance (R_d) with time, for R_d = 2 K-ohm and C_d = 50 nF is shown in Fig.4.4. It can be seen from Fig.4.4, that the sensitivity is negative from 0 to 160 micro sec., positive from 160 to 440 micro sec., and again negative from 440 to 600 micro sec. This variation of sensitivity can be validated from the valve voltage waveforms given in Fig.4.3 by comparison of the two curves corresponding to R_d = 2K and R_d = 4K.

The peak of the valve voltage for R_d = 2 K-ohm is occurring at 225 micro sec. (from Fig.4.3). The sensitivity corresponding to this time is positive (14.5 volts/ohm). This indicates the increase in R_d will reduce the valve voltage at this time. The time to peak of the valve voltage is reduced with increase in R_d, which confirms the results obtained in Chapter 3.

The effect of damping circuit capacitance (C_d) on valve voltage has been shown in Chapter 3, which are reproduced here in Fig.4.5. The variation of the sensitivity of the valve voltage with respect to damping circuit capacitance (C_d) with time for R_d = 2 K-ohm and C_d = 50 nF is shown in Fig.4.6. It can be seen from Fig.4.6, that the sensitivity is positive from 0 to 290 micro sec., and negative from 290 to 600 micro sec.

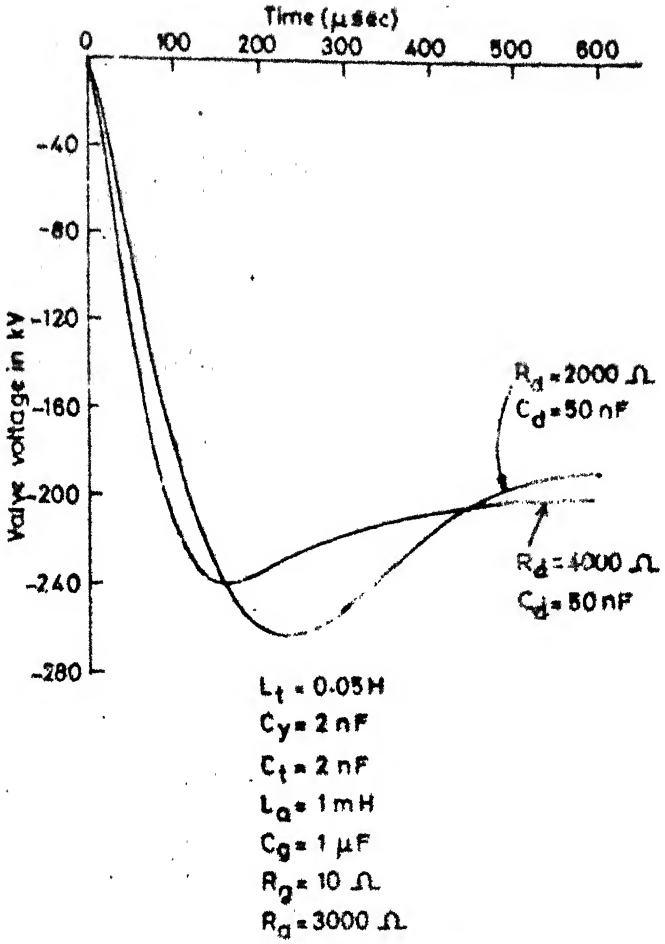

Fig. 4.3 Valve voltage vs. time

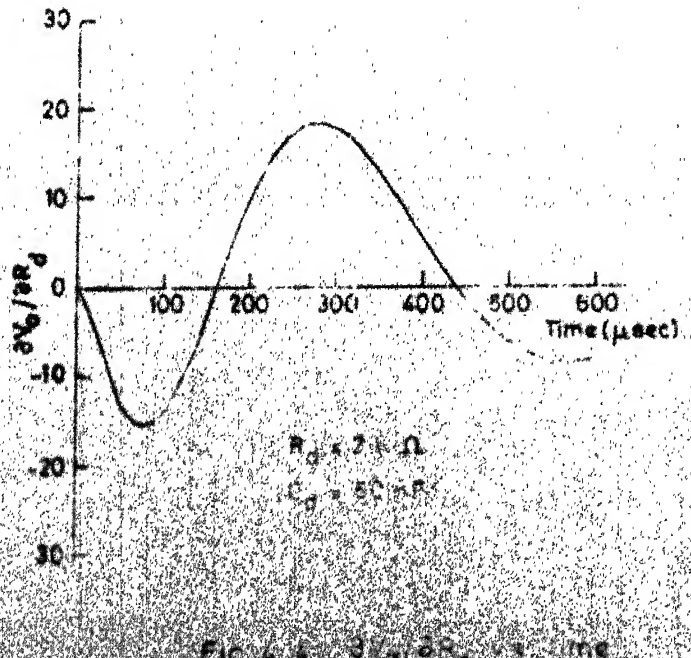

Fig. 4.4 $\partial V_b / \partial R_d$ vs. time

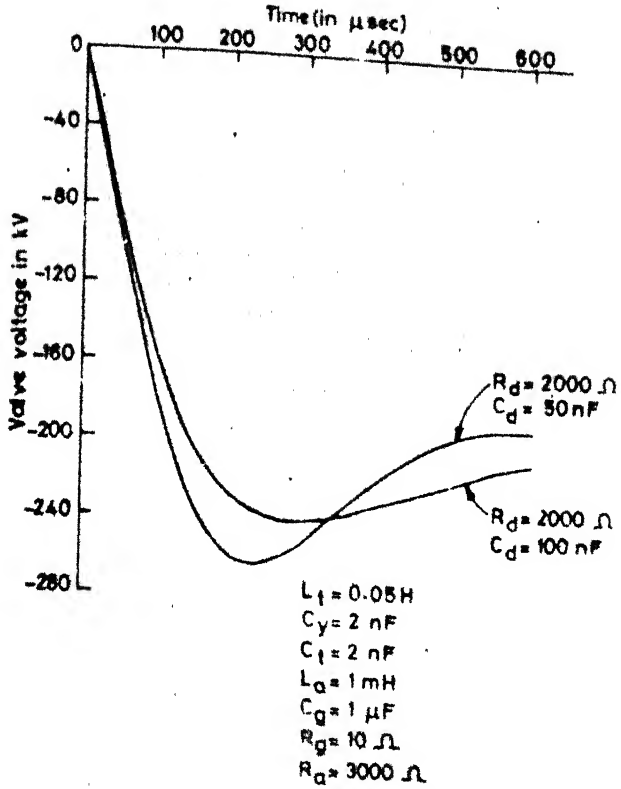

Fig.4.5 Valve voltage vs. time

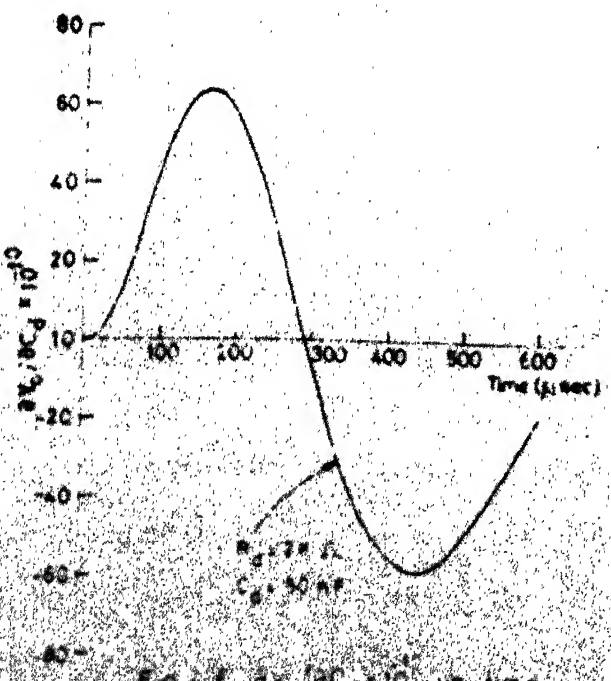

Fig. 4. $\partial V_d / \partial C_d \times 10^{-10}$ vs time

This variation of sensitivity can be validated from the valve voltage waveforms given in Fig.4.5, by comparision of the two curves corresponding to C_d = 50 nF and C_d = 100 nF. The sensitivity corresponding to the peak value voltage for C_d = 50 nF is positive (450 volts/nF) which indicates that the increase in C_d reduces the valve voltage at this instant. Because of the negative sensitivity observed at the subsequent interval the time to peak of valve voltage is delayed with increase in C_d. This is also validated from the results obtained in Chapter 3.

Effect of R_d and C_d on Sensitivity:

The variation of sensitivity of the valve voltage with respect to damping circuit resistance with time for different values of R_d is shown in Fig.4.7. The variations in sensitivity of the valve voltage with respect to R_d with time for different values of C_d are shown in Fig.4.8. The sensitivity curves obtained for different values of R_d are similar in shape but the magnitudes are reduced as R_d is increased. It can be concluded that over a wide range of variation in R_d, the effect of increase in R_d is to reduce the time to peak of the overvoltage. The behaviour of $\partial v_o/\partial R_d$ for different values of C_d is different. The magnitude of the sensitivity is slightly increased in the first interval (when the sensitivity is negative) and reduced in the subsequent interval. The transition from

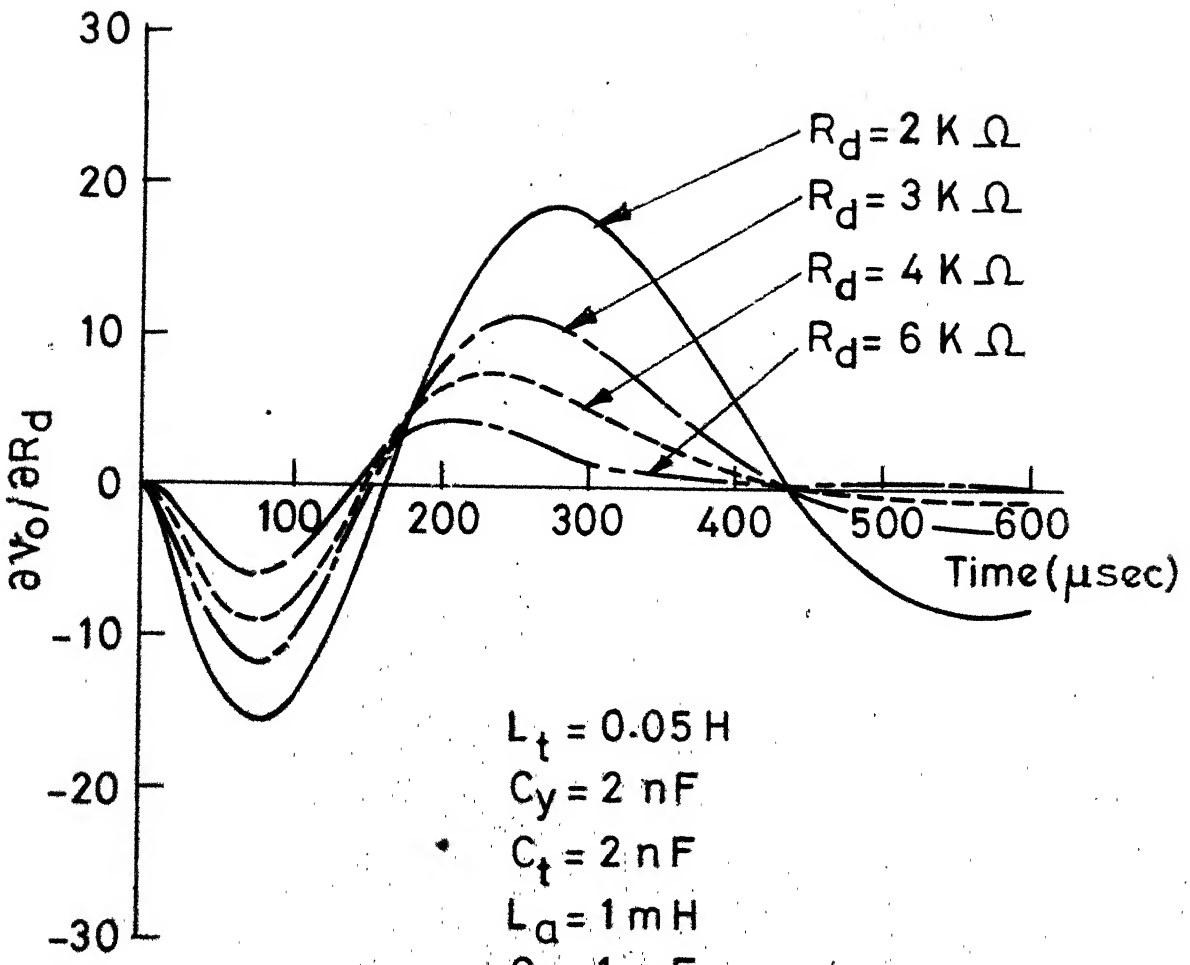

$L_t = 0.05\ H$
$C_y = 2\ nF$
$C_t = 2\ nF$
$L_a = 1\ mH$
$C_g = 1\ \mu F$
$R_g = 10\ \Omega$
$R_a = 3000\ \Omega$
$C_d = 50\ nF$

Fig. 4.7 $\partial V_o / \partial R_d$ vs. time for different R_d

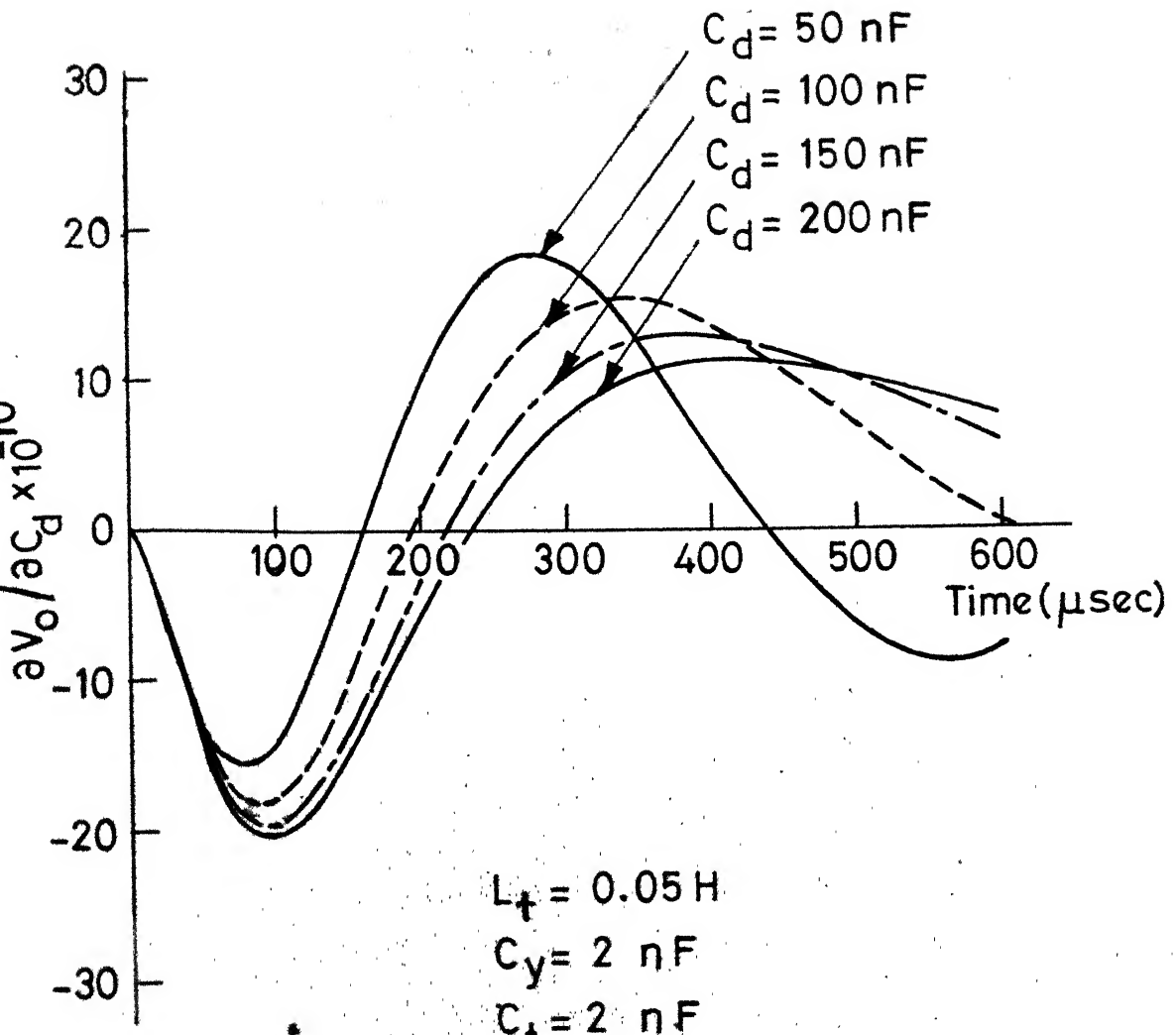

L_t = 0.05 H
C_y = 2 nF
C_t = 2 nF
L_a = 1 mH
C_g = 1 μF
R_g = 10 Ω
R_a = 3000 Ω
R_d = 2000 Ω

Fig.4.8 $\partial V_o/\partial R_d$ vs time for different C_d

negative values to the positive is also delayed and hence the peak overshoot is reduced with increase in R_d from the initial value of 2 K-ohm. However, from the Fig.4.7, it can be observed that the peak overshoot is not necessarily reduced as R_d is increased. For a given value of C_d, there is an optimum value of R_d for which the peak overshoot is a minimum.

The variation of sensitivity of the valve voltage with respect to damping circuit capacitance for different c_d is shown in Fig.4.9. The variations of sensitivity of the valve voltage with respect to C_d with time for different Rd are shown in Fig.4.10. The sensitivity curves obtained for different values of C_d are similar in shape but the transition from positive to negative is delayed with increase in C_d. The magnitude of the sensitivity is also reduced with increase in C_d. It can be concluded as C_d increases the valve voltage peak occurs at later instant and the effect on the peak voltage is diminished. The sensitivity curves for different R_d are similar in shape, but the increase in R_d reduces the magnitude of sensitivity.

4.4.3 Calculation of Sensitivities of the Valve Voltage with respect to Damping Circuit Resistance and Capacitance considering Turn-off Process:

A detailed model which is presented in Chapter 3 for considering the valve as a number of thyristor groups which turn-off sequentially according to their storage charge

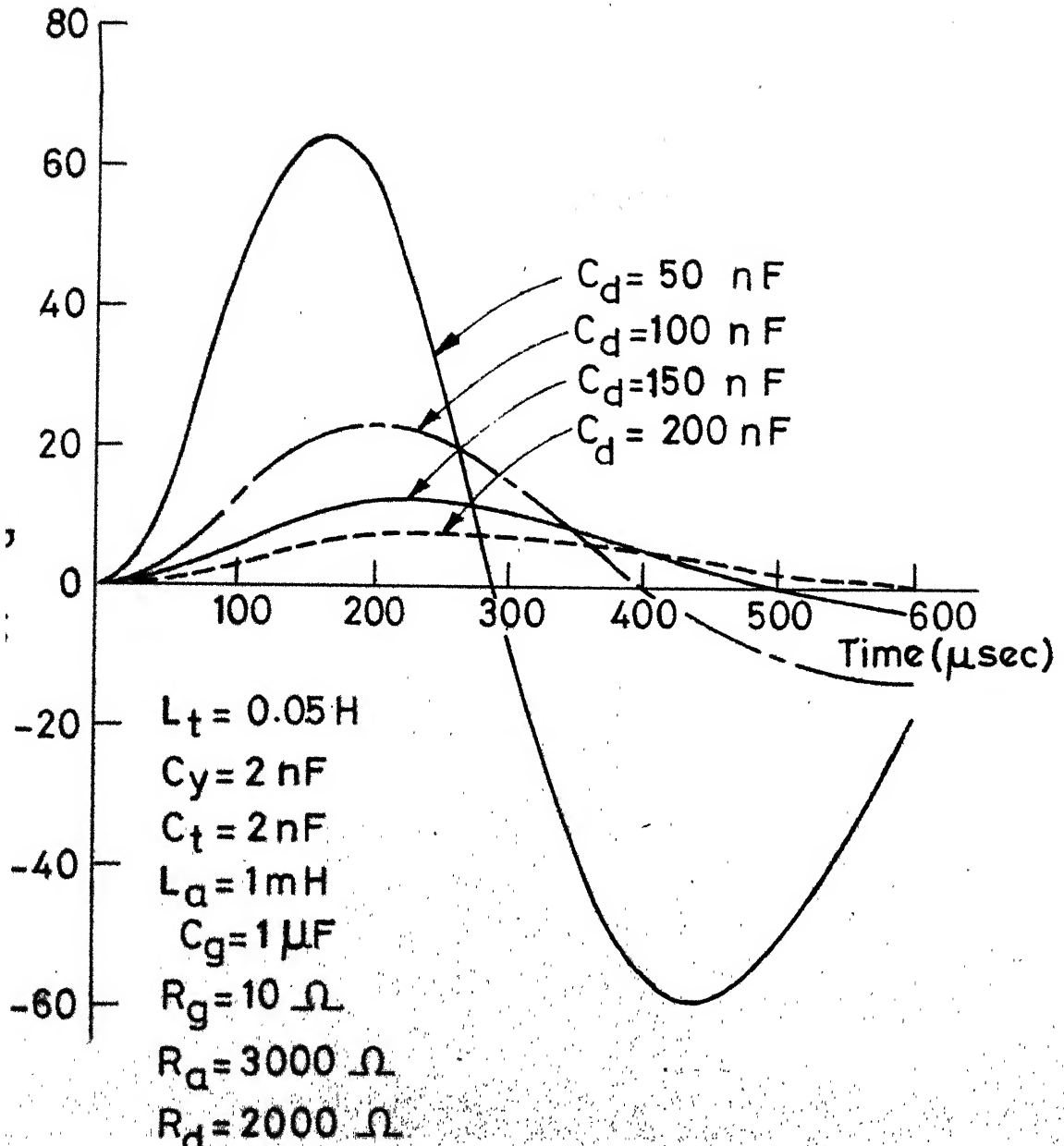

Fig. 4.9 $\partial V_o / \partial C_d \times 10^{-10}$ vs. time FOR different C_d

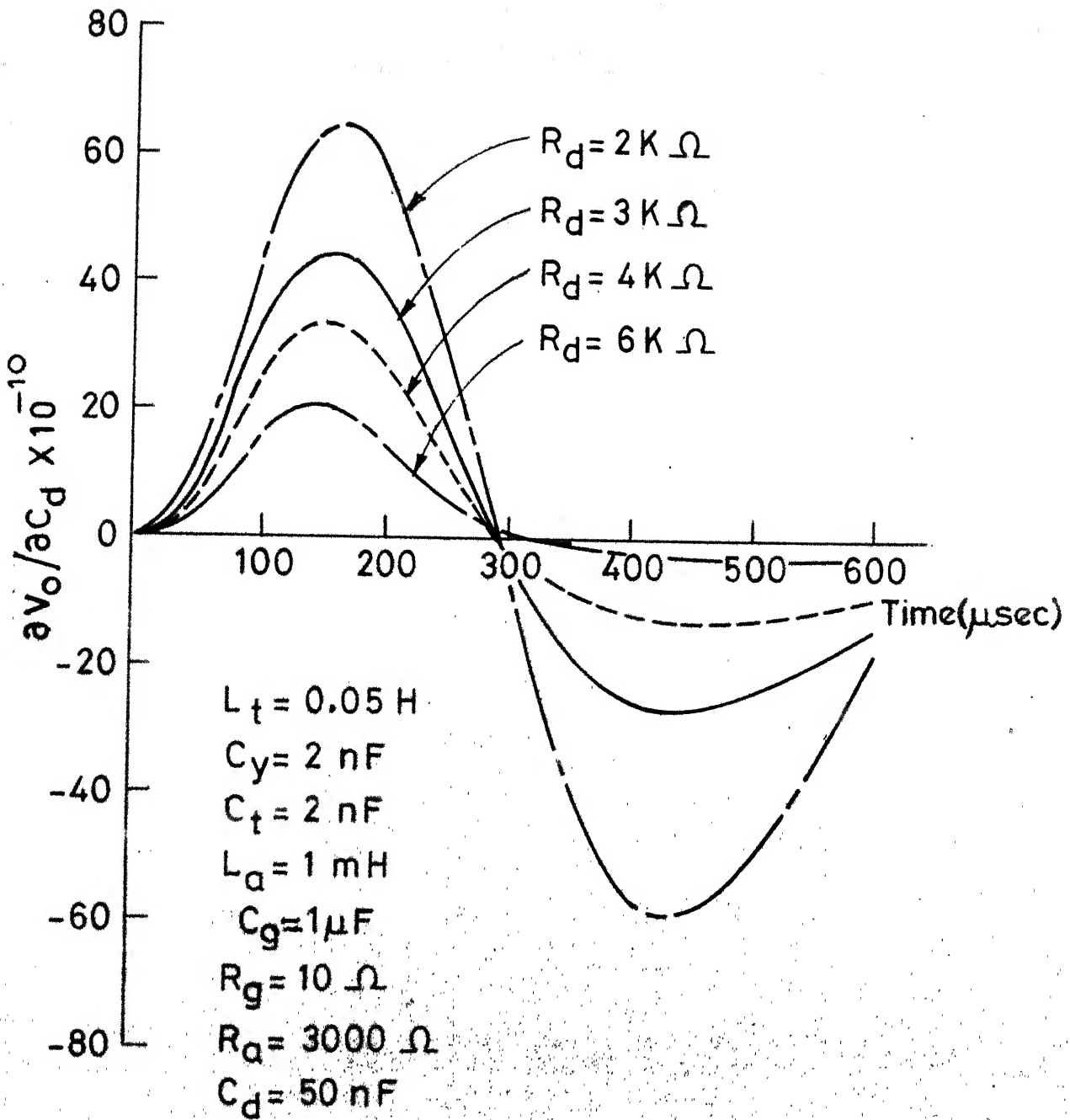

Fig.4.10 $\partial V_o/\partial C_d \times 10^{-10}$ vs time for different R_d

distribution, is incorporated in the sensitivity analysis. Effectively the turn-off process is incorporated by increasing the values of grading circuit resistance (R) and capacitance (C) in steps, till the last group of thyristors turns-off. Thus the system can be still represented by the equivalent circuit shown in Fig.4.1 and the adjoint network is similar to that shown in Fig.4.2. The only difference is the R and C are considered as variable elements depending on the turn-off process.

The sensitivities of the valve voltage with respect to R_d and C_d for R_d = 2 K-ohm and C_d = 50 nF are shown in Figs.4.11 and 4.12 respectively. The curves are qualitatively similar to those obtained in the previous section but the peak magnitudes are almost doubled. This indicates that the valve voltage variation with R_d or C_d is more if the turn-off process is considered in detail.

4.5 Conclusions

A computer program has been developed to calculate the sensitivities of the valve voltage with respect to damping circuit resistance and capacitance using the adjoint network approach. The effect of damping circuit resistance and capacitance on sensitivities has been studied by taking a representative valve.

From the sensitivity information it can be concluded that the effect of increase in R_d is to advance the instant of peak voltage whereas the effect of increase in C_d is to

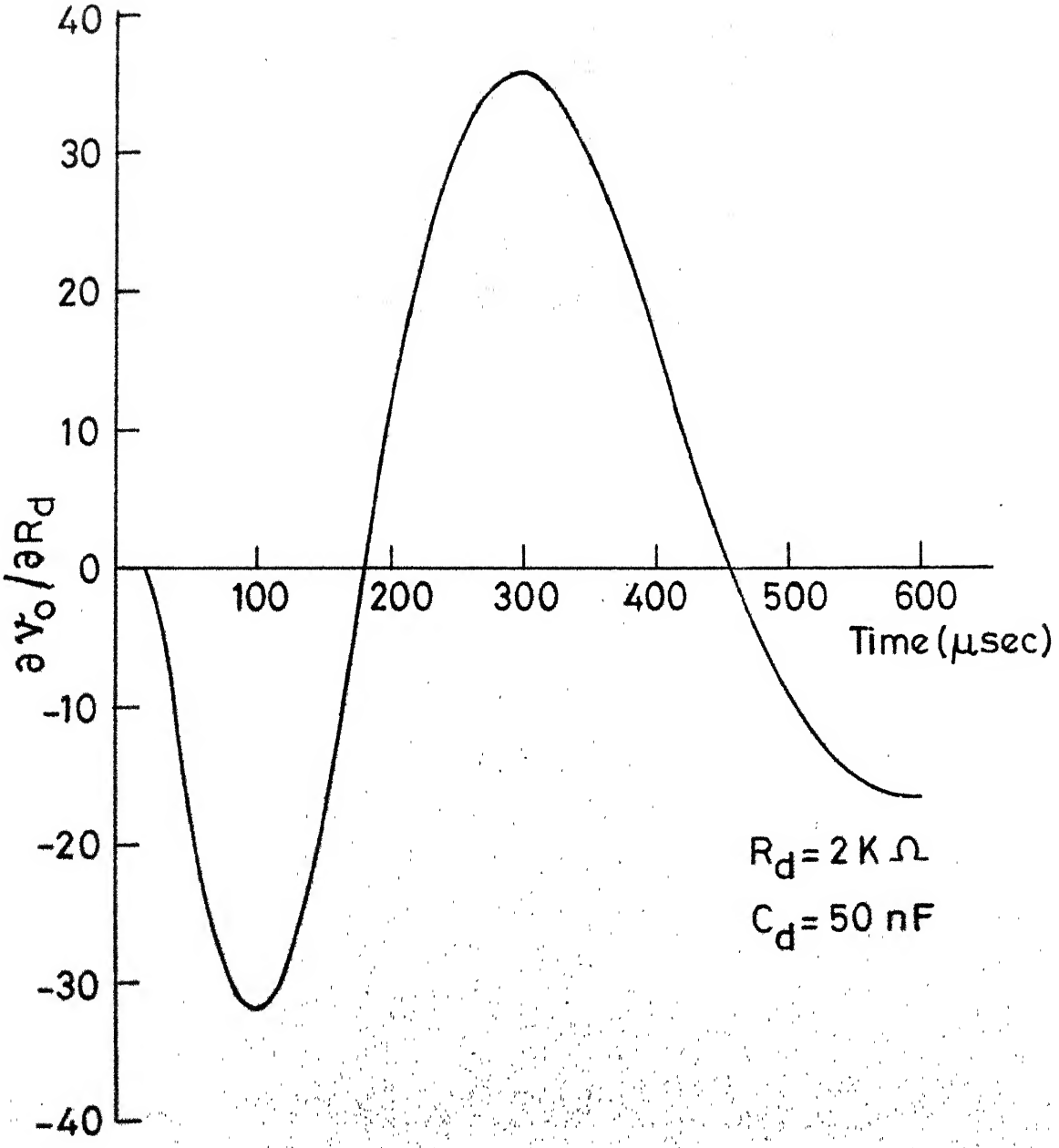

Fig. 4.11 $\partial V_o / \partial R_d$ vs. time (considering turn – off)

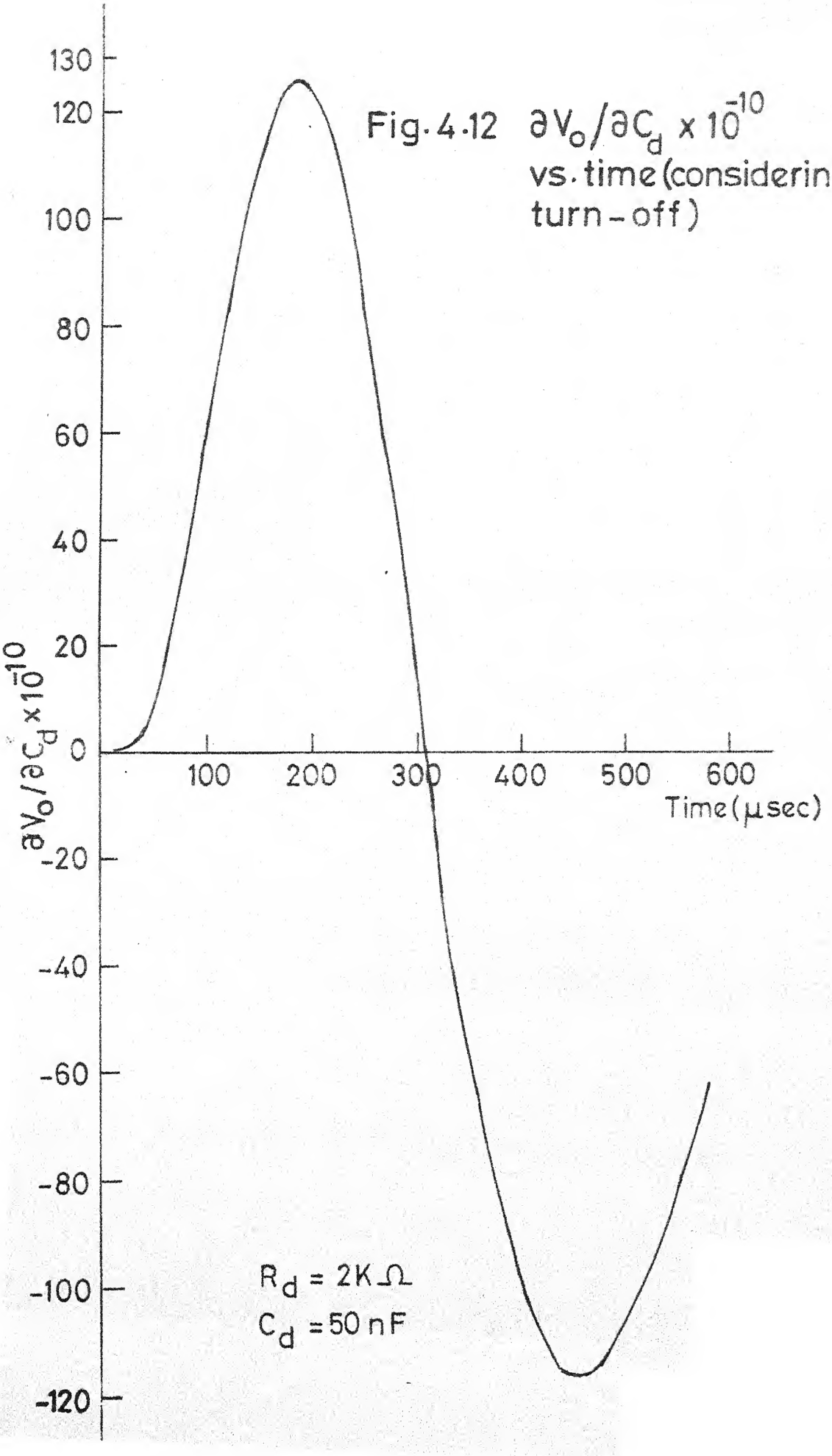

Fig. 4.12 $\partial V_o/\partial C_d \times 10^{-10}$ vs. time (considering turn-off)

delay the valve voltage peak. The sensitivity is reduced at higher values of R_d and C_d. The sensitivities of the valve voltage with respect to R_d and C_d have also been calculated considering the turn-off process in the valve. For a given value of R_d and C_d, it is observed that the sensitivity is increased compared to the case neglecting turn-off process.

CHAPTER 5

CALCULATION OF DAMPING CIRCUIT LOSSES

5.1 Introduction

The power loss in damping circuits is a significant component of the total losses in a convertor station. Also the amount of heat to be dissipated from the damper resistance affects their size, cooling requirement, and cost. A method of calculating the damping circuit losses has been developed representing the exact equivalent circuit of the convertor system during each interval of conduction over a cycle. Computer program is developed and the effect of bridge operation (commutating and delay angles) and damping circuit parameters on losses is analysed using a numerical example. The results are compared (1) with the results obtained using the approximate formulas given by Ainsworth [7], (2) and with the results obtained using an approximate second order model for simulating valve voltage oscillations [4].

5.2 Ideal Valve Voltage Waveform

The three phase bridge circuit (shown in Fig.3.1) is considered. In the normal operation of the bridge circuit, two or three valves conduct alternately. Considering the firing of valve 5 at the instant α, neglecting transients,

the voltage appearing across the valve 3 over a cycle is given in Table 5.1, with the supply voltages given by Eq.(5.1)[4].

$$\begin{aligned} v_a &= \sqrt{\frac{2}{3}}\, E_L \sin(\omega t + 90^\circ) \\ v_b &= \sqrt{\frac{2}{3}}\, E_L \sin(\omega t - 30^\circ) \\ v_c &= \sqrt{\frac{2}{3}}\, E_L \sin(\omega t - 150^\circ), \end{aligned} \tag{5.1}$$

where E_L is the line-to-line r.m.s. voltage.

The valve voltage waveform for $\alpha = \mu = 15^\circ$ is shown in Fig. 5.1.

5.3 Ainsworth's Formulas for Damping Circuit Loss Calculation[7]

It is assumed that the current in the damper resistor is that obtained by applying the ideal valve voltage shown in Fig. 5.1 directly to the R-C circuit, neglecting the transient voltage drop in the commutating reactance. One cycle of the waveform of the ideal valve voltage consists of eight arcs of fundamental frequency sine waves, separated by vertical discontinuities or jumps - one such arc (for the period of conduction of the valve) being of zero amplitude. The current resulting from this voltage wave in each of the eight intervals corresponding to the separate sinusoidal arcs has two components: (a) a transient component i_t resulting from the preceding voltage jump and (b) a sinusoidal component i_s resulting from the sinusoidal arc of voltage.

Table 5.1: Definition of the Valve Voltage Waveform

Section	Time Interval (in radians)	Valves conducting	Theoretical voltage across valve 3, $V(\omega t)$
1	$\alpha \leq \omega t < \alpha + \mu$	3,4,5	$v_1 = 0$
2	$\alpha + \mu \leq \omega t < \frac{\pi}{3} + \alpha$	4,5	$v_2 = \sqrt{2} E_L \sin \omega t$
3	$\frac{\pi}{3} + \alpha \leq \omega t < \frac{\pi}{3} + \alpha + \mu$	4,5,6	$v_3 = \sqrt{\frac{3}{2}} E_L \sin(\omega t + \frac{\pi}{6})$
4	$\frac{\pi}{3} + \alpha + \mu \leq \omega t < \frac{2\pi}{3} + \alpha$	5,6	$v_4 = \sqrt{2} E_L \sin \omega t$
5	$\frac{2\pi}{3} + \alpha \leq \omega t < \frac{2\pi}{3} + \alpha + \mu$	5,6,1	$v_5 = \sqrt{\frac{3}{2}} E_L \sin(\omega t - \frac{\pi}{6})$
6	$\frac{2\pi}{3} + \alpha + \mu \leq \omega t < \pi + \alpha$	6,1	$v_6 = \sqrt{2} E_L \sin(\omega t - \frac{\pi}{3})$
7	$\pi + \alpha \leq \omega t < \pi + \alpha + \mu$	6,1,2	$v_7 = \sqrt{\frac{3}{2}} E_L \sin(\omega t - \frac{\pi}{2})$
8	$\pi + \alpha + \mu \leq \omega t < \frac{4\pi}{3} + \alpha$	1,2	$v_8 = \sqrt{2} E_L \sin(\omega t - \frac{\pi}{3})$
9	$\frac{4\pi}{3} + \alpha \leq \omega t < \frac{4\pi}{3} + \alpha + \mu$	1,2,3	$v_9 = 0$
10	$\frac{4\pi}{3} + \alpha + \mu \leq \omega t < \frac{5\pi}{3} + \alpha$	2,3	$v_{10} = 0$
11	$\frac{5\pi}{3} + \alpha \leq \omega t + \frac{5\pi}{3} + \alpha + \mu$	2,3,4	$v_{11} = 0$
12	$\frac{5\pi}{3} + \alpha + \mu \leq \omega t < 2\pi + \alpha$	3,4	$v_{12} = 0$

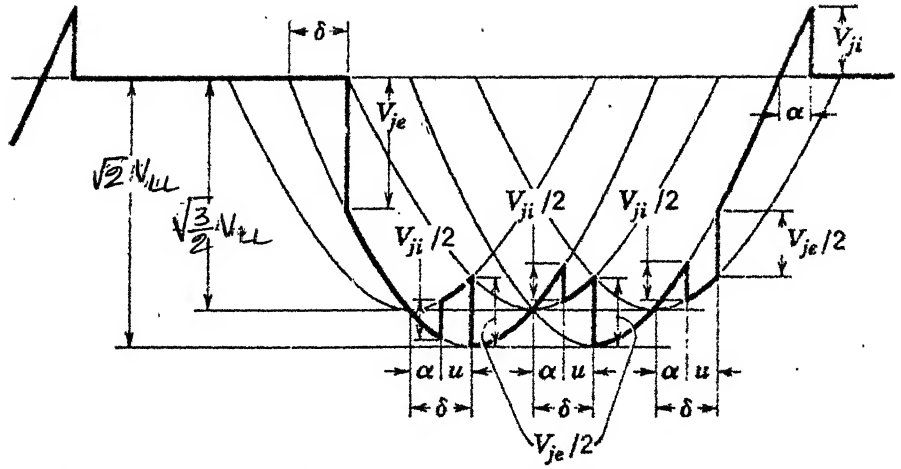

Fig. 5.1 Theoretical voltage across rectifier valve, showing voltage jumps. Drawn for $\alpha = u = 15°$: $V_{ji} = \sqrt{2}V_{LL}\sin\alpha$ is ignition voltage jump; $V_{je} = \sqrt{2}V_{LL}\sin\delta$ is extinction voltage jump. The smaller jumps ($V_{ji}/2$ and $V_{je}/2$) occur at ignition and extinction of other valves.

The sinusoidal component of current is an arc of fundamental frequency leading the corresponding voltage wave by 90^{o}, since at this frequency the reactance of the capacitor predominates. The instantaneous power consumed by the resistor is given by

$$p = R\, i^2 = R(i_t^2 + 2i_t i_s + i_s^2) \text{ Watts} \qquad (5.2)$$

In the above equation, the first term is the high frequency loss, and the sum of the second and third terms is arbitrarily called the low frequency loss, although the second term depends on both components of current. It is obvious that the first and third terms are always positive but that the second term may have either sign. The expression must be integrated with respect to time over the eight parts of one cycle; and the result must then be multiplied by fundamental frequency in order to find the energy dissipated per second, which is the power loss.

Ainsworth has derived the loss formulae which are as follows:

$$P_d = P_{hf} + P_{Lf} \qquad (5.3)$$

where

$$P_{hf} = 1.75\, f_1 V_{LL}^2 (C+C_s)(\sin^2\alpha + \sin^2\delta) \qquad (5.4)$$

$$P_{Lf} = 2\pi f_1^2 V_{LL}^2 C^2 R[2.46+0.875(\sin 2\alpha + 3 \sin 2\delta - 2u) + 0.433(\cos 2\alpha + \cos 2\delta)] \qquad (5.5)$$

f_1 = fundamental frequency, Hz

V_{LL} = r.m.s. line-to-line secondary voltage, volts

C = damper capacitance, farads

C_s = stray capacitance across the valve, farads

R = damper resistance, ohms

α = ignition delay angle ; δ = extinction delay angle,

u = overlap angle, radians

P_d = power loss in damper for one valve, watts

P_{hf} = high frequency component of P_d

P_{Lf} = low frequency component of P_d.

High Frequency Loss:

The voltage jump V_j applied across an R-C circuit causes a loss of energy of $CV_j^2/2$ joules in the resistor. The voltage across a valve has eight jumps per cycle, the largest of which are the ignition jump $V_{ji} = \sqrt{2}V_{LL} \sin\alpha$ and the extinction jump $V_{je} = \sqrt{2}\, V_{LL} \sin\delta$. In addition, there are six smaller jumps due to commutations in other valves; three of these are equal to $V_{ji}/2$ and three are equal to $V_{je}/2$. The energy loss per cycle is, therefore,

$$W_{hf} = 0.5C \Sigma V_j^2 = 0.5C(\sqrt{2}\, V_{LL})^2 (\sin^2\alpha + \sin^2\delta)[1+3(0.5)^2] \text{ joules} \qquad (5.6)$$

which multiplied by f_1, gives the high frequency power loss as given in Eq. (5.4).

In the total power loss, high frequency loss constitutes a major part and as an approximation the low frequency loss may be ignored. The high frequency loss is independent of the resistance and is directly proportional to the fundamental frequency, to the capacitance, and to the sum of the squares of the voltage jumps.

5.4 Calculation of Damping Circuit Losses using a Second Order Model for Voltage Oscillations [4].

After each commutation, the exact valve voltage consists of a damped oscillation which is superimposed on the sinewave. The frequency and amplitude of the superimposed damped oscillation are calculated as explained in 3.8 of recovery voltage calculation in Chapter 3. In this analysis, it is assumed that the same type of damped oscillation is superimposed on the ideal valve voltage at each commutation.

The equivalent circuit used for power loss calculation is shown in Fig.5.2 where the valve voltage is generated by switching one of the generators (V_2 - V_9 of Table 5.1) to a linear second order system which superimposes a damped oscillation on the sinewave. The output voltage of the second order system is applied to the damping circuit.

The loss in the damping resistance, R_d, is given by

$$P = (R_d/T) \int_0^T i_{R_d}^2(t)dt \qquad (5.7)$$

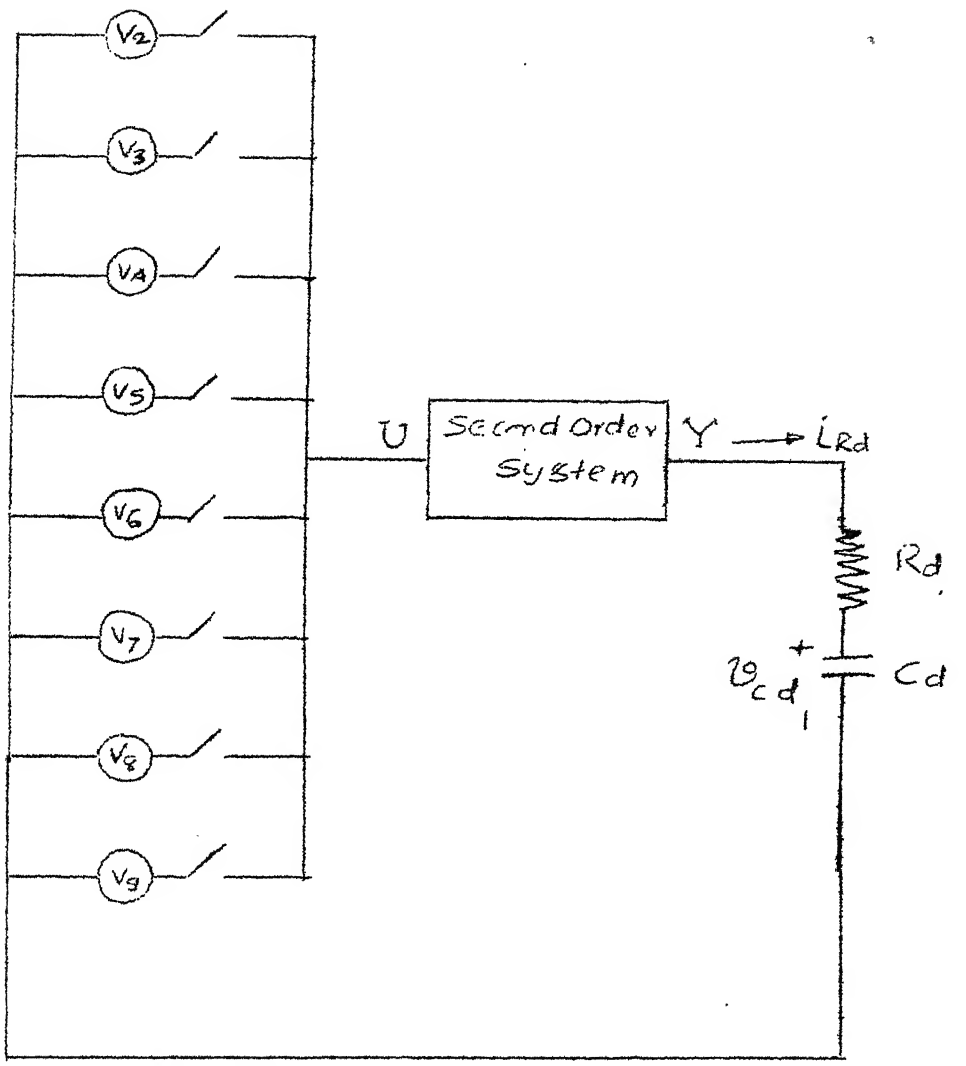

fig 5.2 Equivalent Circuit for the Power Loss Calculation using a Second order System for Oscillations.

where $i_{R_d}(t)$: instantaneous current through R_d

R_d : damping resistance

T : power frequency period.

The transfer function of the second order system is of the form

$$Y(s)/U(s) = \omega_n^2/(s^2 + 2\zeta\omega_n s + \omega_n^2) \qquad (5.8)$$

where ζ : damping factor

ω_n : undamped natural frequency.

Choosing the state variables as x_1, x_2 ($x_1 = Y$, $x_2 = dY/dt$), where Y is the output of the second order system), and the capacitance voltage v_{C_d}, the system equations are developed [6] and are given by

$$\begin{bmatrix} px_1 \\ px_2 \\ pv_{C_d} \end{bmatrix} = \begin{bmatrix} 0 & 1 & 0 \\ -\omega_n^2 & -2\zeta\omega_n & 0 \\ 1/C_dR_d & 0 & -1/C_dR_d \end{bmatrix} \begin{bmatrix} x_1 \\ x_2 \\ v_{C_d} \end{bmatrix} + \begin{bmatrix} 0 \\ \omega_h^2 \\ 0 \end{bmatrix} [U]$$

$$i_{Rd} = (x_1 - v_{C_d})/R_d \qquad (5.9)$$

These equations are solved numerically using Runge-Kutta fourth order method. After knowing the state variables x_1, x_2 and v_{C_d} at any time instant t, the current through the damping resistance (R_d) can be evaluated. Trapezoidal rule is used for performing the numerical integration required in Eq. (5.7) of power loss calculation.

5.5 A Detailed Analysis for Damping Circuit Loss Calculation

5.5.1 Detailed Equivalent Circuit Representation:

In the previous section, the ideal valve voltage is superimposed with a damped oscillation at each commutation. This is generated using a fixed second order model which is an approximation. Using the exact waveform of valve voltage is necessary to calculate the damping circuit losses more accurately. This can be achieved by representing an exact equivalent circuit during each interval of conduction over a cycle and carrying out the transient analysis.

The equivalent circuits of the thyristor valve converter system during each interval corresponding to sections 2 to 9 of Table 5.1 are developed. The equivalent circuit during the interval $\alpha+\mu \leq \omega t < (\pi/3)+\alpha$ (valves 4 and 5 conducting) is given in Fig.5.3. In deriving this equivalent circuit, the conducting valves are represented by short circuits, and the non-conducting valves are represented by their corresponding grading circuits in parallel with their damping circuits. The anode damper R_a -L_a is neglected for all the valves except for valve 3.

The state variable equations are written (using the algorithm in Appendix A) to the equivalent circuits developed for Sections 2 to 9 of Table 5.1 and are solved numerically using Runge-Kutta fourth order method. The final state vector

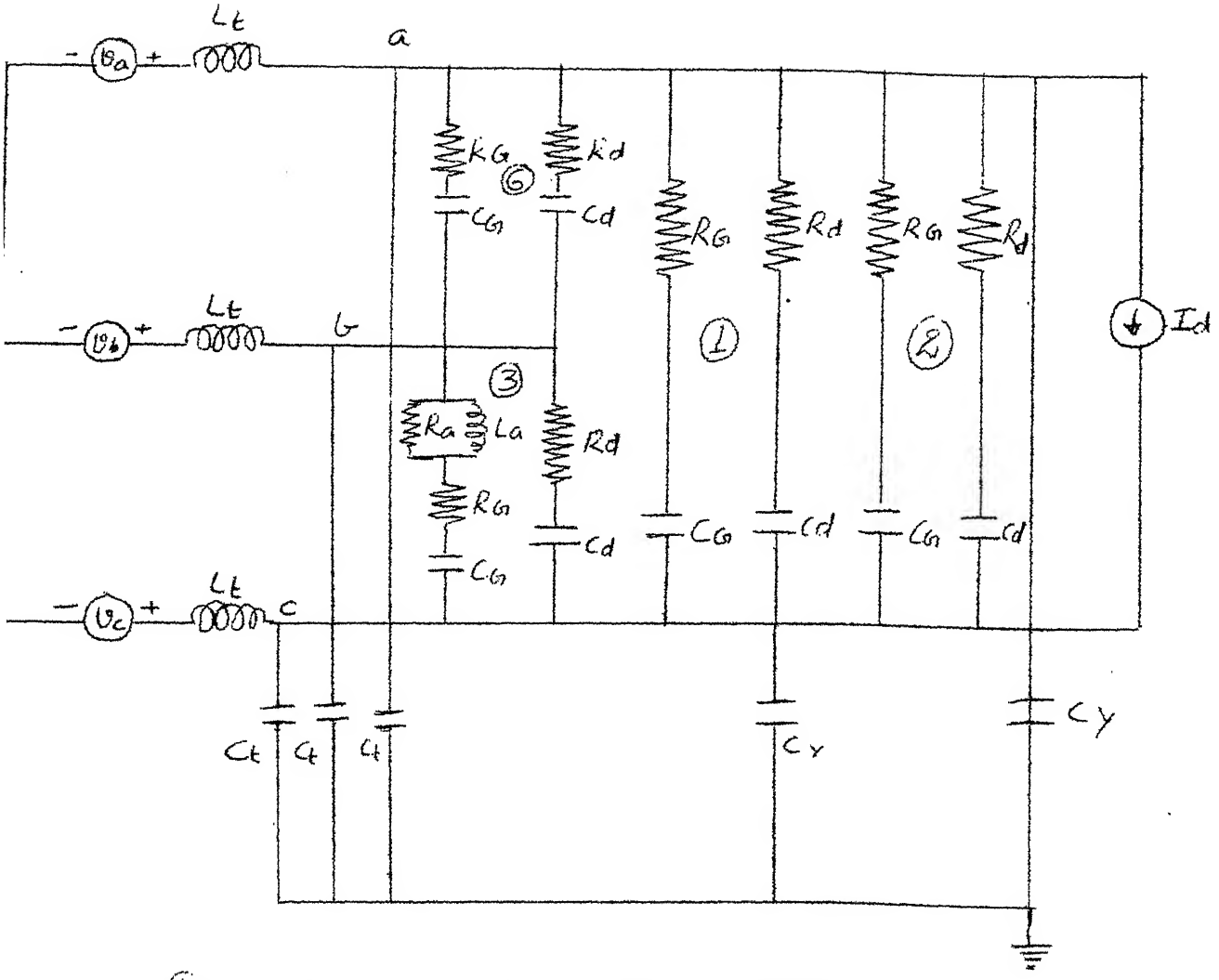

Fig 5.3 Equivalent Circuit of the Converter System during the period $\alpha + \mu \leq \omega t < \pi/3 + \alpha$ (Valves 4 and 5 are Conducting).

at the end of each interval is taken as the initial state vector to the subsequent interval. The current flowing through R_d of valve 3 during each interval is evaluated. Trapezoidal rule [10] is used for performing the numerical integration required in Eq.(5.7).

5.5.2 Simplified Equivalent Circuit Representation:

The equivalent circuit of Fig.5.3 can be simplified by neglecting capacitances C_t and C_y and the anode damper (R_a - L_a) of valve 3. The state equations for the simplified equivalent circuits are developed and solved numerically; and the power loss in the damping circuit of a valve is evaluated as explained earlier. The equivalent circuits for sections 2 to 9 (see Table 5.1) and the state equations for the first two intervals (sections 2 and 3 of Table 5.1) are given in Appendix C.

5.5.3 Computer Program:

The flow chart of the computer program is shown in Fig.5.4.

5.6 An Example

5.6.1 System Data:

Supply System: L_t = 0.05 H

C_t = 2 nF

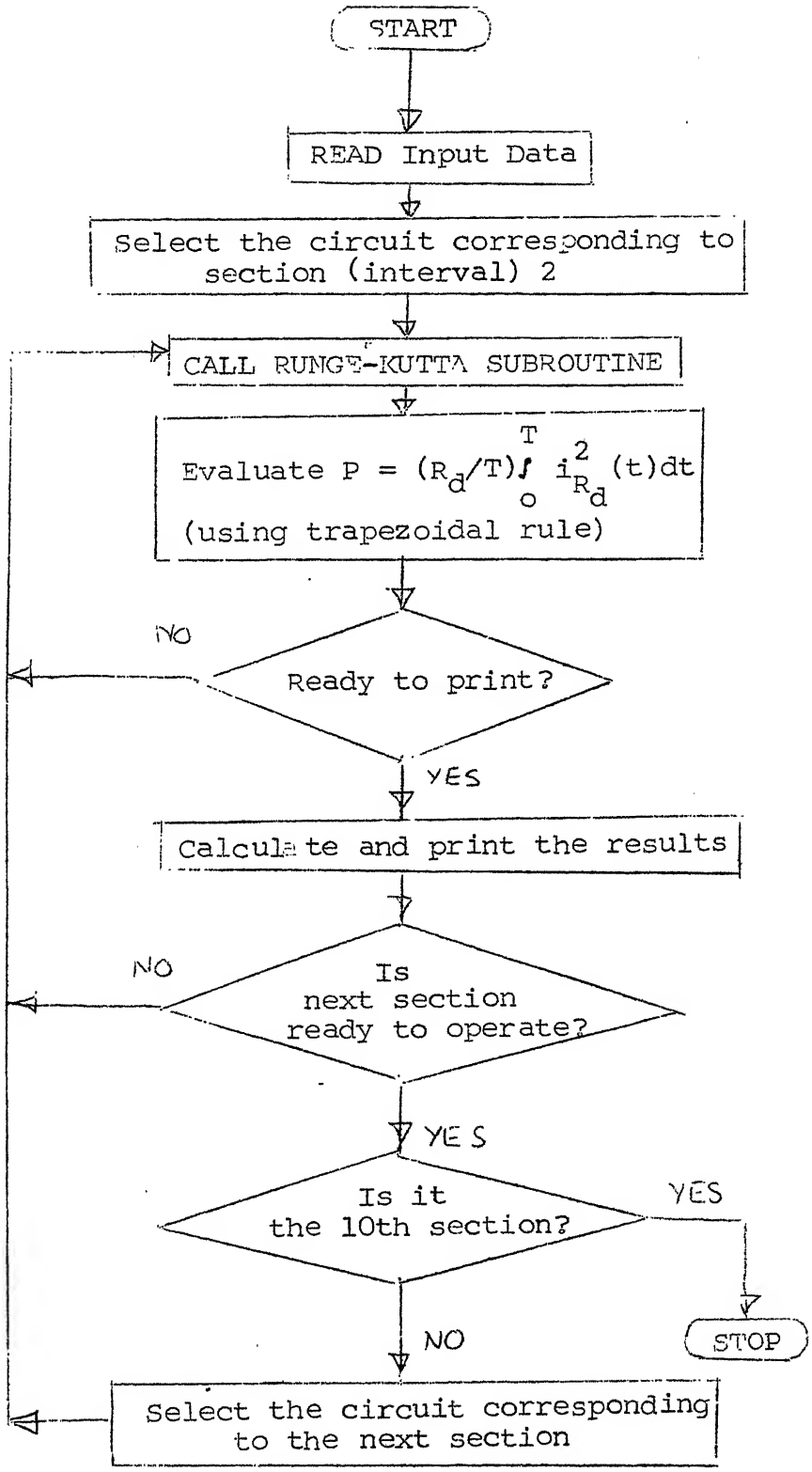

Fig. 5.4: Flow chart of the computer program.

C_y = 2 nF

L_a = 1 mH

R_a = 3 K-ohm

E_L = 200/√2 Kv

f = 60 Hz

Valve: R_d = 2 K-ohm

C_d = 100 nF

R_g = 10 Ohm

C_g = 1 microfarad

N = 200

5.6.2 Results:

Computed valve voltage, current in the damping circuit, and the damping circuit loss for $\alpha = 90^\circ$, $\mu = 15^\circ$ are shown in Figs. 5.5, 5.6 and 5.7 respectively. It can be seen from the curves that at each commutation, the valve voltage jump with a subsequent oscillation which in turn produces a current oscillation, the magnitude of which is relatively large compared to power frequency current. It can be seen from the power loss curve, loss increases rapidly at each commutation while varying slightly between commutations. This confirms that the losses are produced mainly by charging and discharging of C_d when voltage jumps appear across it.

Effect of Commutation Angle (μ) and Delay Angle (α) on Damping Circuit Loss:

The effects of commutation and delay angles are shown in Figs. 5.8 and5.9. In Fig.5.8 the solid lines

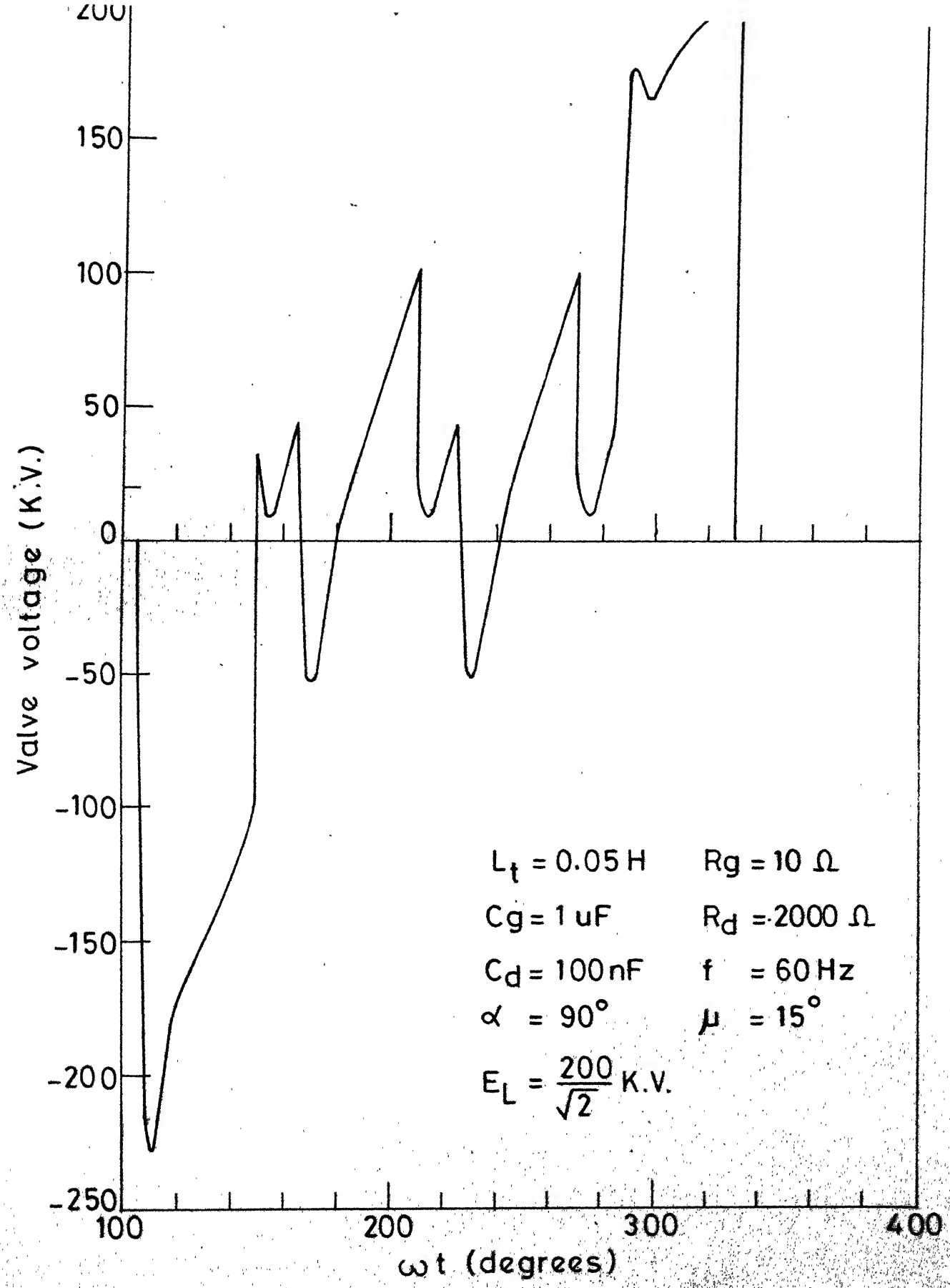

Fig. 5.5 Computed valve voltage waveform.

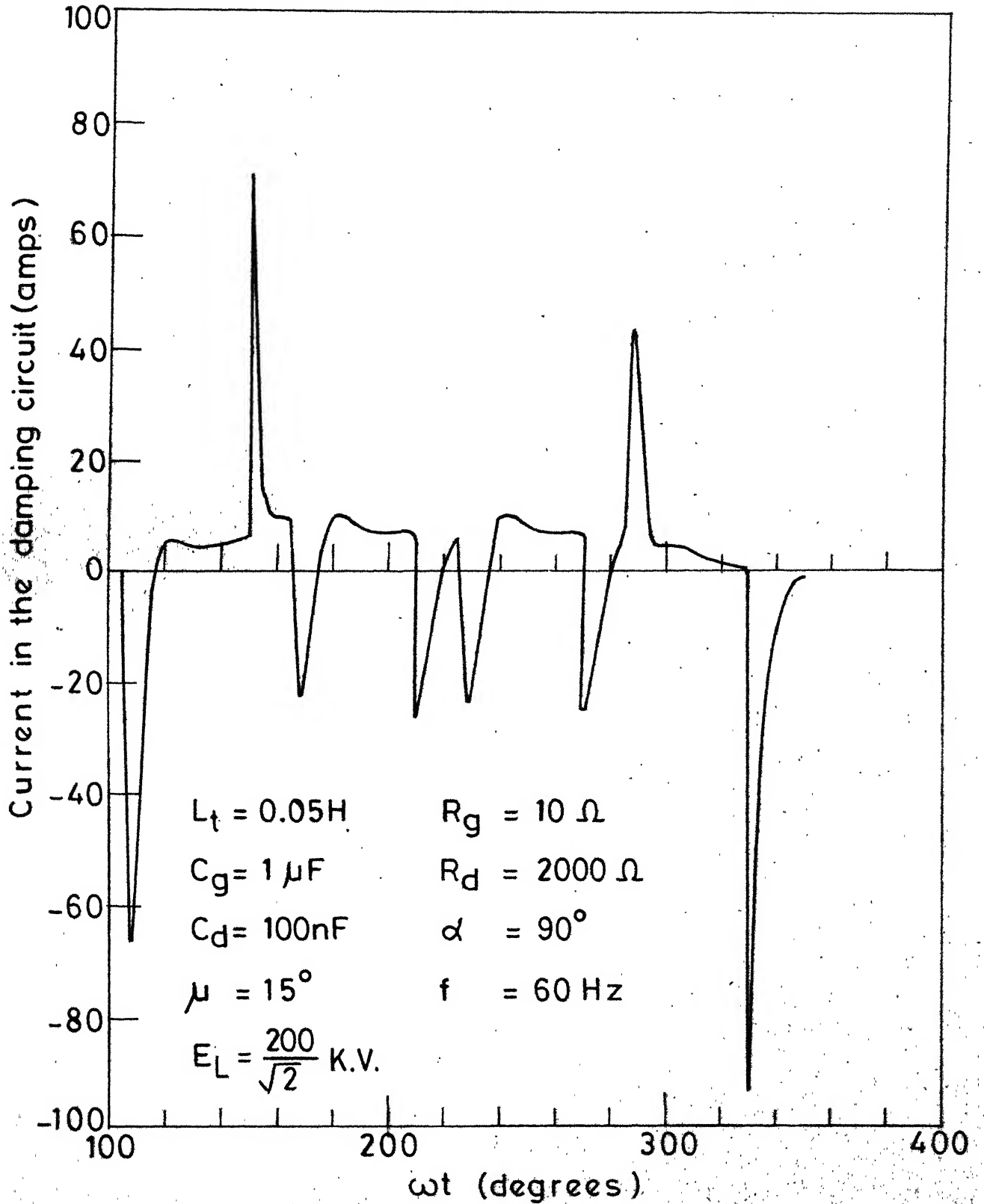

Fig. 5.6 Computed current waveform.

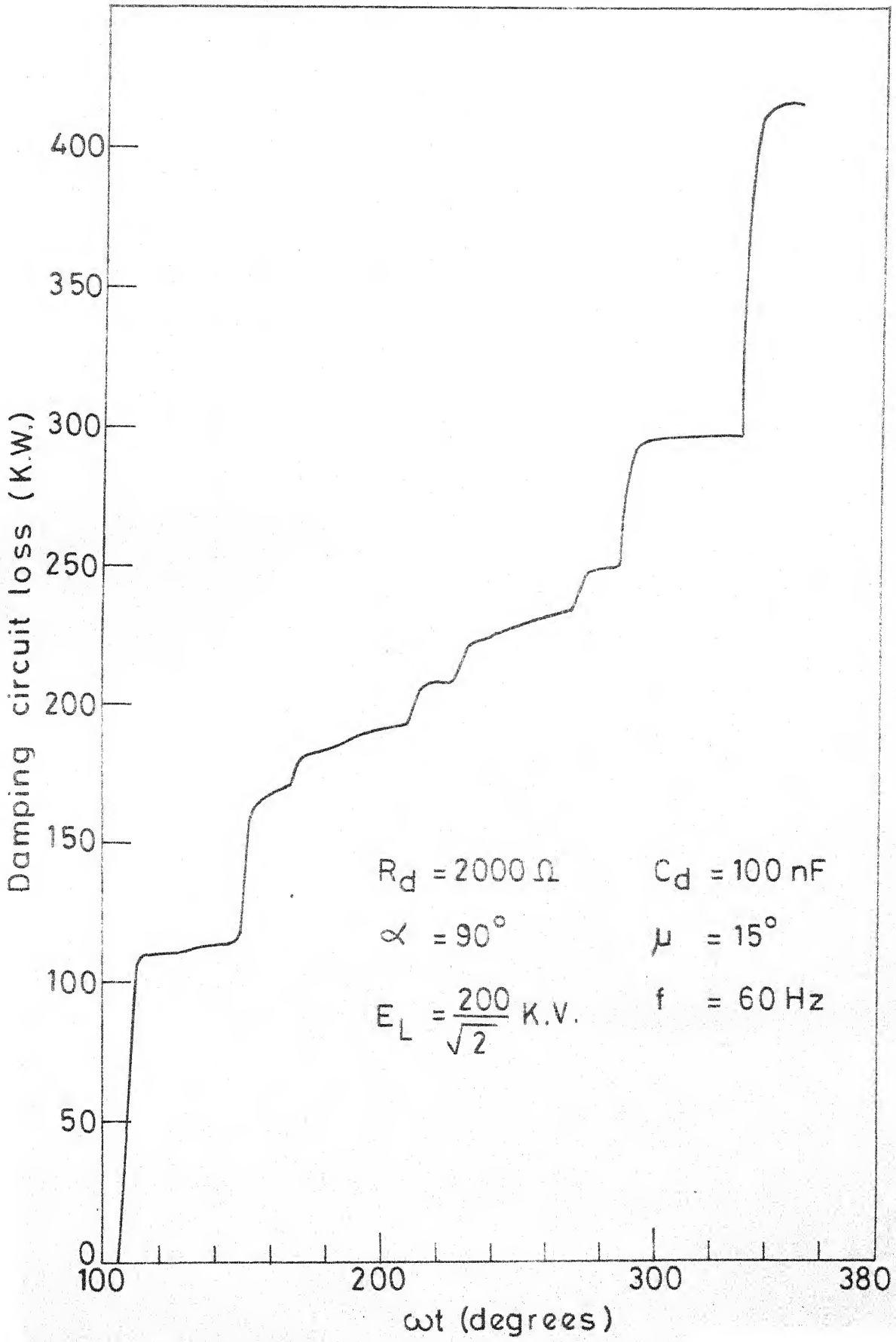

Fig. 5.7 Damping loss vs time

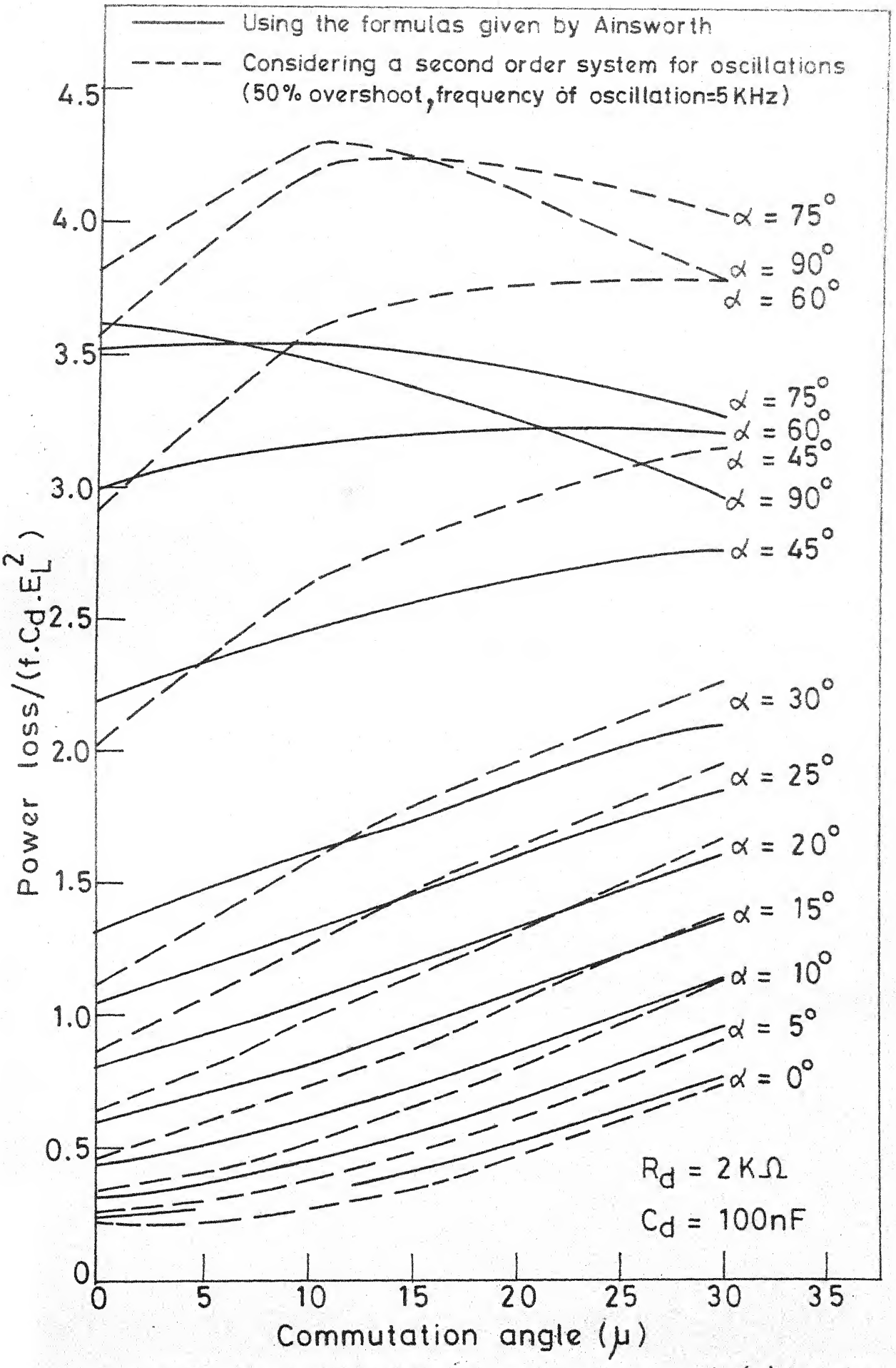

Fig. 5.8 The effect of the commutation angle (μ) and delay angle (α) on the power loss.

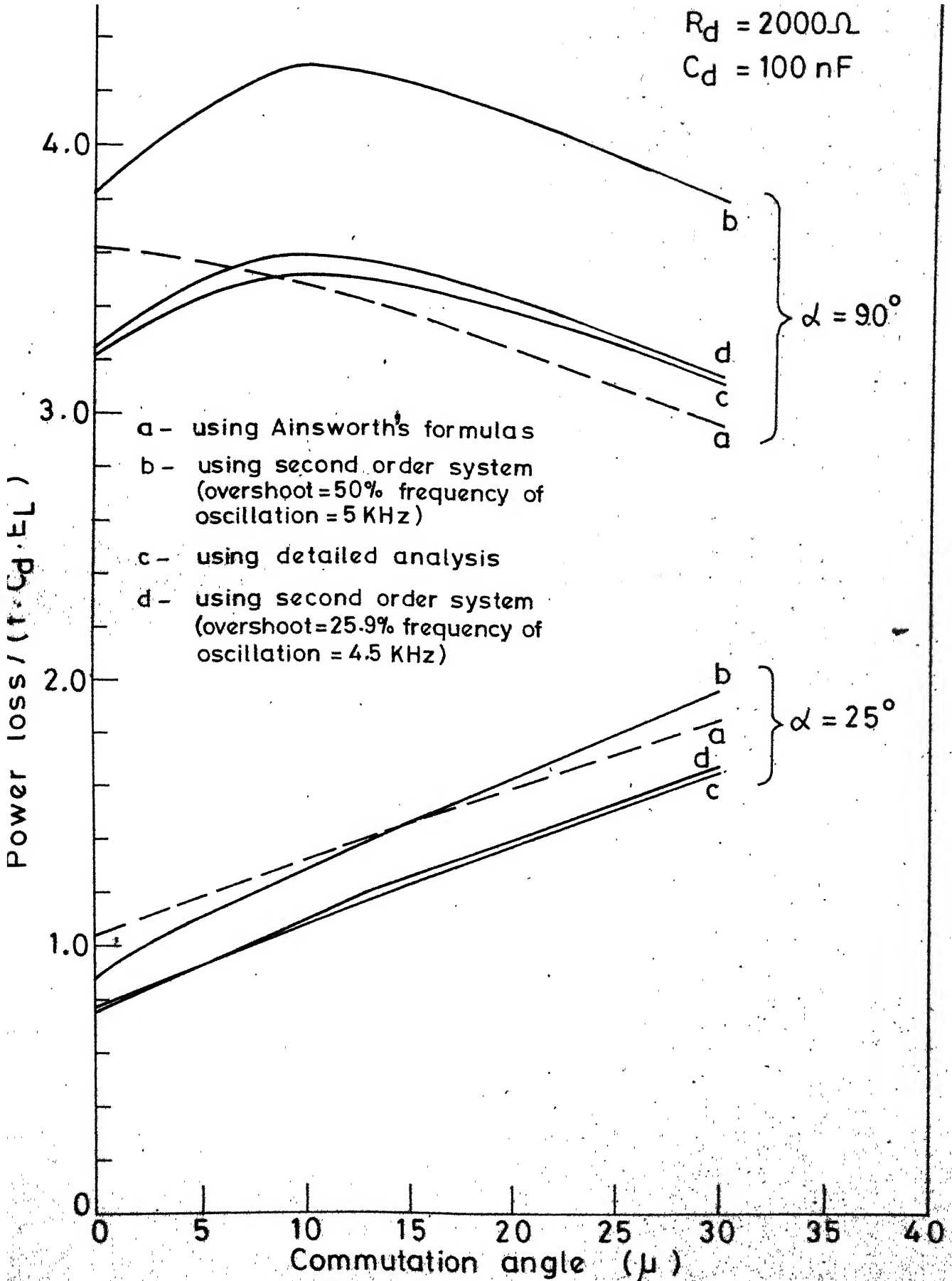

Fig. 5.9 Effect of the commutation angle (μ) and the delay angle (α) on the damping circuit loss.

represent the calculations by Ainsworth's formulas, whereas the dashed lines represent the calculations using a second order system for oscillations. It can be seen from Fig 5.8 that the increase in α increases losses, because for high α the heights of the extinction and ignition voltage jumps which appear across the valve are more, which in turn increases the peaks of the current spikes. The increase of losses with μ is less significant compared to that of α.

The effect of μ on losses for two different values of α (25° and 90°) for the three methods described is shown in Fig. 5.9.

Effect of Damping Circuit Parameters on Damping Circuit Loss:

The effects of R_d and C_d on damping circuit losses are shown in Figs. 5.10 and 5.11 respectively. It is observed that losses increases drastically with increasing C_d, whereas R_d does not significantly affect the circuit losses. The capacitance C_d must therefore be kept to a minimum to reduce losses, whereas the selection of the value of R_d depends mainly on the recovery voltage transient.

5.6.3 Discussion:

Three methods have been studied for calculating the damping circuit losses. In the case of Ainsworth's formulae an ideal valve voltage waveform is considered for loss calculation neglecting the valve voltage oscillations during

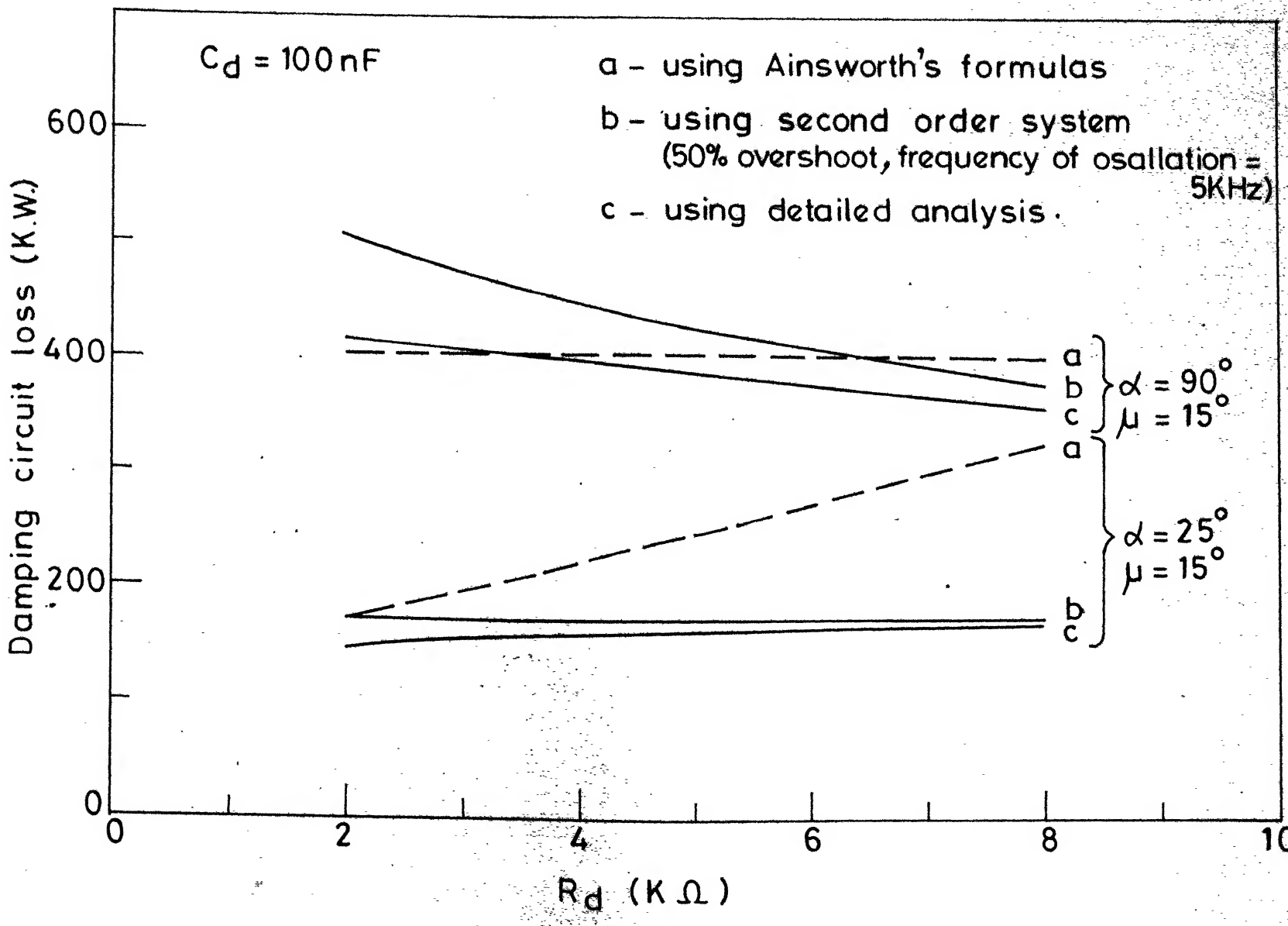

Fig. 5.10 Effect of R_d on damping circuit loss.

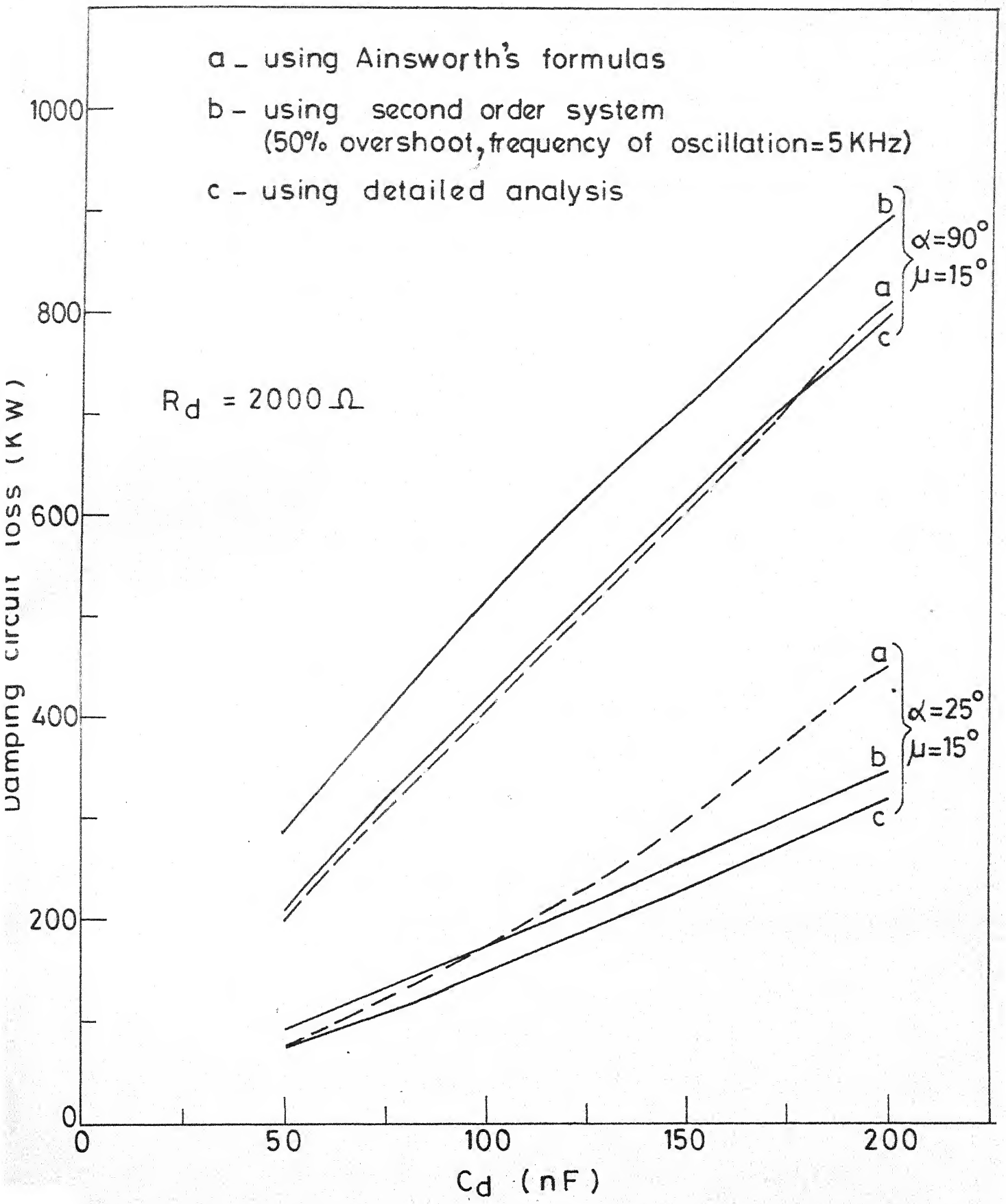

Fig . 5 .11 Effect of C_d on damping circuit loss.

commutation. In the second method, an improvement is made by assuming a fixed second order model for simulating high frequency valve voltage oscillations, that are imposed on the ideal valve voltage. A detailed analysis is carried out in the third method, in which the exact equivalent circuits are represented during different intervals to evaluate the exact valve voltage waveform which can be used for calculating the losses more accurately.

It is observed that Ainsworth's formulae give inaccurate results at lower values of α both qualitatively and quantitatively. From Fig.5.10, it can be seen that increase in R_d gives rise to rapid increase in losses at lower values of α which is not true; and also the losses are almost constant with increase in R_d at higher values of α, although the exact losses are decreasing. At higher values of α the formulae give reasonably accurate results.

In the method considering a second order model, reasonably accurate results can be obtained (though the deviation is considerable at higher values of α), provided the overshoot is chosen correctly. In Fig.5.9, the curves with two different overshoots, 50 percent (which is assumed), 25.9 percent (which is obtained from the transient analysis) show that the results can be improved by considering the overshoot obtained from transient analysis. It is to be noted that the losses increase significantly with increase in the overshoot, whereas the effect of frequency of oscillation on losses is not significant [4].

A comparision in terms of accuracy and computational time for different methods is shown in Table 5.2.

It can be observed from Table 5.2, the step length required in the detailed analysis is half the step length required in the second order system model. The detailed analysis, of course, requires much more computational effort than the first two methods and is used here mainly to investigate the accuracy of the earlier methods.

5.7 Conclusions

Three methods of calculating the damping circuit losses are studied. An exact calculation of the circuit loss is carried out by using detailed equivalent circuits during each section of the valve voltage waveform.

The effects of varying the bridge operation parameters (α and μ) and the damping circuit parameters (R_d and C_d) are analysed for a representative thyristor valve. The damping circuit losses are increased by C_d but less affected by R_d.

Table 5.2: Comparison of various methods used for damping circuit loss calculation.

Method	Damping circuit loss for $\alpha = 90^{o}$, $\mu = 15^{o}$ (KW)	Step length used (seconds)	C.P.U.time on DEC-1090 computer (seconds)
Using Ainsworth's formulas	404.859	-	0.09
Using second order model for oscillations (overshoot 25.9 percent, frequency of oscillation 4.5 KHz)	423.6	0.15625×10^{-5}	5.07
Using second order model for oscillations (overshoot 50 percent, frequency of oscillation 5 KHz)	507.11	0.15625×10^{-5}	5.07
Using detailed analysis-simplified equivalent circuit representation	416.039	0.78125×10^{-6}	39.04
Using detailed analysis-detailed equivalent circuit representation	391.442	0.78125×10^{-6}	55.00

CHAPTER 6

VALVE DAMPING CIRCUIT DESIGN FOR HVDC SYSTEMS

6.1 Introduction

The electrical design of HVDC valve depends upon the overvoltages generated in the system and those generated within the valve. These overvoltages will depend upon the valve parameters. In the case of thyristor valves, the voltag grading circuit, the firing method, and the mechanical design are the most important factors. The overvoltages developed during the turn-on and turn-off periods are among the most severe internal overvoltages. The valve damping circuit which consists of a resistance and a capacitance in series is used to limit the recovery voltage during turn-off.

One of the important factors to be considered in the design of valve damping circuit is the damping circuit loss that takes place because of the voltage applied across the damping circuit, when the valve is not conducting. Proper selection of damping resistance and capacitance limit the recovery voltage to an economic value without undue increase in the losses of the damping circuit. Calculation of turn-on and turn-off overvoltages has been presented in Chapters 2 and 3 respectively. Calculation of recovery voltage and damping circuit losses has been described in the Chapters 3 and 5 respectively. In this chapter, a method has

been proposed to optimize the damping circuit with the objective of limiting both recovery voltage transient and damping circuit loss.

6.2 Equivalent Circuit

The equivalent circuit used in this analysis is the same as the equivalent circuit used in the case of turn-off overvoltage calculations (which is given in Fig. E.1 of Appendix E) except the following changes:

(1) The source voltages are taken to be sinusoidal voltages.

(2) The turn-off process is neglected. That is, the values of R and C in Fig. E.1 are set equal to R_G and C_G respectively.

6.3 A Method for Parameter Optimization

Given a system described by

$$\dot{x} = A(p)\, x \tag{6.1}$$

where $p = (p_1, p_2, \ldots, p_n)$

$p_i, i=1,2,\ldots,n$ are the system parameters,

the problem of optimization of the parameters p, for the above system is defined by the objective of minimizing an index of performance η, given by

$$\eta = \int_0^\infty x^T Q\, x\, dt \tag{6.2}$$

where Q is a positive semidefinite matrix.

The criterion for selecting a performance index (PI) is dependent on the desired objective to be achieved and is accordingly expressed as a function of the design variables. It can be shown that for any asymptotically stable system, the PI can be expressed as given

$$\eta = x_o^T P x_o \qquad (6.3)$$

where p, a symmetric positive semidefinite matrix for any stable system, is given by the matrix Liapunov equation

$$A^T P + PA = -Q \qquad (6.4)$$

x_o is the initial state vector. For a given set of initial values of parameters $p_1, \ldots, p_n$, the matrix A is determined and the matrix Liapunov equation is solved. The matrix P is used to evaluate the PI. By searching through the parameter space, it is possible to determine the optimal values of parameters that minimize the PI.

A solution procedure of the matrix Liapunov equation (Eq. 6.4) is given in Appendix D.

6.4 State equations

The state equations for the equivalent circuit considered, is given in Appendix E. These are of the form

$$p\,x = F\,x + G\,u \qquad (6.5)$$

where u is a vector given by

$$u = [v_1 \quad v_2]^T \tag{6.6}$$

where

$$v_1 = v_b - v_a$$

$$v_2 = v_b - v_c \tag{6.7}$$

In order to use the method described in the previous section, the Eq.(6.5) should be transformed to the form of Eq.(6.1). Since the vector u consists of sinusoidal voltages direct transformation will make the system critically stable and the technique cannot be used. To avoid this difficulty damped sinusoidal voltages are assumed. The damping term is chosen arbitrarily. A second order system of the following form

$$\frac{d^2y}{dt^2} + 2\zeta\omega_n \frac{dy}{dt} + \omega_n^2 y = 0$$

gives the solution

$$y(t) = \exp(-\zeta\omega_n t) \sin\omega t$$

with the following initial conditions

$$y(o) = 0$$

$$\dot{y}(o) = \omega$$

Taking the state variables x_{12} and x_{13} as $y(t)$ and $\dot{y}(t)$ respectively, the expressions for v_1 and v_2 in terms of x_{12} and x_{13} are given by

$$v_1 = \sqrt{\frac{3}{2}}\, E_L\left[\left(\frac{1}{\sqrt{3}} \mp \frac{\zeta\omega_n}{\omega}\right) x_{12} \mp x_{13}\right]$$

$$v_2 = \sqrt{\frac{3}{2}}\, E_L\left[\left(-\frac{1}{\sqrt{3}} \mp \frac{\zeta\omega_n}{\omega}\right) x_{12} \mp x_{13}\right)$$

Eq. (6.5) is transformed to an unforced system of the form

$$p\, x_1 = F_1\, x_1$$

where the state vector x_1 is given as

$$x_1 = [v_6, v_7, v_9, v_{11}, v_{13}, v_{15}, v_{18}, v_{22}, i_3, i_5, i_{19}, x_{12}, x_{13}]^T$$

F_1 is a 13 x 13 matrix with the following non-zero elements

$$F_1(i,j) = F(i,j) \qquad \text{for } i, j = 1,2,\ldots,11$$

$$F_1(9,12) = \left[\sqrt{\frac{3}{2}}\, E_L\left(\frac{\zeta\omega_n}{\omega} \mp \sqrt{3}\right)\right]/3L_t$$

$$F_1(9,13) = \left[\sqrt{\frac{3}{2}}\, E_L(1/\omega)\right]/3L_t$$

$$F_1(10,12) = \left[\sqrt{\frac{3}{2}}\, E_L\left(-\frac{\zeta\omega_n}{\omega} \mp \sqrt{3}\right)\right]/3L_t$$

$$F_1(10,13) = -\sqrt{\frac{3}{2}}\, E_L(1/\omega)/3L_t$$

$$F_1(12,13) = 1$$

$$F_1(13,12) = \mp\omega_n^2$$

$$F_1(13,13) = -2\zeta\omega_n$$

6.5 Selection of the Performance Index and Initial Vector

The performance index chosen for limiting both recovery voltage transient and damping circuit loss is given by

$$\eta = \eta_1 + K\eta_2 = \int_0^\infty x^T Q\, x\, dt \tag{6.13}$$

where $\eta_1 = \int_0^\infty (e-e_d)^2\, dt = \int_0^\infty x^T Q_1\, x\, dt$ (6.14)

$$\eta_2 = \int_0^\infty i_{R_d}^2\, R_d\, dt = \int_0^\infty x^T Q_2\, x\, dt \tag{6.15}$$

e is the transient voltage (appears across the valve) which is given by

$$e = C_1 x \tag{6.16}$$

where

$$C_1 = \left[\frac{R_G}{R_G+R_a}\ \ \frac{R_G}{R_G+R_a}\ 0\ 0\ 0\ 0\ 0\ \frac{R_a}{R_G+R_a}\ \ 0\ 0\ \frac{R_G R_a}{R_G+R_a}\ 0\ 0\right] \tag{6.17}$$

e_d is the steady state voltage across the valve which is given by

$$e_d = C_2 x \tag{6.18}$$

where

$$C_2 = [0\ 0\ 0\ 0\ 0\ 0\ 0\ 0\ 0\ 0\ 0\ -\sqrt{2E_L}\ \ 0] \tag{6.19}$$

i_{R_d} is the current through the damping circuit which is given by

$$i_{R_d} = D x \tag{6.20}$$

where

$$D = [1/R_d\ \ 1/R_d\ 0\ 0\ 0\ 0\ -1/R_d\ 0\ 0\ 0\ 0\ 0\ 0] \tag{6.21}$$

K is weighting factor given to the powerloss component.

The above performance index consists of integrals that are to be evaluated from zero to infinity. Although, the damping circuit loss is to be considered only during a finite period, it is assumed here that minimizing the PI η_2 is equivalent to the minimization of the actual power losses.

The weighting matrix Q is given by

$$Q = Q_1 + K Q_2 \tag{6.22}$$

where

$$Q_1 = (C_1 - C_2)^t (C_1 - C_2) \tag{6.23}$$

$$Q_2 = (D^t \; D \; R_d) \tag{6.24}$$

The initial state vector considered, corresponds to the instant $\alpha + \mu = 90^\circ$, and is given by

$$x_o = [0 \;\; 0 \;\; 0 \;\; 0 \;\; 0 \;\; 0 \;\; 0 \;\; 0 \;\; 0 \;\; 0 \;\; 0 \;\; 0 \;\; \omega]^T \tag{6.25}$$

6.6 An Example

6.6.1 Description of the Problem:

A valve which contains 200 thyristors and operates at a peak repetitive voltage of 200 KV, is considered with the following supply system and valve parameters.

Supply system:

L_t = 0.05 H

C_t = 2 nF

C_y =2 nF

R_a = 3 K-ohm

L_a = 1 mH

E_L = 200/√2 KV

φ = 0.05

f = 60 Hz

Valve: R_d = 2 K-ohm to 8 K-ohm ; C_d = 50 nF - 200 nF

R_g = 10 ohms

C_g = 1 microfarad.

6.6.2 Computed Results and Discussion:

Fig. 6.1 shows the variation of PI with R_d for C_d = 100 nF. When K = 0, the optimum R_d (at which PI is minimum) is obtained as 6.0 K-ohm.

As verification to the optimum R_d obtained for C_d = 100 nF, the recovery voltage transient for different R_d is computed from the transient analysis of the equivalent circuit (which is explained in 3.5). The effect of R_d on the recovery voltage transient is shown in Fig.6.2. It can be seen from Fig.6.2 that the recovery voltage transient is minimum for R_d = 6 K-ohm compared to that obtained with other values of R_d. Though the peak overvoltage is less for R_d=4K-ohm, the deviation of the transient voltage from the steady state voltage is more and persists longer (whereas for R_d = 8 K-ohm, the deviation of the transient voltage from the steady state voltage is less but the overvoltage peak is more compared to

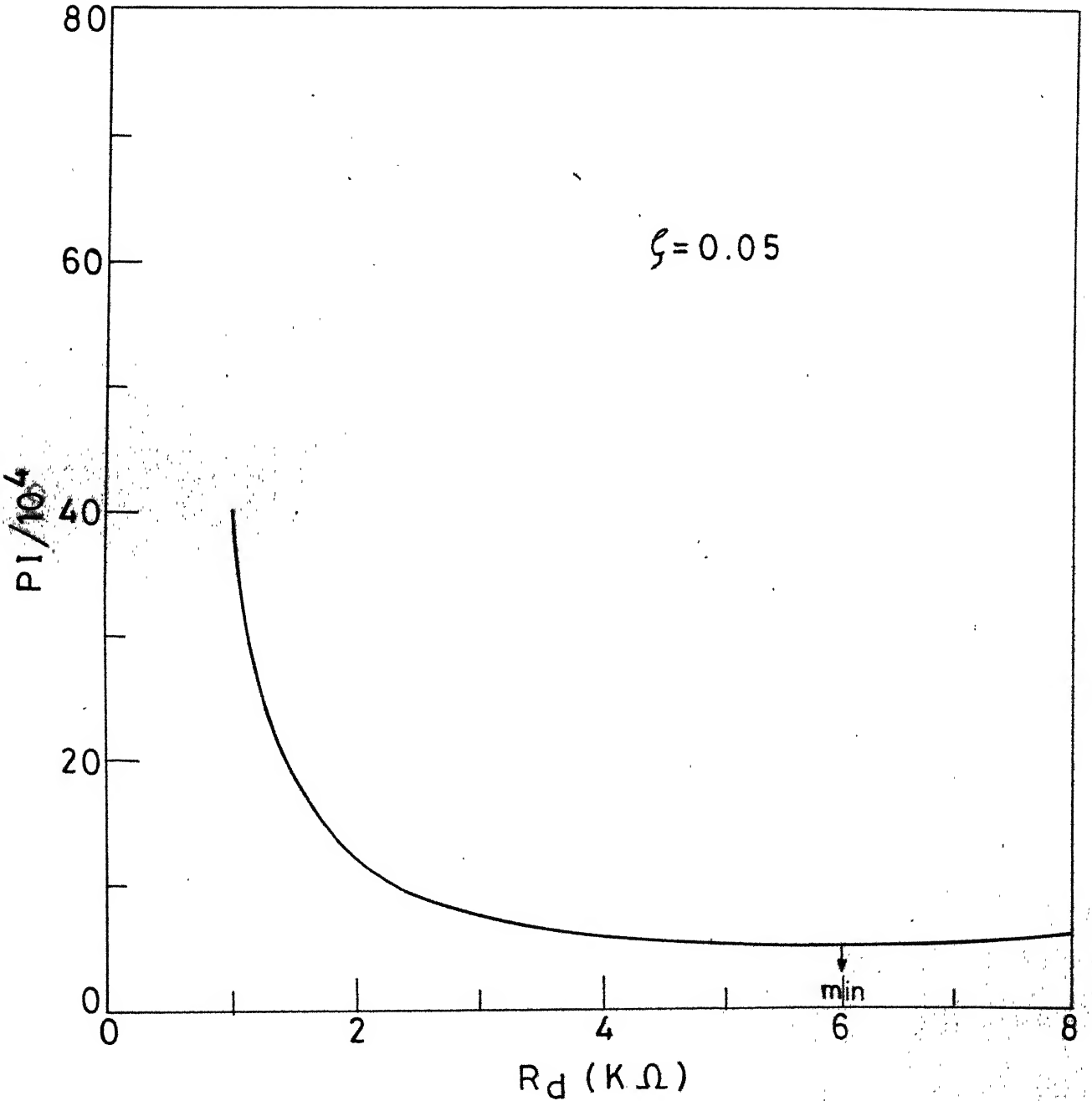

Fig. 6.1 Variation of PI with R_d for $C_d = 100\,nF$.

R_d = 6 K-ohm case). Thus it is observed for C_d = 100 nF, R_d = 6 K-ohm gives the minimum recovery voltage transient.

For different values of C_d the optimum R_d is evaluated and the PI values corresponding to optimum R_d are given in Table 6.1. It can be seen from the table (with K = 0) that the optimum value of C_d is around 100 nF. Therefore, for limiting the recovery voltage transient the optimum damping circuit parameters are R_d = 6 K-ohm, C_d = 100 nF.

Table 6.1 PI Values corresponding to optimum R_d for different C_d.

C_d	Optimum R_d	PI
50 nF	6.5 K-ohm	0.574543×10^5
100 nF	6.0 K-ohm	0.533494×10^5
150 nF	6.0 K-ohm	0.555074×10^5
200 nF	6.0 K-ohm	0.594936×10^5

Optimal damping circuit parameters with inclusion of power loss.

The effect of the inclusion of the power loss in the PI is shown in Table 6.2 which gives the optimum values of R_d and C_d for different weighting factors K.

Table 6.2: Optimum damping circuit parameters for different weighting factors(K).

Weightage given to power loss (K)	Optimum R_d	Optimum C_d
1	5.5 k-ohm	100 nF
10	6.0 K-ohm	50 nF
50	4.5 K-ohm	50 nF

6.7 Conclusions

The design of the damping circuit requires the determination of the capacitance and resistance which reduce the recovery voltage transient without undue increase in losses in the damping circuit. An objective function is defined which takes into account both the recovery voltage transient and the damping circuit loss. The optimum damping circuit parameters are evaluated for a representative valve using the approach of minimization of the objective function.

CHAPTER 7

CONCLUSIONS

7.1 Summary

The electrical design of HVDC valves depends upon the overvoltages generated in the system and those generated within the valve. The overvoltages, developed during the turn-on and turn-off periods, because of the non-simultaneous operation of the thyristors in a valve, are among the most severe overvoltages. The grading and damping circuits are used to limit these overvoltages instead of derating the valve. The design of damping circuit also depends upon the losses that take place in it. Proper selection of damping resistance and capacitance limit the overvoltages to an economic value without undue increase in the losses of the damping circuit.

In Chapters 2 and 3 of this thesis, an attempt has been made to calculate the turn-on and turn-off overvoltages in a HVDC valve. Computer programs are developed and the effect of various parameters on these overvoltages has been studied. The approach adopted for simulation of a valve during turn-on and turn-off periods is along the lines given in refs. [1] and [3], but the equivalent circuits are simulated by developing the state equations on the basis of topological considerations, instead of using the ECAP program for simulation as in refs. [1] and [3].

In connection with damping circuit design, a computer program is developed to calculate the sensitivities of the valve voltage with respect to the damping circuit resistance and capacitance in time domain using adjoint network approach using the algorithm given in refs. [5, 11], in Chapter 4.

In Chapter 5, a detailed method has been developed to calculate the damping circuit losses by representing exact equivalent circuit of the converter system during each interval of conduction over a cycle. The results obtained are comparable (1) with the results obtained using a second order system for valve voltage oscillations [4], and (2) with the results obtained using the approximate formulas given by Ainsworth.

In Chapter 6, an objective function, which considers both recovery voltage transient and damping circuit loss, is defined and optimal damping circuit parameters are obtained by minimizing the objective function.

7.2 Scope for Further Work

The calculations of turn-on and turn-off overvoltages can be greatly improved by considering the number of thyristors which turn-on and turn-off non-simultaneously as a random variable and then evaluating the expected value and variance of the overvoltages, instead of considering the groups of thyristors which turn-on and turn-off at a specific time.

The sensitivities of the valve voltage with respect to damping circuit resistance and capacitance can be used for optimizing damping circuit parameters by defining an error function. The gradient of the error function can be ascertained and the parameter values can be altered according to some gradient technique to efficiently reduce the error.

The technique presented in Chapter 6, for optimization of damping circuit parameters is a first step in the application of mathematical optimization methods to damping circuit design. The assumptions used in applying this technique have to be examined critically, particularly regarding the choice of a suitable performance index. This can lead to improved method of selection of damping circuit parameters.

APPENDIX A

FORMULATION OF STATE EQUATIONS FOR LINEAR NETWORKS [12]

Consider a network containing only two terminal components each of which is either a voltage (or current) source or is a passive element (resistor, or inductor, or capacitor). The voltage current relationships of the passive elements are

$$v(t) = R\, i(t) \qquad \text{for resistors} \qquad (A.1)$$

$$i(t) = C(dv(t)/dt) \qquad \text{for capacitors} \qquad (A.2)$$

$$v(t) = = L(di(t)/dt) \qquad \text{for inductors} \qquad (A.3)$$

where $v(t)$ and $i(t)$ represent the voltage and current variables of the elements.

If the edges in the network graph corresponding to the voltage sources do not form circuits and the edges corresponding to current sources do not form cutsets, then the network can be characterized by a set of linear differential equations which can be derived as follows. Let the voltage and current variables associated with the edges of an arbitrary tree T be designated by the vectors v_T and i_T. If the vectors $\psi_p = (v_T, i'_T)$ and $\psi_s = (v'_T, i_T)$ represent,

respectively, the primary and secondary variables corresponding to the tree T and the cotree T', it is possible, by proper partitioning of these vectors, to write the terminal equations for the components in the form

$\mathcal{Y}_{po}$ = specified functions of time (voltage and current sources)

$$\frac{d}{dt}\mathcal{Y}_{p1} = D_1 \mathcal{Y}_{s1} \qquad (A.4)$$

and

$$\begin{bmatrix} \mathcal{Y}_{p2} \\ \mathcal{Y}_{p3} \end{bmatrix} = \begin{bmatrix} D_2(d/dt) & 0 \\ 0 & D_3 \end{bmatrix} \begin{bmatrix} \mathcal{Y}_{s2} \\ \mathcal{Y}_{s3} \end{bmatrix} \qquad (A.5)$$

Although it is not evident from the development so far, it can be seen later that the vector $\mathcal{Y}_{p1}$ represents the state vector of the system. The matrices $D_i (i = 1,2,3)$ in Eqs.(A.4) and (A.5) are all diagonal with positive diagonal entries, and D_3 corresponds to the resistance elements.

The vectors of primary variables $\mathcal{Y}_{pi}$, $i = 0,1,2,3$ contain exactly one variable for each edge of the graph and are identified with the voltage and current variables of the various elements. The vectors of secondary variables $\mathcal{Y}_{si}$, $i = 0,1,2,3$, likewise contain exactly one variable for each edge of the graph and represent the complimentary variables of the respective primary vectors. The circuit and cutset equations of the system

graph for any tree T can be written in the form

$$\begin{bmatrix} \psi_{so} \\ \psi_{s1} \\ \psi_{s2} \\ \psi_{s3} \end{bmatrix} + \begin{bmatrix} \phi_{o1} & \phi_{o2} & \phi_{o3} \\ \phi_{11} & \phi_{12} & \phi_{13} \\ \phi_{21} & \phi_{22} & \phi_{23} \\ \phi_{31} & \phi_{32} & \phi_{33} \end{bmatrix} \begin{bmatrix} \psi_{p1} \\ \psi_{p2} \\ \psi_{p3} \end{bmatrix} + \begin{bmatrix} \phi_{oo} \\ \phi_{10} \\ \phi_{20} \\ \phi_{30} \end{bmatrix} \begin{bmatrix} \psi_{po} \end{bmatrix}$$

$$= 0 \qquad \text{(A.6)}$$

where each one of the submatrices ϕ_{ij} has the form

$$\phi_{ij} = \begin{bmatrix} 0 & A_{ij} \\ B_{ij} & 0 \end{bmatrix} \qquad i,j=0,1,2,3,$$

where A_{ij} is the fundamental cutset matrix and B_{ij} is the fundamental circuit matrix.

A maximally selected tree and cotree by definition include a maximum number of edges corresponding to capacitors in T and a maximum number of edges corresponding to inducters in T'. It can be shown, for such a tree, certain of the submatrices in Eq.(A.6) are identically zero and that the vector of primary variables ψ_{p1} identified with the tree and cotree represents the state vector of the network.

A systematic procedure for identifying a maximally selected tree in the network graph G is based on a sequence of subgraphs of the network graph selected as follows:

1. Consider a subgraph G_1 of G consisting of all the edges corresponding to voltage sources. Select a tree T_1 in G_1. By a hypothesis of the theorem, the voltage sources form no circuits. Consequently, in G_1 the compliment T_1' of T_1 contains no edges.

2. Consider a subgraph G_2 of G consisting of all the edges in G_1 and the edges corresponding to capacitors. Select a tree T_2 in G_2 containing T_1. In G_2, the compliment of T_2 contains at most edges corresponding to capacitors, i.e. the edges associated with the voltage variables in ψ_{s2} or the current variables in ψ_{p2}.

3. Consider a subgraph G_3 consisting of all the edges in G_2 and the edges corresponding to the resistors, i.e. the edges corresponding to the variables in ψ_{p3}. Select a tree T_3 in G_3 containing T_2. In G_3, the compliment T_3' of T_3 contains at most edges corresponding to capacitors and resistors, i.e., the edges corresponding to the voltage variables in ψ_{s2} and ψ_{p3}, respectively.

4. Consider a subgraph G_4 of G consisting of all the edges in G_3 and the edges corresponding to inductors. Select a tree T_4 in G_4 which includes T_3. In G_4, the compliment T_4 includes, at most edges corresponding to capacitors, resistors and inductors, i.e., edges corresponding to the voltage variables in ψ_{s2}, ψ_{s3}, and ψ_{s1} respectively.

5. Consider the entire graph G. Select a tree $T_5 = T$ which includes T_4. Since, by hypothesis, the graph contains no cutsets of edges corresponding only to current sources, $T_5' = T_4' = T'$ and the maximally selected tree and cotree have been identified.

From the second step in selecting the tree, it is evident that the fundamental circuits defined by T_2' span only those edges of the graph that are contained in T_2. It thus follows that the fundamental circuit equations introduce only zero entries in $\emptyset_{22}$ and $\emptyset_{23}$, that is, $B_{22} = 0$, $B_{23} = 0$. Likewise the circuits defined by the edges of T_3' span only those edges of the graph contained in T_3, and the fundamental circuit equations can introduce only zero entries in $\emptyset_{32}$, that is, $B_{32} = 0$.

From Step 4, it follows that the cutsets defined by the edges of T_4 corresponding to inductors contain only those edges corresponding to inductors and specified current sources. It follows, therefore, that the fundamental cutset equations introduce only zero entries in $\emptyset_{22}$ and $\emptyset_{23}$, that is $A_{22} = 0$, $A_{23} = 0$, and it can be concluded that $\emptyset_{22} = 0$ and $\emptyset_{23} = 0$. Likewise, since the cutsets defined by the edges of T_3 do not include edges corresponding to current variables in ψ_{pl}, it follows that $\emptyset_{32} = 0$.

The state equations for the system are developed by substituting Eq.(A.6) into Eqs.(A.4) and (A.5) with $\phi_{22} = 0$, $\phi_{23} = 0$, and $\phi_{32} = 0$. The results are

$$\frac{d\psi_{p1}}{dt} = -D_1[\phi_{12} \quad \phi_{13}]\begin{bmatrix}\psi_{p2}\\ \psi_{p3}\end{bmatrix} - D_1\phi_{11}\psi_{p1} - D_1\phi_{10}\psi_{p0} \tag{A.7}$$

and

$$\begin{bmatrix} U & 0 \\ 0 & U + D_3\phi_{33}\end{bmatrix}\begin{bmatrix}\psi_{p2}\\ \psi_{p3}\end{bmatrix} = -\begin{bmatrix} D_2\phi_{21}(d/dt) \\ D_3\phi_{31}\end{bmatrix}\psi_{p_1} - \begin{bmatrix} D_2\phi_{20}(d/dt) \\ D_3\phi_{30}\end{bmatrix}\psi_{po} \tag{A.8}$$

If the coefficient matrix to the left of the equality sign in Eq.(A.8) is nonsingular, then Eq.(A.8) can be solved explicitly for ψ_{p2} and ψ_{p3}. The result is

$$\begin{bmatrix}\psi_{p2}\\ \psi_{p3}\end{bmatrix} = -\begin{bmatrix} D_2\phi_{21}(d/dt) & D_2\phi_{20}(d/dt) \\ M_{21} & M_{22}\end{bmatrix}\begin{bmatrix}\psi_{p1}\\ \psi_{p0}\end{bmatrix} \tag{A.9}$$

where

$$M_{21} = (U + D_3 \, \phi_{33})^{-1} \, D_3 \, \phi_{31}$$

$$M_{22} = (U + D_3 \, \phi_{33})^{-1} \, D_3 \, \phi_{30} \qquad \text{(A.10)}$$

Substituting the indicated solution in Eq.(A.9) into Eq.(A.7) gives a system of differential equations of the form

$$(U - D_1 \phi_{12} \, D_2 \, \phi_{21})(d/dt)\psi_{p1} = N_1 \psi_{p1} + N_2 \, \psi_{p0} + N_3 (d/dt)\psi_{p0} \qquad \text{(A.11)}$$

where

$$N_1 = D_1 \, \phi_{13} \, M_{21} + D_1 \, \phi_{11}$$

$$N_2 = D_1 \, \phi_{13} \, M_{22} + D_1 \, \phi_{10}$$

$$N_3 = D_1 \, \phi_{12} \, D_2 \, \phi_{20}$$

The above equations can be reduced to the following form

$$\frac{d\psi_{p1}}{dt} = P \psi_{p1} + Q_1 \psi_{p0} + Q_2 \, \frac{d}{dt} \psi_{p0} \qquad \text{(A.12)}$$

where

$$P = [U + D_1 \, \phi_{12} \, D_2 \, \phi_{21}]^{-1} \, N_1$$

$$Q_1 = [U + D_1 \, \phi_{12} \, D_2 \, \phi_{21}]^{-1} \, N_2$$

$$Q_2 = [U + D_1 \, \phi_{12} \, D_2 \, \phi_{21}]^{-1} \, N_3$$

if the coefficient matrix on the vector $(d/dt)\psi_{p1}$ is non-singular. These coefficient matrices are indeed non-singular[12].

An Example for Illustration:

Consider the network shown in Fig. A.1. The system graph is shown in Fig.A.2. The tree is selected maximally putting all the capacitors in the tree and all the inductors in the link.

$$\psi_{po} = [v_o \quad V]^T$$

$$\psi_{so} = [i_o \quad i]^T$$

where i_o and i are the currents through the voltage sources V_o and V.

$$\psi_{p1} = [v_2 \quad v_3 \quad v_6 \quad i_7 \quad i_8 \quad i_{10}]^T$$

$$\psi_{s1} = [i_2 \quad i_3 \quad i_6 \quad v_7 \quad v_8 \quad v_{10}]^T$$

$$D_1 = \begin{bmatrix} 1/C_{bc} & 0 & 0 & 0 & 0 & 0 \\ 0 & 1/C_{yc} & 0 & 0 & 0 & 0 \\ 0 & 0 & 1/C & 0 & 0 & 0 \\ 0 & 0 & 0 & 1/2L_t & 0 & 0 \\ 0 & 0 & 0 & 0 & 1/L_a & 0 \\ 0 & 0 & 0 & 0 & 0 & 1/L_a \end{bmatrix}$$

There are no capacitors in the cotree, no inductors in the tree Therefore $\psi_{p2} = 0$

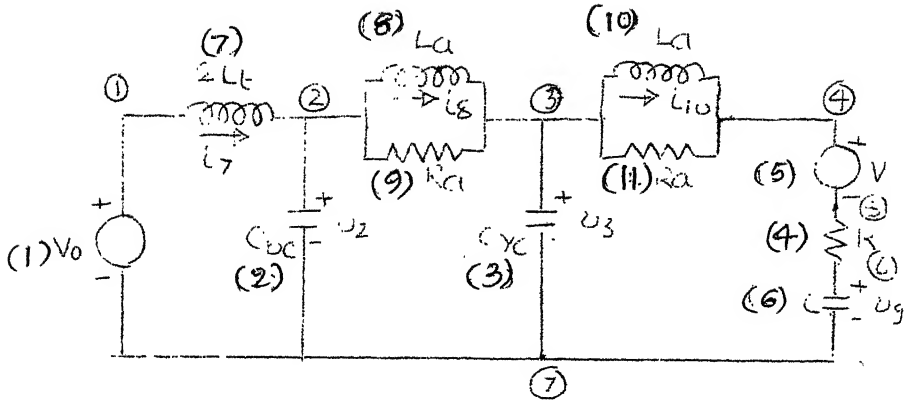

FIG A·1 NETWORK CONSIDERED FOR WRITING STATE EQUATIONS (EQUIVALENT CIRCUIT USED IN FUNCTION drop VOLTAGE CALCULATION)

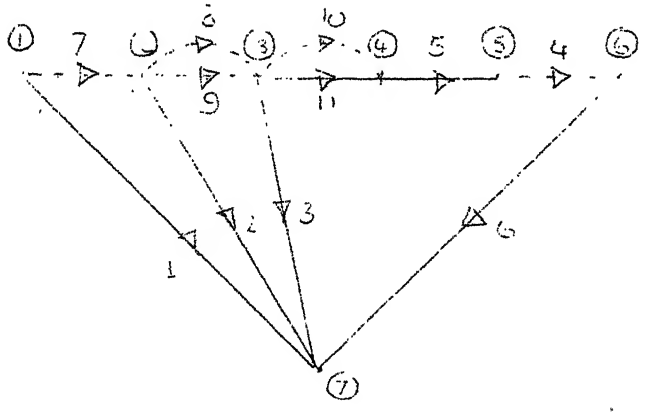

FIG A·2 GRAPH OF FIG A 1

$$\Psi_{p3} = [i_4 \quad i_9 \quad v_{11}]^T$$

$$\Psi_{s3} = [v_4 \quad v_9 \quad i_{11}]^T$$

$$D_3 = \begin{bmatrix} G & 0 & 0 \\ 0 & G_a & 0 \\ 0 & 0 & R_a \end{bmatrix}$$

The circuit and cutset equations of the system graph are given by Eq.(A.6). For this example, the nonzero matrices of Ø are as follows:

$$\emptyset_{01} = \begin{bmatrix} 0 & 0 & 0 & 1 & 0 & 0 \\ 0 & 0 & 0 & 0 & 0 & 0 \end{bmatrix}$$

$$\emptyset_{03} = \begin{bmatrix} 0 & 0 & 0 \\ -1 & 0 & 0 \end{bmatrix}$$

$$\emptyset_{10} = \begin{bmatrix} 0 & 0 \\ 0 & 0 \\ 0 & 0 \\ -1 & 0 \\ 0 & 0 \\ 0 & 0 \end{bmatrix}; \quad \emptyset_{11} = \begin{bmatrix} 0 & 0 & 0 & -1 & 1 & 0 \\ 0 & 0 & 0 & 0 & -1 & 0 \\ 0 & 0 & 0 & 0 & 0 & 0 \\ 1 & 0 & 0 & 0 & 0 & 0 \\ -1 & 1 & 0 & 0 & 0 & 0 \\ 0 & 0 & 0 & 0 & 0 & 0 \end{bmatrix}$$

$$\phi_{13} = \begin{bmatrix} 0 & 1 & 0 \\ 1 & -1 & 0 \\ -1 & 0 & 0 \\ 0 & 0 & 0 \\ 0 & 0 & 0 \\ 0 & 0 & -1 \end{bmatrix}; \qquad \phi_{30} = \begin{bmatrix} 0 & 1 \\ 0 & 0 \\ 0 & 0 \end{bmatrix}$$

$$\phi_{31} = \begin{bmatrix} 0 & -1 & 1 & 0 & 0 & 0 \\ -1 & 1 & 0 & 0 & 0 & 0 \\ 0 & 0 & 0 & 0 & 0 & 1 \end{bmatrix}; \quad \phi_{33} = \begin{bmatrix} 0 & 0 & 1 \\ 0 & 0 & 0 \\ -1 & 0 & 0 \end{bmatrix}$$

Substituting the above defined matrices in Eq.(A.12) and simplifying, the state equations are obtained which are given by Eq. (A.13).

$$
\begin{bmatrix} pv_2 \\ pv_3 \\ pv_g \\ pi_7 \\ pi_8 \\ pi_{10} \end{bmatrix} = \begin{bmatrix} \frac{-1}{C_{bc}R_a} & \frac{1}{C_{bc}R_a} & 0 & \frac{1}{C_{bc}} & \frac{-1}{C_{bc}} & 0 \\ \frac{1}{C_{yc}R_a} & \frac{-1}{C_{yc}R_a} - \frac{1}{C_{yc}(R+R_a)} & \frac{1}{C_{yc}(R+R_a)} & 0 & \frac{1}{C_{yc}} & \frac{-R_a}{C_{yc}(R+R_a)} \\ 0 & \frac{1}{C(R+R_a)} & \frac{-1}{C(R+R_a)} & 0 & 0 & \frac{R_a}{C(R+R_a)} \\ \frac{-1}{2L_t} & 0 & 0 & 0 & 0 & 0 \\ \frac{1}{L_a} & \frac{-1}{L_a} & 0 & 0 & 0 & 0 \\ 0 & \frac{R_a}{L_a(R+R_a)} & \frac{-R_a}{L_a(R+R_a)} & 0 & 0 & \frac{-R_aR}{L_a(R+R_a)} \end{bmatrix} \begin{bmatrix} v_2 \\ v_3 \\ v_g \\ i_7 \\ i_8 \\ i_{10} \end{bmatrix} + \begin{bmatrix} 0 & 0 \\ 0 & \frac{1}{C_{yc}(R+R_a)} \\ 0 & \frac{-1}{C(R+R_a)} \\ \frac{1}{2L_t} & 0 \\ 0 & 0 \\ 0 & \frac{-R_a}{L_a(R+R_a)} \end{bmatrix} \begin{bmatrix} V_o \\ V \end{bmatrix} \qquad (A.13)
$$

APPENDIX B

TIME DOMAIN SENSITIVITY CALCULATIONS [5]

The adjoint network method will be used for sensitivity calculations in the time domain for linear dynamic networks. The problem to be investigated in this section is the determination of $\partial v_o(t_f)/\partial x_j$ or $\partial i_o(t_f)/\partial x_j$, where x_j is some element parameter (R,L,C,g_m, temperature, etc.); and $v_o(t_f)$ or $i_o(t_f)$ is the output voltage or current at the specific time $t = t_f$. According to Tellegen's theorem,

$$v^t(t)\,\hat{i}(\tau) = i^t(t)\,\hat{v}(\tau) = \hat{i}^t(\tau)v(t) = \hat{v}^t(\tau)i(t) = 0 \qquad (B.1)$$

where v(t)and i(t) are the element voltage and current vectors corresponding to the original network (N), $\hat{v}(\tau)$ and $\hat{i}(\tau)$ are voltage and current vectors corresponding to adjoint network $(\hat{N})$. The following equations can also be derived using Tellegen's theorem.

$$\begin{aligned} &\hat{i}^t(\tau)\,\Delta v(t) = 0 \\ &\hat{v}^t(\tau)\,\Delta i(t) = 0 \\ &\hat{i}^t(\tau)\,\Delta v(t) - \hat{v}^t(\tau)\,\Delta i(t) = 0 \end{aligned} \qquad (B.2)$$

where $\Delta v(t)$ and $\Delta i(t)$ are the deviations of voltage and current of the perturbed network from the original network.

Let i, $(i + \Delta i)$, and $\hat{i}$ be the currents associated with the original network N, perturbed network N_p, and adjoint Network $\hat{N}$ respectively, and similarly for the voltage vectors.

Subscript P indicates port variables, and subscript b indicates variables for nonsource branches. With such partitioning of voltage and current vectors, Eq. (B.2) becomes

$$\hat{i}^t(\tau)\Delta v(t) - \hat{v}^t(\tau)\Delta i(t) = [\hat{i}_p^t(\tau)\Delta v_p(t) + \hat{i}_b^t(\tau)\Delta v_b(t)]$$

$$-[\hat{v}_p^t(\tau)\Delta i_p(t) + \hat{v}_b^t(\tau)\Delta i_b(t)]$$

$$= 0$$

It follows that

$$[-[\hat{i}_p^t(\tau)\Delta v_p(t) - \hat{v}_p^t(\tau)\Delta i_p(t)] = [\hat{i}_b^t(\tau)\Delta v_b(t) - \hat{v}_b^t(\tau)\Delta i_b(t)] \tag{B.3}$$

These equations are valid regardless of the values of t and τ. In particular, Eq. (B.3) is valid if we let t and τ be related by $\tau = t_f - t$, where $t_f > 0$ is the time instant at which v_o or i_o is to be investigated. With t and τ so related, further integration of Eq. (B.3) on both sides from t = 0 to $t = t_f$ leads to the following equation

$$\int_0^{t_f} [-\hat{i}_p(\tau)\Delta v_p(t) + \hat{v}_p^t(\tau)\Delta i_p(t)]\, dt \Big|_{\tau = t_f - t}$$

$$= \int_0^{t_f} [\hat{i}_b^t(\tau)\Delta v_b(t) - \hat{v}_b^t(\tau)\Delta i_b(t)]dt \Big|_{\tau = t_f - t} \tag{B.4}$$

To evaluate the integrals in Eq. (B.4), first the transient analysis of N and $\hat{N}$ are performed to obtain the

required voltages and currents. In the analysis of N, the time variable is designated at t; in the analysis of $\hat{N}$ the time variable is designated as τ. Responses of N are obtained for the interval $0 \leq t \leq t_f$; the response of $\hat{N}$ are obtained for $0 \leq \tau \leq t_f$. Since $\tau = t_f - t$, as t increases from 0 to t_f, the variable τ actually decreases from t_f to 0. For this reason, the adjoint network is sometimes said to be analysed in backward time, whereas the original network is analysed in forward time.

Let there be b non-source branches in N (and hence in $\hat{N}$). The left side of Eq.(B.4) which is considered with the independent sources in N and $\hat{N}$ is evaluated as follows. It is considered any output voltage in N as the voltage across an independent current source, and any output current in N is considered to be the current through an independent voltage source. To get the left side of Eq.(B.4) as one term, which is precisely the desired change in output (Δv_o or Δi_o) at $t = t_f$. If the desired change to be Δv_o, the unit impuse function $\delta(\tau)$ is used and let $\hat{i}_o(\tau) = -\delta(\tau)$ is applied across the output terminals and all other independent sources in $\hat{N}$ be zero valued. The L.H.S. of Eq.(B.4) becomes

$$\int_o^{t_f} \left[-\hat{i}_p^t(\tau)\Delta v_p(t) + \hat{v}_p^t(\tau)\Delta i_p(t)\right] dt \Big|_{\tau=t_f-t} = -\int_o^{t_f} \left[\hat{i}_o(\tau)\Delta v_o(t)\right] dt \Big|_{\tau=t_f-t}$$

$$= \int_o^{t_f} \delta(t-t_f)\Delta v_o(t)\, dt = \Delta v_o(t_f).$$

If the desired change to be Δi_o, the unit impulse function $\delta(\tau)$ is used and let $\hat{v}_o(\tau) = \delta(\tau)$ and all other independent sources in $\hat{N}$ be zero valued. The L.H.S. of Eq. (B.4) becomes

$$\int_o^{t_f} [\hat{i}_{pk}^t(\tau)\,\Delta v_p(t) + \hat{v}_p^t(\tau)\,\Delta i_p(t)]\,dt \Big|_{\tau=t_f-t} = \int_o^{t_f} [\hat{v}_o(\tau)\Delta i_o(t)]\,dt \Big|_{\tau=t_f-t}$$

$$= \int_o^{t_f} \delta(t-t_f)\Delta i_o(t)dt = \Delta i_o(t_f).$$

The R.H.S. of Eq. (B.4) in scalar notations can be written as

$$\sum_{k=1}^{b} \int_o^{t_f} [\hat{i}_{bk}(\tau)\,\Delta v_{bk}(t) - \hat{v}_{bk}(\tau)\Delta i_{bk}(t)]\,dt \Big|_{\tau = t_f-t} \qquad (B.5)$$

Thus, the integrals in Eq.(B.5) are evaluated for each individual RLC branch and for each group of coupled branches. The results are then added to give the R.H.S. of Eq.(B.5). The evaluation of integrals for R and C is given below. For other types, the final results are shown in Table B.1.

Resistance branch:

$v(t) = R\,i(t)$ and $\hat{v}(\tau) = R\,\hat{i}(\tau)$

$$\int_o^{t_f} [\hat{i}(\tau)\Delta v(t) - \hat{v}(\tau)\Delta i(t)]\,dt \Big|_{\tau = t_f-t}$$

$$= \int_o^{t_f} [\hat{i}(\tau)[R\,\Delta i(t) - i(t)\Delta R] - R\,\hat{i}(\tau)\Delta i(t)]\,dt \Big|_{\tau = t_f-t}$$

$$= \left[\int_o^{t_f} [\hat{i}(\tau)\,i(t)]\,dt \Big|_{\tau = t_f-t}\right]\Delta R \qquad (B.6)$$

Capacitance branch

$i(t) = dq/dt$, $q(t) = Cv(t)$; and $\hat{i}(\tau) = d\hat{q}/d\tau$, $\hat{q}(\tau) = C\hat{v}(\tau)$

$$\int_0^{t_f} [\hat{i}(\tau)\Delta v(t) - \hat{v}(\tau)\Delta i(t)]\, dt \qquad \tau = t_f - t$$

$$= \int_0^{t_f} [\hat{i}(\tau)\Delta v(t) - \hat{v}(\tau)(\Delta dq/dt)]\, dt \qquad \tau = t_f - t$$

$$= \int_0^{t_f} [\hat{i}(\tau)\Delta v(t) - \hat{v}(\tau)(d/dt)[C\Delta v(t) + v(t)\Delta C]]\, dt \qquad \tau = t_f - t \qquad \text{(B.7)}$$

$$\triangleq I_1 + I_2 + I_3$$

The evaluation of I_3 of Eq.(B.7) is straight-forward.

$$I_3 = -\int_0^{t_f} [\hat{v}(\tau)\, \dot{v}(t)\Delta C]\, dt \qquad \tau = t_f - t$$

$$= \left[-\int_0^{t_f} [\hat{v}(\tau)\, \dot{v}(t)]\, dt \right]\Delta C \qquad \text{(B.8)} \qquad \tau = t_f - t$$

The evaluation of $I_1 + I_2$ in Eq.(B.7) makes use of the method of integration by parts, which states

$$\int_a^b x(t)(dy/dt)dt = -\int_a^b (dx/dt)y(t)dt + [x(t)y(t)]_a^b \qquad \text{(B.9)}$$

we have

$$I_1 + I_2 = \int_0^{t_f} [\hat{i}(\tau)\Delta v(t) - \hat{v}(\tau)(d/dt[C\Delta v(t)])]\, dt \qquad \tau = t_f - t$$

In evaluating I_2, we make use of Eq.(B.9) with $x(t) = \hat{v}(\tau) = \hat{v}(t_f - t)$, and $y(t) = C\Delta v(t)$. Then, recalling that $dt = -d\tau$, we have

$$I_1+I_2 = \int_0^{t_f} \left[\hat{i}(\tau)\Delta v(t) - (d\hat{v}/d\tau)C\Delta v(t)\right] dt \Big|_{\tau=t_f-t}$$

$$- \left[\left(\hat{v}(\tau)C\Delta v(t)\right)\Big|_{\tau=t_f-t}\right]_0^{t_f}$$

$$= \int_0^{t_f} \left[\hat{i}(\tau)\Delta v(t) - \hat{i}(\tau)\Delta v(t)\right] dt \Big|_{\tau=t_f-t}$$

$$- C\hat{v}(o)\Delta v(t_f) + C\hat{v}(t_f)\Delta v(o)$$

$$= -C\hat{v}(o)\Delta v(t_f) + C\hat{v}(t_f)\Delta v(o) \qquad (B.10)$$

Since nothing has been said about the initial condition of a capacitor in the adjoint network $\hat{N}$, we can exploit this freedom to achieve some simplification of the analysis of $\hat{N}$. We shall assume that any capacitor in $\hat{N}$ always has a zero initial condition; i.e.,

$$\hat{v}_C(\tau) = 0, \text{ when } \tau = 0$$

Then Eq.(B.10) becomes

$$I_1 + I_2 = C\hat{v}(t_f)\Delta v(o) \qquad (B.11)$$

In many situations the initial voltage of the capacitor in N remains fixed when other element parameters vary. Then $\Delta v(o) = 0$, and Eq.(B.7) finally becomes

$$\int_0^{t_f} \left[\hat{i}(\tau)\Delta v(t) - \hat{v}(\tau)\Delta i(t)\right] dt \Big|_{\tau=t_f-t}$$

$$= \left[-\int_0^{t_f} \left[\hat{v}(\tau)\dot{v}(t)\right] dt \Big|_{\tau=t_f-t}\right]\Delta C \qquad (B.12)$$

The various steps involved in calculating $\partial v_o(t_f)/\partial x_j$ or $\partial i_o(t_f)/\partial x_j$ are as follows:

Step 1: Perform a transient analysis of the original network (N) for the time interval $t = [0, t_f]$. Obtain $i(t)$ or $v(t)$ for resistive branches, $v(t)$ for capacitive branches, and $i(t)$ for inductive branches.

Step 2: In the adjoint network $(\hat{N})$, impose the following two conditions:

1. All capacitor voltages and inductor currents in $\hat{N}$ are zero at $\tau = 0$.
2. All independent sources in $\hat{N}$ are set to zero except for $\hat{i}_o(\tau) = -\delta(\tau)$ (impulse function), when $\Delta v_o(t_f)$ is of interest, or $\hat{v}_o(\tau) = \delta(\tau)$ when $\Delta i_o(t_f)$ is of interest.

Step 3: Perform a transient analysis of the adjoint network $(\hat{N})$ for the time interval $\tau = [0, t_f]$. Obtain $\hat{i}(\tau)$ or $\hat{v}(\tau)$ for resistive branches, $\hat{v}(\tau)$ for capacitive branches and $\hat{i}(\tau)$ for inductive branches.

Step 4: Evaluate Eq.(B.4) to obtain the sensitivity components. With the excitations for $\hat{N}$ chosen as described in step 3, the L.H.S. of Eq.(B.4) should be exactly $\Delta v_o(t_f)$ or $\Delta i_o(t_f)$. The R.H.S. is evaluated with the aid of Table B.1.

Step 5: Find $\partial v_o(t_f)/\partial x_j$ or $\partial i_o(t_f)/\partial x_j$ from the result of step 4, using the fact that $\partial f/\partial x_j = \Delta f/\Delta x_j$ where x_j is the only parameter that varies, and $\Delta x_j \rightarrow 0$.

Table B.1 Time Domain Sensitivity Components.

Element type	Description	$\int_0^{t_f} [\hat{i}(\tau)\Delta v(t) + \hat{v}(\tau)\Delta i(t)]\, dt \Big\vert_{\tau=t_f-t}$
R	$v_R = R\, i_R$	$\left[\int_0^{t_f} [\hat{i}_R(\tau)\; i_R(t)]\, dt \Big\vert_{\tau=t_f-t}\right]\Delta R$
C	$i_C = dq/dt$ $q = Cv_C$	$\left[-\int_0^{t_f} [\hat{v}_C(\tau)\; \dot{v}_C(t)]\, dt \Big\vert_{\tau=t_f-t}\right]\Delta C$
G	$i_G = Gv_G$	$\left[-\int_0^{t_f} [\hat{v}_G(\tau)\; v_G(t)]\, dt \Big\vert_{\tau=t_f-t}\right]\Delta G$
L	$v_L = d\lambda/dt$ $\lambda = Li_L$	$\left[-\int_0^{t_f} [\hat{i}_L(\tau)\; i_L(t)]\, dt \Big\vert_{\tau=t_f-t}\right]\Delta L$
μ	$v_2 = \mu v_1$ $i_1 = 0$	$\left[\int_0^{t_f} [\hat{i}_2(\tau)\; v_1(t)]\, dt \Big\vert_{\tau=t_f-t}\right]\Delta\mu$
β	$i_2 = \beta i_1$ $v_1 = 0$	$\left[-\int_0^{t_f} [\hat{v}_2(\tau)\; i_1(t)]\, dt \Big\vert_{\tau=t_f-t}\right]\Delta\beta$
g_m	$i_2 = g_m v_1$ $v_1 = 0$	$\left[-\int_0^{t_f} [\hat{v}_2(\tau)\; v_1(t)]\, dt \Big\vert_{\tau=t_f-t}\right]\Delta g_m$
r_m	$v_2 = r_m i_1$ $v_1 = 0$	$\left[\int_0^{t_f} [\hat{i}_2(\tau) i_1(t)]\, dt \Big\vert_{\tau=t_f-t}\right]\Delta r_m$
T	$v_2 = nv_1$ $i_1 = -ni_2$	$\left[\int_0^{t_f} [\hat{i}_2(\tau)\; v_1(t) + \hat{v}_1(\tau)\; i_2(t)]dt \Big\vert_{\tau=t_f-t}\right.$

APPENDIX C

EQUIVALENT CIRCUITS AND STATE EQUATIONS FOR DETAILED ANALYSIS OF DAMPING CIRCUIT LOSS CALCULATION.

The simplified equivalent circuits of the converter system during the sections 2 to 9 of Table 5.1 are given in Figs. C.1 to C.8. The state equations and the expression for current through valve 3 damping resistance for the section 2 are given by Eqs.(C.1) and (C.2) respectively. Similarly the equations for the section 3 are given by Eqs.(C.3) and (C.4) respectively.

$$pv_8 = v_7/C_G R_G$$

$$pv_{10} = (-v_{10}+v_7+v_8)/C_d R_d$$

$$pv_{12} = v_{11}/C_G R_G$$

$$pv_{14} = (-v_{14}+v_{11}+v_{12})/C_d R_d$$

$$pv_{16} = (-v_{16} + v_7 + v_8 + v_{11} + v_{12})/C_G R_G$$

$$pv_{18} = (-v_{18} + v_7 + v_8 + v_{11} + v_{12})/C_d R_d$$

$$pv_{20} = (-v_{20} + v_7 + v_8 + v_{11} + v_{12})/C_G R_G$$

$$pv_{22} = (-v_{22} + v_7 + v_8 + v_{11} + v_{12})/C_d R_d$$

$$pi_4 = (1/3L_t)[-2v_7-2v_8+v_b-2v_a+v_c-v_{11}-v_{12}]$$

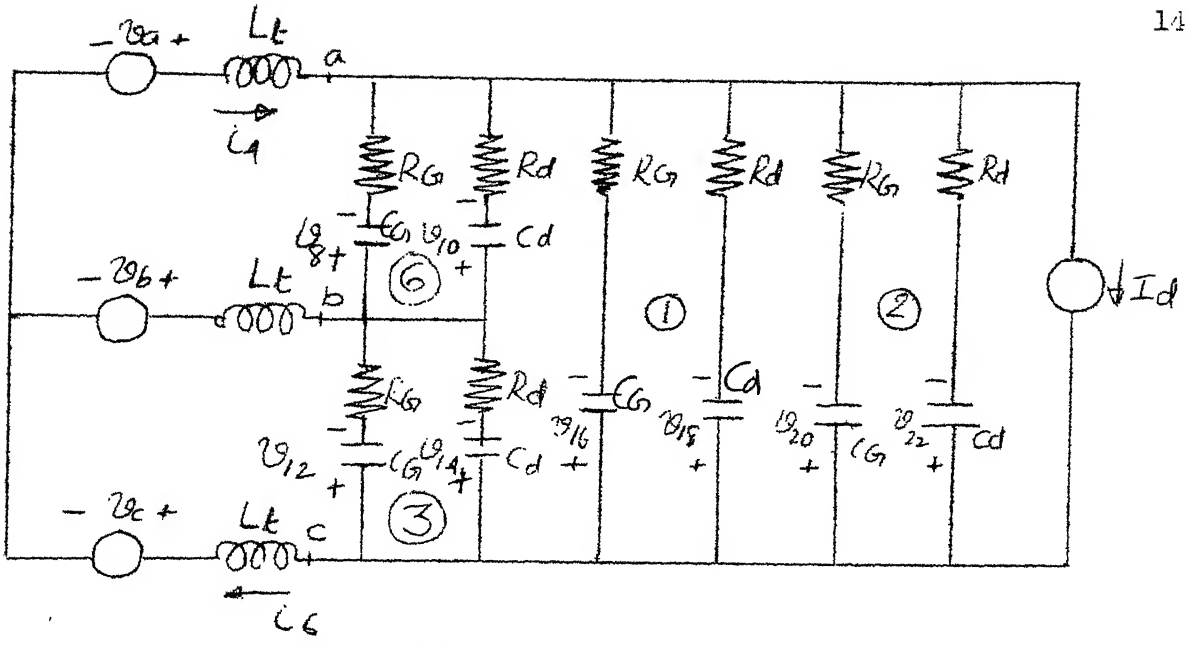

fig c.1 Simplified Equivalent Circuit of the Converter System during the period $\alpha + \mu \leq \omega t < \pi/3 + \alpha$ (Valves 4 and 5 are Conducting).

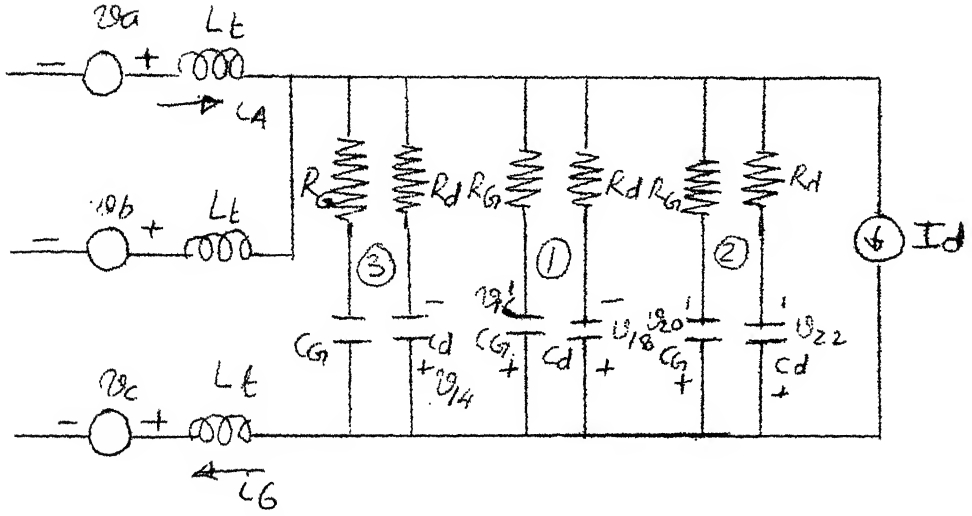

fig c 2. Simplified Equivalent Circuit of the Converter System during the period $\pi/3 + \alpha \leq \omega t < \pi/3 + \alpha + \mu$ (1, 5 and 6 Valves are conducting).

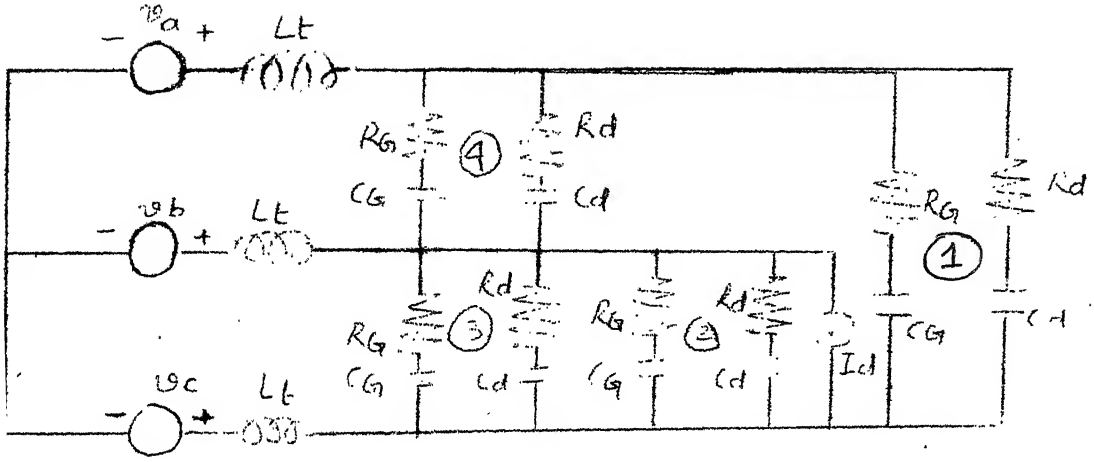

fig c.3 simplified Equivalent circuit of the Converter system during the period $\pi/3 + \alpha + \mu \leq \omega t < 2\pi/3 + \alpha$ (5 and 6 Values are Conducting).

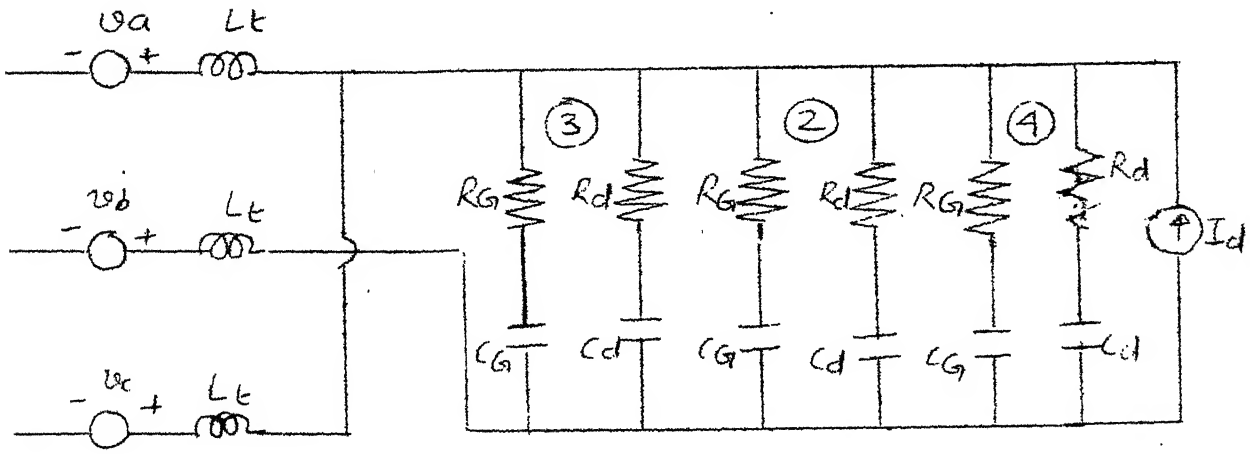

fig c.4 Simplified Equivalent Circuit of the Converter system during the period $2\pi/3 + \alpha \leq \omega t < 2\pi/3 + \alpha + \mu$ (5, 6 and 1 Values are Conducting)

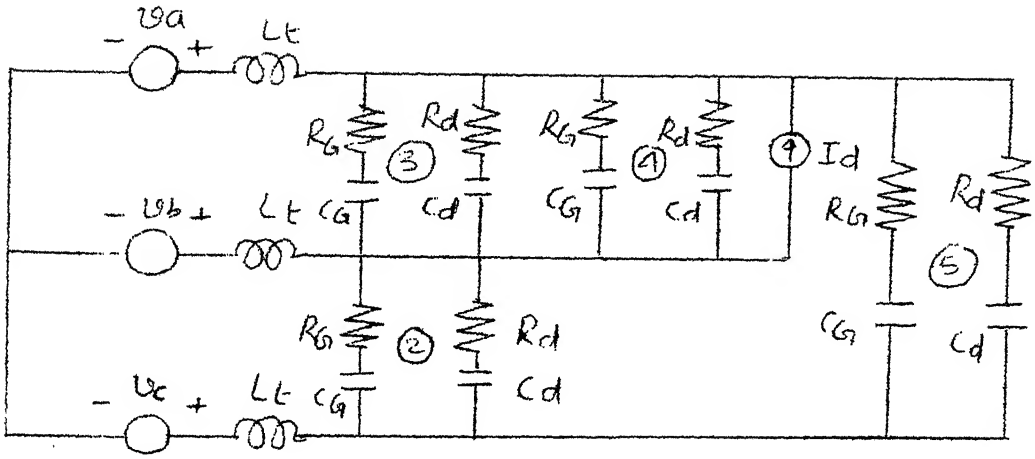

fig C·5 Simplified Equivalent Circuit of the Converter System during the period $2\pi/3 + \alpha + \mu \leq \omega t < \pi + \alpha$ (6 and 1 valves are conducting).

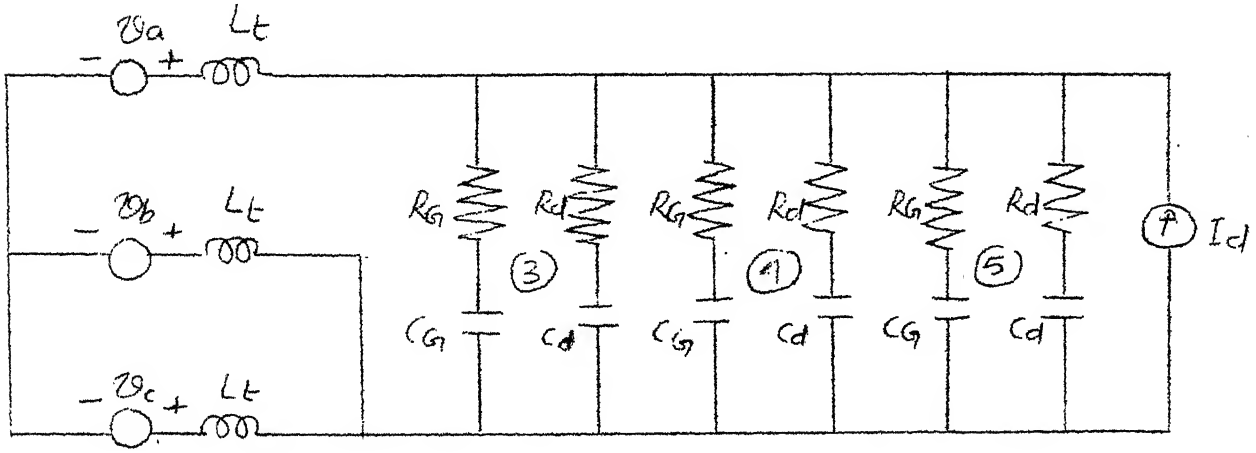

fig C·6 Simplified Equivalent circuit of the Converter System during the period $\pi + \alpha \leq \omega t < \pi + \alpha + \mu$.
(6, 1 and 2 valves are conducting)

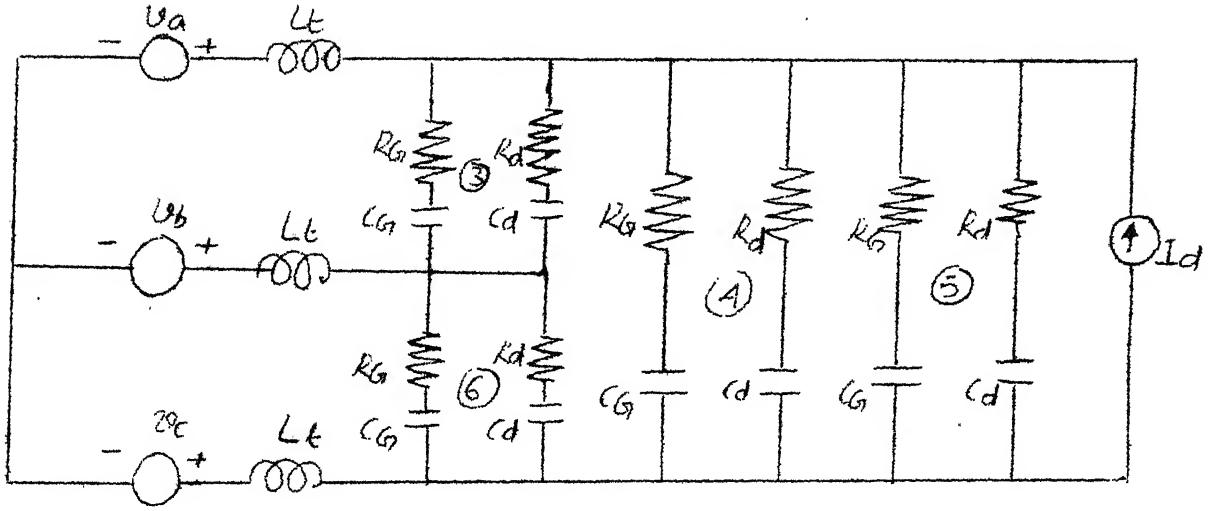

fig C.7 Simplified Equivalent circuit of the Converter system during the period $\pi + \alpha + \mu \leq \omega t < 4\pi/3 + \alpha$ (1 and 2 Valves are Conducting.)

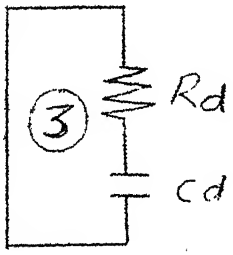

fig C 8 Simplified Equivalent circuit of the Converter system during the period $4\pi/3 + \alpha \leq \omega t < 4\pi/3 + \alpha + \mu$ (1, 2 and 3 Valves are Conducting.)

$$p_{i_6} = (1/3L_t)[-v_7 - v_8 - v_b - v_a + 2v_c - 2v_{11} - 2v_{12}]$$

$$i_{R_d} = (-v_{14} + v_{11} + v_{12})/R_d \qquad (C.2)$$

where

$$v_7 = [Q/(Q^2-PR)]X - [P/(Q^2-PR)]Y$$

$$v_{11} = [R/(PR-Q^2)]X - [Q/(PR-Q^2)]Y$$

and Y

where P,Q,R,X are defined as below.

$$P = \left(\frac{3}{R_G} + \frac{3}{R_d}\right)$$

$$Q = \left(\frac{2}{R_G} + \frac{2}{R_d}\right)$$

$$R = \left(\frac{3}{R_G} + \frac{3}{R_d}\right)$$

$$X = i_6 + \frac{v_{14} - v_{12}}{R_d} + \frac{v_{16} - v_8 - v_{12}}{R_G} + \frac{v_{18} - v_8 - v_{12}}{R_d}$$

$$+ \frac{v_{20} - v_8 - v_{12}}{R_G} + \frac{v_{22} - v_8 - v_{12}}{R_d} - I_d$$

$$Y = i_4 + \frac{v_{10} - v_8}{R_d} + \frac{v_{16} - v_8 - v_{12}}{R_G} + \frac{v_{18} - v_8 - v_{12}}{R_d}$$

$$+ \frac{v_{20} - v_8 - v_{12}}{R_G} + \frac{v_{22} - v_8 - v_{12}}{R_d} - I_d$$

The initial state variable vector for Eq.(C.1)is given by

$$v_8(t_1) = -3v_a/2$$

$$v_{10}(t_1) = -3v_a/2$$

$$v_{12}(t_1) = 0$$

$$v_{14}(t_1) = 0$$

$$v_{16}(t_1) = -3v_a/2$$

$$v_{18}(t_1) = -3v_a/2$$

$$v_{20}(t_1) = -3v_a/2$$

$$v_{22}(t_1) = -3v_a/2$$

$$i_4(t_1) = -I_d$$

$$i_6(t_1) = -I_d$$

$$pv_{12} = v_{11}/C_G R_G$$

$$pv_{14} = (-v_{14} + v_{11} + v_{12})/C_d R_d$$

$$pv_{16} = (-v_{16} + v_{11} + v_{12})/C_G R_G$$

$$pv_{18} = (-v_{18} + v_{11} + v_{12})/C_d R_d \qquad \text{(C.3)}$$

$$pv_{20} = (-v_{20} + v_{11} + v_{12})/C_G R_G$$

$$pv_{22} = (-v_{22} + v_{11} + v_{12})/C_d R_d$$

$$pi_4 = (1/3L_t)[-2v_a - v_{11} - v_{12} + v_c + v_b]$$

$$pi_6 = (1/3L_t)[-v_a - 2v_{11} - 2v_{12} - v_b + 2v_c]$$

$$i_{R_d} = (-v_{14} + v_{11} + v_{12})/R_d \qquad \text{(C.4)}$$

where $v_{11} = M/N$

and $$M = i_6 + \frac{v_{14} - v_{12}}{R_d} + \frac{v_{16} - v_{12}}{R_G} + \frac{v_{18} - v_{12}}{R_d} + \frac{v_{20} - v_{12}}{R_G} + \frac{v_{22} - v_{12}}{R_d} - I_d$$

$$N = \frac{3}{R_G} + \frac{3}{R_d}$$

APPENDIX D

DERIVATION AND METHOD OF SOLUTION OF LIAPUNOV MATRIX EQUATION AND EVALUATION OF PERFORMANCE INDEX [8]

Derivation of the Matrix Liapunov Equation

Considering the unforced system

$$\dot{x} = A\,x \tag{D.1}$$

For stability of the above system there must exist a Liapunov function, or a V function, which is positive definite.

Considering a general quadratic V function

$$V(x) = x^T\,p\,x \tag{D.2}$$

where P is any arbitrary positive definite matrix. The time derivation of V(x) is given by

$$\dot{V}(x) = \dot{x}^T\,P\,x + x^T P\,\dot{x} \tag{D.3}$$

and substitution of $\dot{x}$ from Eq.(D.1) gives

$$\begin{aligned}\dot{V}(x) &= x^T\,A^T\,P\,x + x^T\,P\,A\,x \\ &= x^T(A^TP + P\,A)x\end{aligned} \tag{D.4}$$

which can be written as

$$\dot{V}(x) = -x^T\,Q\,x \tag{D.5}$$

where Q is given by

$$A^T P + P A = -Q \qquad (D.6)$$

with any arbitrarily chosen positive definite P matrix, Q and hence V are, in general, indefinite. On the other hand arbitrarily selecting a positive semidefinite matrix Q and solving Eq.(D 6), we get P, which is positive semi-definite for an asymptotically stable system.

Solution of the matrix Liapunov Equation

The matrix Liapunov equation is a linear equation in terms of the elements of the matrix P which has to be determined. Since P is symmetric matrix only m(m+1)/2 elements of the P matrix are independent where m is the order of the matrix.

The method of solution of Liapunov equation used here is based on rewriting the equation as

$$[S]\,\underline{r} = \underline{q} \qquad (D.7)$$

where, the matrix S is of order N = m(m+1)/2. If [S] and $\underline{q}$ are known then $\underline{r}$ can be determined.

The vector $\underline{r}$ and $\underline{q}$ are defined as

$$\underline{r} = [P_{11}, P_{12}, \cdots, P_{1n}, P_{22}, \cdots, P_{rr}, \cdots, P_{rn}, \cdots, P_{nn}]^T \qquad (D.8)$$

$$\underline{q} = [Q_{11}, Q_{12}, \cdots, Q_{1n}, Q_{22}, \cdots, Q_{rr}, \cdots, Q_{rn}, \cdots, Q_{nn}]^T \qquad (D.9)$$

the elements of vector r can be expressed in general form as

$$= P_{LK} \qquad L \leq K, \text{ for } L = 1,2,\ldots,m$$
$$K = 1,2,\ldots,m$$

The matrix S is defined by

$$NR = (2m - i + 2)(i - 1)/2 + (j - i + 1)$$

$$NC = 2m - L+2)(L-1)/2 + (K - L + 1)$$

then

(a) for $i = j$

$$S(NR, NC) = 2\, a_{KL} \quad \text{for } L = i,\ L \geq K$$
$$= 2a_{LK} \quad \text{for } K = i,\ L < K$$
$$= 0 \quad \text{for } L \neq i$$

(b) for $i < j$

$$S(NR, NC) = a_{ii} + a_{jj} \quad \text{for } L = i,\ K = j$$
$$= a_{Kj} \quad \text{for } L = i,\ K \neq j$$
$$= a_{Ki} \quad \text{for } L = j,\ K \geq L$$
$$= 0 \quad \text{other conditions.}$$

Evaluation of performance index

The performance index η, defined as

$$\eta = \int_0^\infty x^T Q\, x\, dt \qquad (D.10)$$

can be obtained by substituting value of Q from Eq.(D.6)

$$\eta = -\int_0^\infty x^T(A^T P + P A)x\, dt$$

or

$$\eta = -\int_0^\infty x^T A^T P\, x\, dt - \int_0^\infty x^T P\, A\, x\, dt \qquad (D\ 11)$$

From Eq. (D .1)

$$\dot{x}^T = x^T A^T$$

and thus Eq. (D .11) can be written as

$$\eta = -\int_0^\infty \dot{x}^T P\, x\, dt - \int_0^\infty x^T P\, \dot{x}\, dt$$

$$= -[x^T P\, x]_0^\infty + \int_0^\infty x^T P\, \dot{x}\, dt - \int_0^\infty x^T P\, \dot{x}\, dt$$

$$= x_0^T P\, x_0 - x_\infty^T P\, x_\infty$$

For any asymptotically stable system $x_\infty \to 0$, so we get

$$\eta = x_0^T P\, x_0 \qquad (D\ 12)$$

APPENDIX E

EQUIVALENT CIRCUIT FOR CALCULATION OF TURN-OFF OVERVOLTAGES AND VALVE DAMPER DESIGN

The state equations for Fig.E.1 are derived using the algorithm given in Appendix A. These equations are written in the form

$$p\,x = F\,x + G\,u \qquad \text{(E.1)}$$

where x is the state variable vector with 11 state variables given by

$$[x] = [v_6,\ v_7,\ v_9,\ v_{11},\ v_{13},\ v_{15},\ v_{18},\ v_{22},\ i_3,\ i_5,\ i_{19}]^T \qquad \text{(E.2)}$$

F is a 11 x 11 matrix with the following non-zero elements

$$F(1,1) = \left[-\left(1 + \frac{C_{bc}}{C_{ca}}\right)\left(\frac{1}{R_G} + \frac{1}{R_d}\right) - \frac{1}{R_d} - \frac{1}{R+R_a}\right] \Big/ \left[C_{ab}\left(1 + \frac{C_{bc}}{C_{ab}} + \frac{C_{bc}}{C_{ca}}\right)\right]$$

$$F(1,2) = \left[\left(C_{bc}/C_{ca}\right)\left(\frac{2}{R_G} + \frac{2}{R_d}\right) - \frac{1}{R_d} - \frac{1}{R+R_a}\right] \Big/ \left[C_{ab}\left(1 + \frac{C_{bc}}{C_{ab}} + \frac{C_{bc}}{C_{ca}}\right)\right]$$

$$F(1,3) = \left(1 + \frac{C_{bc}}{C_{ca}}\right)(1/R_G) \Big/ \left[C_{ab}\left(1 + \frac{C_{bc}}{C_{ab}} + \frac{C_{bc}}{C_{ca}}\right)\right]$$

$$F(1,4) = \left(-C_{bc}/C_{ca}\right)(2/R_G) \Big/ \left[C_{ab}\left(1 + \frac{C_{bc}}{C_{ab}} + \frac{C_{bc}}{C_{ca}}\right)\right]$$

$$F(1,5) = \left(1 + \frac{C_{bc}}{C_{ca}}\right)(1/R_d) \Big/ \left[C_{ab}\left(1 + \frac{C_{bc}}{C_{ab}} + \frac{C_{bc}}{C_{ca}}\right)\right]$$

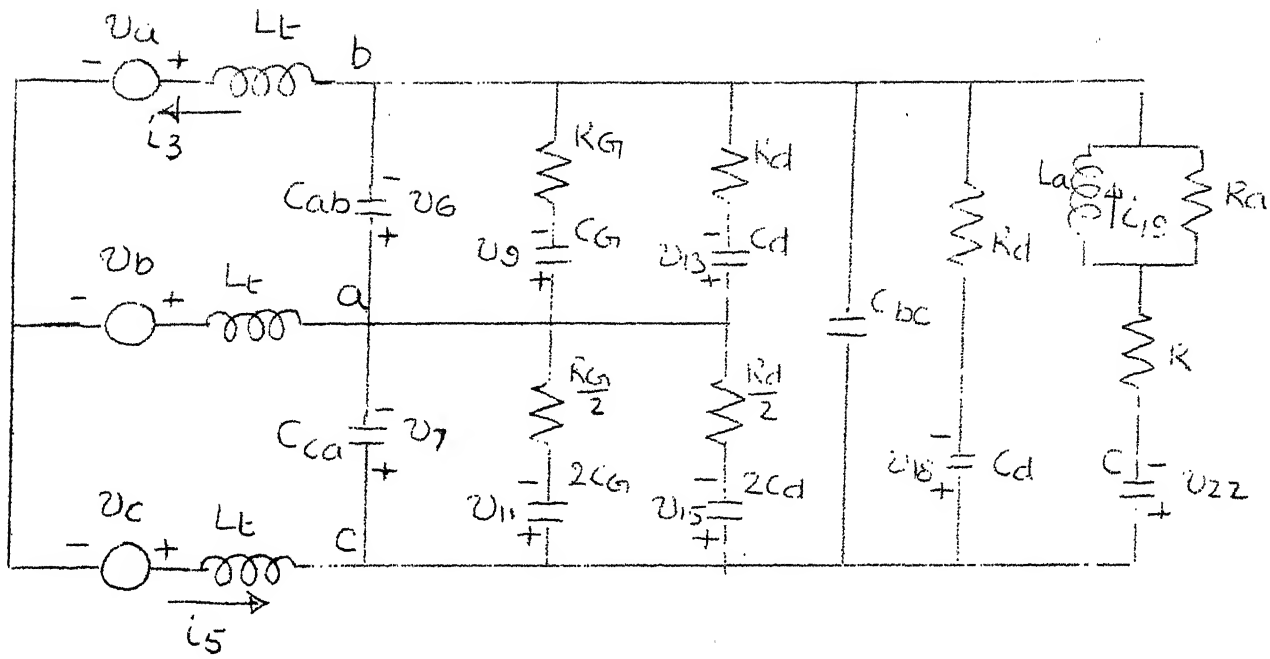

FIG E-1. EQUIVALENT CIRCUIT FOR CALCULATION OF TURN OFF OVER VOLTAGES AND VALVE DAMPER DESIGN

$$F(1,6) = (-C_{bc}/C_{ca})(2/R_d)/[C_{ab}(1 + \frac{C_{bc}}{C_{ab}} + \frac{C_{bc}}{C_{ca}})]$$

$$F(1,7) = (1/R_d)/[C_{ab}(1 + \frac{C_{bc}}{C_{ab}} + \frac{C_{bc}}{C_{ca}})]$$

$$F(1,8) = [-1/(R+R_a)] / [C_{ab}(1 + \frac{C_{bc}}{C_{ab}} + \frac{C_{bc}}{C_{ca}})]$$

$$F(1,9) = -(1+ \frac{C_{bc}}{C_{ca}})/[C_{ab}(1+ \frac{C_{bc}}{C_{ab}} + \frac{C_{bc}}{C_{ca}})]$$

$$F(1,10)= (C_{bc}/C_{ca})/[C_{ab}(1 + \frac{C_{bc}}{C_{ab}} + \frac{C_{bc}}{C_{ca}})] \qquad (E.3)$$

$$F(1,11) = [R_a/(R+R_a)]/[C_{ab}(1 + \frac{C_{bc}}{C_{ab}} + \frac{C_{bc}}{C_{ca}})]$$

$$F(2,1) = [(C_{bc}/C_{ab})(\frac{1}{R_G} + \frac{1}{R_d}) - \frac{1}{R_d} - \frac{1}{R+R_a}]/ [C_{ca}(1 + \frac{C_{bc}}{C_{ab}} + \frac{C_{bc}}{C_{ca}})]$$

$$F(2,2) = [-(1 + \frac{C_{bc}}{C_{ab}})(\frac{2}{R_G} + \frac{2}{R_d}) - \frac{1}{R_d} - (1/(R+R_a))]/ [C_{ca}(1 + \frac{C_{bc}}{C_{ab}} + \frac{C_{bc}}{C_{ca}})]$$

$$F(2,3) = (-C_{bc}/C_{ab})(1/R_G)/[C_{ca}(1 + \frac{C_{bc}}{C_{ab}} + \frac{C_{bc}}{C_{ca}})]$$

$$F(2,4) = (1 + \frac{C_{bc}}{C_{ab}})(2/R_G) /[C_{ca}(1 + \frac{C_{bc}}{C_{ab}} + \frac{C_{bc}}{C_{ca}})]$$

$$F(2,5) = (-C_{bc}/C_{ab})(1/R_d)/[C_{ca}(1 + \frac{C_{bc}}{C_{ab}} + \frac{C_{bc}}{C_{ca}})]$$

$$F(2,6) =[(1 + \frac{C_{bc}}{C_{ab}})(2/R_d)]/[C_{ca}(1 + \frac{C_{bc}}{C_{ab}} + \frac{C_{bc}}{C_{ca}})]$$

$$F(2,7) = (1/R_d)/[C_{ca}(1 + \frac{C_{bc}}{C_{ab}} + \frac{C_{bc}}{C_{ca}})]$$

$$F(2,8) = [-1/(R+R_a)]/[C_{ca}(1+ \frac{C_{bc}}{C_{ab}} + \frac{C_{bc}}{C_{ca}})]$$

$$F(2,9) = (C_{bc}/C_{ab})/[C_{ca}(1 + \frac{C_{bc}}{C_{ab}} + \frac{C_{bc}}{C_{ca}})]$$

$$F(2,10) = -(1 + \frac{C_{bc}}{C_{ab}})/ [C_{ca}(1 + \frac{C_{bc}}{C_{ab}} \quad \frac{C_{bc}}{C_{ca}})]$$

$$F(2,11) = [R_a/(R+R_a)]/[C_{ca}(1 + \frac{C_{bc}}{C_{ab}} + \frac{C_{bc}}{C_{ca}})]$$

$$F(3,1) = 1/C_G R_G$$

$$F(3,3) = -1/C_G R_G$$

$$F(4,2) = 4/C_G R_G$$

$$F(4,4) = -4/C_G R_G$$

$$F(5,1) = 1/C_d R_d$$

$$F(5,5) = -1/C_d R_d$$

$$F(6,2) == 4/C_d R_d$$

$$F(6,6) = -4/C_d R_d$$

$$F(7,1) = 1/C_d R_d$$

$$F(7,2) = 1/C_d R_d$$

$$F(7,7) = -1/C_d R_d$$

$$F(8,1) = -1/C(R+R_a)$$

$$F(8,2) = -1/C(R+R_a)$$

$$F(8,8) = -1/C(R+R_a)$$

$$F(8,11) = R_a/C(R+R_a)$$

$$F(9,1) = 2/3L_t$$

$$F(9,2) = 1/3L_t$$

$$F(10,1) = 1/3L_t$$

$$F(10,2) = 2/3L_t$$

$$F(11,1) = -R_a/L_a(R+R_a)$$

$$F(11,2) = -R_a/L_a(R+R_a)$$

$$F(11,8) = -R_a/L_a(R+R_a)$$

$$F(11,11) = -RR_a/L_a(R+R_a)$$

G is a 11x2 matrix with the following non-zero elements:

$$G(9,1) = -2/3L_t$$

$$G(9,2) = -1/3L_t \qquad \text{(E.4)}$$

$$G(10,1) = -1/3L_t$$

$$G(10,2) = -2/3L_t$$

u is a vector given by

$$u = (v_1 \quad v_2 \ ]^T \qquad \text{(E.5)}$$

where

$$v_1 = v_b - v_a \qquad \text{(E.6)}$$

$$v_2 = v_c - v_a$$

where

$$v_a = \sqrt{\frac{2}{3}} E_L \sin(\omega t + 90)$$

$$v_b = \sqrt{\frac{2}{3}} E_L \sin(\omega t - 30) \qquad \text{(E.7)}$$

$$v_c = \sqrt{\frac{2}{3}} E_L \sin(\omega t - 150)$$

In Chapters 3 and 4, the constant voltage sources V_{01} and V_{02} are considered which are given by

$$V_{01} = V_1[\omega t = \alpha + \mu]$$

$$V_{02} = V_2[\omega t = \alpha + \mu] \qquad \text{(E.8)}$$

REFERENCES

[1]. G. Karady and T. Gilsig, "The calculation of turn-on overvoltages in a HVDC thyristor valve", IEEE Trans., Power Apparatus and Systems, Vol.PAS-90, pp. 2802-2811, 1971.

[2] J. Reeve and R. Marttila, "Calculation of turn-on stresses in a HVDC valve having parallel thyristor strings", IEEE Trans., Power Apparatus and Systems, Vol.PAS-92, pp. 864-870, May/June 1973.

[3] G. Karady and T.Gilsig, "The calculation of turn-off overvoltages in a High Voltage d.c. thyristor valve", IEEE Trans., Vol.PAS-91, No.2, pp. 565-573, March/April 1972.

[4] Y. Beausejour and G. Karady, "Valve damping circuit design for HVDC systems", IEEE Trans., Vol.PAS-92, No.5, pp. 1615-1621, July-Dec. 1973.

[5] Leon O. Chua and Pen-Min Lin,"Computer aided analysis of Electronic Circuits - Algorithms and computational Techniques", Prentice-Hall Inc., Englewood Cliffs, New Jersey, 1975.

[6] I.J. Nagrath and M. Gopal, "Control systems engineering", Wiley Eastern Limited, New Delhi, 1978.

[7] E.W. Kimbark, "Direct Current Transmission", Vol.1, Wiley Interscience, New York, 1971.

[8] Ajit Kumar Rastogi, "Selection of Parameters of a static oexcitation system for 200 M.W. Obra Unit", M.Tech. Thesis, I.I.T.,Kanpur, Jan.1980.

[9] D.G.Schultz and J.L.Melsa, "State functions and linear control systems", McGraw-Hill Book Company, New York, 1967.

[10] Brice Carnahan, H.A. Luther, and James O. Wilkes, "Applied Numerical Methods", John Wiley & Sons,Inc. New York, 1969.

[11] Stephen W. Director, and Ronald A. Rohrer, "The generalised Adjoint Network and Network Sensitivities", IEEE Transactions on Circuit Theory, Vol.CT-16, No.3, pp. 318-323, August 1969.

[12] Herman E. Koenig, Ylmaz Tokad, and Hiremaglur K.Kesavan, "Analysis of Discrete Physical Systems", McGraw-Hill Book Company, New York, 1967.

[13] K.R. Padiyar, "Problems of EHV AC and DC Transmission", Course notes,I.I.T.Kanpur, Dec. 1978.

[14] E. Uhlmann, "Power Transmission by Direct Current", Springer-Verlag, Berlin, 1975.

[15] B.R.Pelly, "Thyristor phase Controlled Convertors and Cycloconvertors", Wiley Interscience, New York, 1971.

[16] M. Ramamoorty, "An Introduction to Thyristors and their Applications", Affiliated East West Press, New Delhi, 1977.

[17] B.J. Cory "High Voltage Direct Current Convertors and Systems", Macdonald, London,1965.